IMPERIAL COLLEGE LONDON

Department of Earth Science and Engineering

Centre for Petroleum Studies

Analysis of Injectivity Decline in some Deepwater Water Injectors

By

Samuel Legborsi Dambani

A report submitted in partial fulfillment of the requirements for the MSc and/or the DIC.

September 2013

DECLARATION OF OWN WORK

I declare that this thesis

"Analysis of Injectivity Decline in Some Deepwater Water Injectors"

is entirely my own work and that where any material could be construed as the work of others, it is fully cited and referenced, and/or with appropriate acknowledgement given.

Signature:………………………………………………………………………………..

Name of Student: **Samuel Legborsi Dambani**

Name of Academic supervisor: **Prof. Martin Blunt**

Names of industry supervisors: **Fidelis Tendo and Kazeem A. Lawal, Shell Nigeria Exploration and Production Company (SNEPCo).**

Abstract

The challenges and risks relating to injectivity decline due to injection of particulate-laden water are well documented in the petroleum industry and elsewhere. Although different theories have been advanced to rationalize this problem, the modeling aspects remain largely unresolved, putting huge investments at risk. By combining the fractional-flow and deep-bed filtration theories, this work formulates a new model for describing reservoir impairments due to suspension transport by injection water.

The critical settling velocity of the suspended particulates is determined and used to create a condition at which particle settling will occur, dependent on its size. The particle settling velocity as obtained from Stokes law for laminar flow (N_{Re}<<1), is compared to this critical settling velocity, which is a function of the residence time of the particles, to obtain the optimum transported particle size profile in the formation. The average size of transportable particulates and their total volumes are then obtained and used to determine the volume of deposits; this is in turn used to develop a new injectivity decline model for predicting permeability impairment due to the deposition of suspended solids. Model development was done considering linear flow with microscopic displacement and radial flow geometry accounting for the change in Darcy velocity with distance from the well.

The resulting models are validated by analyzing reported datasets from two injectors completed in the same deepwater reservoir, offshore Niger Delta. With the model parameters obtained from history-matching these two injectors, the historic injectivity performance of a third injector, completed in another reservoir in the same field, is then re-constructed in a predictive mode. Overall, the results are reasonable as the impairment model rationalized available field data sets satisfactorily. Furthermore, sensitivity analysis is performed, highlighting the robustness of the models against the typical range of uncertainties in some process and reservoir variables. The developed models can be used for the following field applications: (1) quantification of formation damage; (2) optimized water treatment facilities design; (3) implementing an effective and safe back flush operation; and (4) studying the impact of formation damage on hydrocarbon recovery.
.

Acknowledgements

My unreserved gratitude goes to the Shell Petroleum Development Company of Nigeria for sponsoring my MSc in Petroleum Engineering course at Imperial College London.

I will like to thank my college supervisor Prof. Martin Blunt whose objective criticism and prompt feedback was excellent and molded the analysis to the heights it attained. To my industry supervisors, Fidelis Tendo and Kazeem A. Lawal, words cannot express how grateful I am for the technical assistance you provided out of your tight schedule throughout the project. Your directions and advice guided me and were highly instrumental to the success of this project.

I will not fail to acknowledge all those that contributed via advice and encouraging words such as Marshal Wigwe, Tega Uvieghara, Oluwaseun Smith, Jennifer Aigbogun, Peter Mogbolu, Idris Olatunji, Oluseye Ogunsina, Leo-Andrew Adoghe and many others too numerous to mention. I remain truly grateful.

Finally, I will like to acknowledge and remain forever grateful to my sisters: Sophia, Laura and Deborah for your love, endurance, encouragement and support throughout a very adventurous and challenging year of my life.

Dedication

I dedicate this thesis to the Almighty God who has brought me this far and my parents Pastor Samuel Dambani and Mrs. Florence Dambani whose un-lingering support made me whom I am today.

Table of Contents

LIST OF FIGURES

Figures in Main Body

Figures in Appendix:

LIST OF TABLES

Tables in main body

Tables in appendix

MSc in Petroleum Engineering 2012-2013

Imperial College London

Analysis of Injectivity Decline in Some Deepwater Water Injectors

Samuel Legborsi Dambani

Imperial College supervisor: Prof. Martin Blunt

Industry supervisors: Fidelis Tendo and Kazeem A. Lawal, SNEPCo, Lagos.

Abstract

The challenges and risks relating to injectivity decline due to injection of particulate-laden water are well documented in the petroleum industry and elsewhere. Although different theories have been advanced to rationalize this problem, the modeling aspects remain largely unresolved, putting huge investments at risk. By combining the fractional-flow and deep-bed filtration theories, this work formulates a new model for describing reservoir impairments due to suspension transport by injection water.

The critical settling velocity of the suspended particulates is determined and used to create a condition at which particle settling will occur, dependent on its size. The particle settling velocity as obtained from Stokes law for laminar flow (N_{Re}<<1), is compared to this critical settling velocity, which is a function of the residence time of the particles, to obtain the optimum transported particle size profile in the formation. The average size of transportable particulates and their total volumes are then obtained and used to determine the volume of deposits; this is in turn used to develop a new injectivity decline model for predicting permeability impairment due to the deposition of suspended solids. Model development was done considering linear flow with microscopic displacement and radial flow geometry accounting for the change in Darcy velocity with distance from the well.

The resulting models are validated by analyzing reported datasets from two injectors completed in the same deepwater reservoir, offshore Niger Delta. With the model parameters obtained from history-matching these two injectors, the historic injectivity performance of a third injector, completed in another reservoir in the same field, is then re-constructed in a predictive mode. Overall, the results are reasonable as the impairment model rationalized available field data sets satisfactorily. Furthermore, sensitivity analysis is performed, highlighting the robustness of the models against the typical range of uncertainties in some process and reservoir variables. The developed models can be used for the following field applications: (1) quantification of formation damage; (2) optimized water treatment facilities design; (3) implementing an effective and safe back flush operation; and (4) studying the impact of formation damage on hydrocarbon recovery.

Introduction

The economics and success of deepwater developments in most parts of the world is mostly hinged on the performance of water injectors. Producers whose high rates are solely dependent on these injectors present their own management risk but the maintenance of injectors relative to producers is a major challenge in the oil and gas industry as over time their injectivity may decline as a result of different factors such as: the injection water quality (main cause of impairments due to suspended solids), and the temperature difference between the injected water and the reservoir fluids leading to precipitation of solids and several other factors.

The injected water is either produced water, fresh water or sea water; each of these sources comes with a certain measure of impurities which are either organic or inorganic. Injected seawater contains suspended particulates (sand) and salts which settle out or precipitate in the formation when it is injected if not properly treated. However, even when the water is well treated at the surface, its quality may deteriorate as it travels down hole and this may be owing to corrosion which depends on the water pH or a gain in solids as it flows through piping (David *et al*, 2003). These suspended particles can over time settle and fill-up the wellbore, plug the completion screens and formation pores leading to severe permeability impairment, loss of injectivity, most of all inadequate voidage replacement and low hydrocarbon recovery.

In order to mitigate this issue in the oil and gas industry, different on-line filters are employed to remove solids of defined sizes that might cause injectivity problems and in most cases a down-hole filter assembly is installed to further separate transported solids before the water gets to the down-hole sand control completion (Kumar, 1991; David *et al*, 2003). The finer the filtering, the more expensive and bulky the facilities required to implement it, especially in deepwater operations; hence, a balance has to be reached during water flood project planning between optimized reservoir performance and the economics of the required water treatment systems. For an optimized design of these filter systems, knowledge of the particle size distribution in the injected water is required and this can be used to carry out particle residence time analysis in the porous media to obtain an estimate of how long these particles stay in suspension in the formation before deposition.

Injectivity decline due to the transport of suspended particulates in the injected water is a well-documented problem, in the operation of water injectors, either for oil recovery or water disposal. This menace has been observed in fields all over the world, for instance, in the Gulf of Mexico, as recorded by (Sharma *et al*, 2000; David *et al*, 2003), where the high rate of decline experienced in the field was tied to the quality of the injected water. In order to address this problem, a number of mathematical models for rationalizing the permeability impairment induced by various solids invading the reservoir pore space have been developed. These models come in different forms with similar underlying theory going from phenomenological ones, that consider the suspended solid mass balance (Pang & Sharma, 1997; Bedrikovetsky *et al*., 2001) and its damage on well and reservoir, and through empirical models which are based on experience with a previous field or even historical data (Furtado *et al*, 2007). Two new models are developed: a deposited particle profile model to track the spatial and temporal size of deposited particles in the formation and a permeability impairment model to predict damage to the formation during a well's injection life in order to determine its performance. The developed models can be used for the following field applications: (1) analysis and prediction of injectivity performance of a well; (2) quantification of formation damage; (3) optimized water treatment facilities design; (4) implementing an effective and safe back flush operation; and (5) studying the impact of formation damage on hydrocarbon recovery.

Barkman & Davidson, (1972) introduced the first comprehensive theory for predicting the behaviour of injectors using a measure of the injected water quality called the water quality ratio as obtained from membrane filter test and core data. The half-life (the time it takes for the injection rate to reach 50% of its initial value) of an injector were estimated using four basic models: wellbore narrowing, particle invasion, wellbore fill-up, and perforation plugging, to predict how long an injector will be before the need of stimulation. The results obtained only applied to constant pressure processes and cannot be applied to process control considering rates. In another work, Davidson, (1979) pointed out that there is an inverse relationship between particle size and the velocity required to prevent particle deposition, hence drawing a relationship between the transportation of particles in the porous media and the linear flow velocity. This work did not take into account the combined effect of the concentration of particles and the particle/pore size ratio.

The depth of formation damage is fundamental in determining the impact of particle settling on a wells injectivity performance. Vetter *et al*, (1987) showed that particles with sizes ranging from 0.05 to 7 microns can cause formation damage. Particle filtration test was conducted and the observations made are summarized thus: (1) the penetration depth of a particle increases the higher its linear velocity gets. (2) Instantaneous formation damage is expected when larger particles are injected and the damage region is shallower (closer to the near-wellbore region of the injector). (3) Smaller particles in the submicron range cause gradual permeability decline.(Pang & Sharma, 1997)

Todd *et al*, (1984) observed in a series of experiments using aluminum oxide particles with size classes 0 to 3, 4 to 6, and 8 to 10 microns and cores that: (1) the mean pore throat size is key in determining the extent of the overall formation damage. (2) Particles in the range 0 to 3cause damage over the entire length of the core. (3) The larger the size of the particle, the closer to the injector well is the damage which tends towards the formation of an external filter cake (Pang & Sharma, 1997).

The results obtained from experiments, as highlighted above, were determined by performing core flood and membrane filter test experiments which have their limitations such that they do not incorporate the effect of change in velocity with distance and these cores form discrete parts of the reservoir. The deposited particle profile model does not only give an estimate of the distance where particles of different sizes will settle out in the formation, it also provides useful information on an optimized water quality specification for the field when coupled with the residence time (time it takes for particles to remain in suspension) of the particles in the injected water, thereby assisting in the design of an optimized water treatment facility. It incorporates radial flow and is sensitive to alteration in reservoir wettability, mobility of the water flood and other process variables. It can be applied to a well-reservoir system by just considering the relative permeability data set of the reservoir, the well geometry and the petrophysical properties of the injected and reservoir fluids and does not require any information from core flood test or data.

Pautz *et al*, (1989) used the formation permeability to estimate a minimum particle size that would contribute to permeability decline which supported the claims of the 1/3 to 1/7 rule-of-thumb from core flood test results. The 1/3 to 1/7 rule-of–thumb is the bridging phenomenon of the formation that uses the particle to pore size ratio to determine the mechanism of impairment (external filter cake or internal filter cake formation). From the analysis, particles with diameter greater than 33% of the pore throat diameter are external filter cake threats while those with diameter within 14% to 33% can induce the formation of internal filter cake in the porous medium. Studies implemented in the work of Bennion *et al*, (1994) suggest that plugging process is characterized by entrainment of larger particulates on the surface of the formation interface directly at the wellbore, comprising an external filter cake. Furthermore, the smaller particulates invade deeper and can form internal filter cake which may be several centimetres or more from the wellbore. They went on to point out that internal filter cakes are more damaging owing to their relative inaccessibility by remedial techniques; hence, this reduces the efficiency of conventional mechanical or chemical stimulation treatments. The depositional particle profile model can be applied simultaneously with the 1/3 to 1/7 rule of thumb to determine regions away from the injector that are prone to internal filter cake formation.

Meanwhile, most of the existing phenomenological (Bedrikovetsky *et al*., 2001;Pang and Sharma, 1997) and empirical (Khatib, 1994; Oort *et al*, 1993) models for predicting injectivity decline do not consider the mobility of the carrier fluid. However, the models developed in this work capture the effect of mobility of the filtrate and the displaced hydrocarbon. This improvement stems from the application of the fractional-flow theory, which utilizes the relative-permeability dataset. Hence, the developed models account for the impacts of reservoir wettability and water mobility on formation damage. Furthermore, the existing phenomenological models (Bedrikovetsky *et al*., 2001;Pang and Sharma, 1997) only consider the mass balance equation of the flowing solids as:

$$\boldsymbol{\phi_m \frac{\partial C_s}{\partial t} + q_t(r)\frac{\partial C_s}{\partial r} = -\frac{\partial C_p}{\partial t}; \qquad \frac{\partial C_p}{\partial t} = \lambda q_t(r) C_s} \quad (1)$$

While equation 1 uses the advective velocity of the carrier fluid, the particle velocity is not represented explicitly. In other words, it uses the advective velocity of the carrier fluid as the representative mean particle velocity, thereby assigning the same velocity to solids of different sizes and shapes in the injected water (Bedrikovetsky *et al*, 2009). Usually, the velocity of the flowing particles is saturation-dependent (Blunt and Muggeridge, 2012). Earlier, Bedrikovetsky *et al,* (2009) emphasized that particles can move faster or slower than the carrier fluid and stated that the concentration front speed (ratio of fractional-flow to saturation, that is, F/S) for large particles tends to zero while smaller particles are characterised by higher speed.

Given the limitations of the existing phenomenological models, this study utilizes the saturation-dependent velocity of the suspended solids, enabling particles of different sizes to move at different speeds, governed by their constant plane of saturation at a given time and injection rate. This phenomenon allows these particles to settle out and accumulate at different points in the formation depending on their relative sizes. By applying the fractional-flow theory to estimate the residence time and critical settling velocities of the injected particles and comparing against their Stokes' settling velocity, the conditions for particle transportation, deposition and accumulation is evaluated (Appendix C).

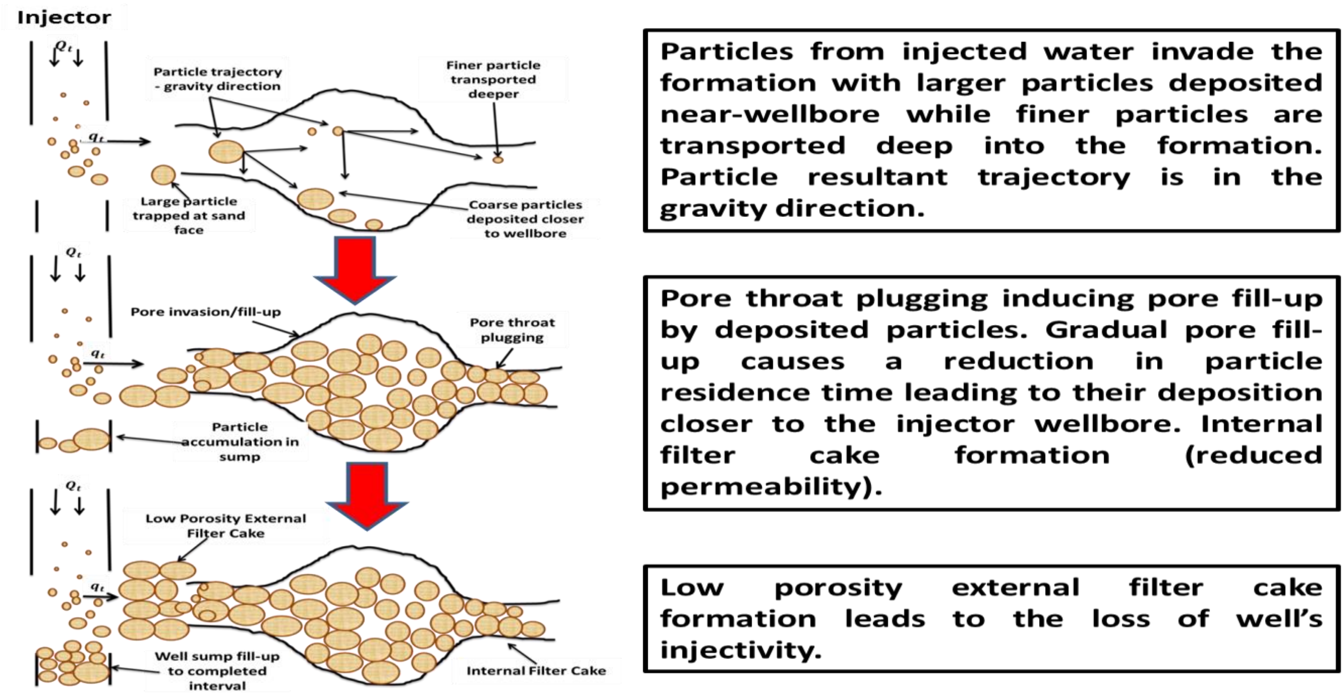

Figure 1: physical process of deposition and accumulation of particles in an isolated pore space and throat showing particle invasion in the formation inducing damage around the wellbore with a corresponding decline in the well's injectivity.

A new method of using Buckley Leverett fractional flow theory coupled with deep bed filtration theory to determine the amount of deposits in the porous media during production to quantify damage is presented in this paper. The proposed model which assumes non-reactive flow, tracks the spatial and temporal variation of deposit-size in the formation using the saturation dependent velocity of the particles at a given time during water flooding. The residence time of the particles in suspension, their critical settling velocity and Stokes' settling velocity are used to create conditions for particle deposition and transportation. Furthermore, a new injectivity decline model is developed considering both linear and radial flow geometry. The volume of deposition obtained during production, which is more significant at the near-wellbore region of the injector, is inputted in the newly developed permeability impairment model to predict the injectivity performance of different wells and to quantify formation damage. Model quality check is performed using sensitivity analysis to picture the impact of injection rate, formation permeability, wettability of the reservoir, viscosity (mobility of the filtrate) and quality of the injected water on the size of transportable particles and the resulting amount of deposits.

Figure 1 shows the physics behind the process of pore space invasion by particles smaller than the pore diameter. This physical process of particle invasion of a pore is modeled in this work. The main mechanisms of permeability impairment are the build-up of an internal filter cake due to deep bed filtration caused by pore space particle invasion (mainly by sub-micron particles) and the formation of an external filter cake (by larger particles trapped by the formation sand-face) as illustrated in figure 1which was prepared for this paper. The parameters that determine whether or not an internal or external filter cake is formed includes: the particle/pore size distribution, injected solids concentration, formation permeability, and fluid velocity (Pang & Sharma, 1997). It (figure 1) shows that over time the build-up of particles in the pore leads to pore throat blocking which initiates the formation of an internal filter cake that later emanates into the build-up of a low porosity external filter cake. This gradual increase in the amount of deposits in the formation near-wellbore, leads to a rise in bottom-hole pressure accompanied by a corresponding decrease in injection rate, hence, a decline in the well's injectivity.

The overall objective of this work is to evaluate/develop a suitable injectivity decline model for the prediction of permeability impairment for well-reservoir systems. As a case study, the developed models are employed to rationalize the performances of three unhealthy injectors in a deepwater field in the Niger Delta. The aim is to combine the fractional flow and deep-bed filtration theories to formulate a new model for describing permeability impairment caused by injection of particulate-laden water.

In conclusion, a recommendation is made on an optimum water treatment facility design in comparison to the effect of other remediation technique and field applications of the developed models are proffered. The questions to be answered by the developed models in the following analysis are: (1) are the injected particles transportable far away from the near-wellbore region of the injector? (2) Considering the fact that the reservoir is unconsolidated and deposited in a turbidite environment with out-of-plane fracture propagation and loose sand, silt and clay grains near-wellbore; are these loose grains contributing to the general permeability impairment recorded in the field? Also, are these loose formation grains transportable at the given rate of injection? (3) If they are not transportable, what is the main mechanism of capture? (4) How effective are remediation techniques currently or previously used on the injectors? Finally, what is an optimized remediation scheme for the field? An attempt will be made to answer all these questions and more in the following sections.

Research Methodology

The methods used to carry out the required analysis involved the development of new models representative of the physics of the process of particle capture and deposition (figure 1) which lead to the implementation of numerical experiments on the application of the developed models and to generate findings on possible areas that could enhance the understanding of the main mechanism responsible for severe permeability impairment in the field. The new methods formulated are listed below:

1. Two mathematical models are developed applying Buckley Leverett fractional flow theory coupled with deep bet filtration theory to track the transported/deposited particles in the porous media and predict permeability impairment. Both linear and radial flow geometry realizations of the models were used for analysis
2. Relative permeability data sets were generated considering an oil-wet and water-wet reservoir using the Corey correlation. They are used to perform sensitivity analysis on the model to capture its response to changes in reservoir properties and some process variables.
3. Diagnostic test using pressure fall off (PFO) analysis, Halls integral and derivative, and pressure-rate plots were used to check wells for pore space and fracture face plugging (appendix F).
4. The particle to pore size ratio and residence time of the injected particles were both combined and used to determine the main mechanism of impairment in order to obtain an estimate of the time when different particles from the injected seawater will settle out.
5. Models were validated using pressure-rate data sets from two injectors (A-2 and A-3) drilled in the same reservoir.
6. The developed permeability impairment model was then used as a predicting tool to evaluate the Injectivity performance of another injector.
7. Important field applications of the developed models are proffered at the end of the analysis.

Model Development

The dynamics of suspended particles flow in water injected into the porous medium is being developed. This is done to track the spatial and temporal variation of deposit size in the formation during production. The concept of particle residence time is used to determine the critical settling velocity of the particles in the suspension which when compared to their Stokes' settling velocity creates a condition for transportation. The developed model will provide information of the average size of particles that can be transported by the water flood at a given injection rate, time and point in the formation away from the injector. It uses ideas from the formation of sediments in a river or sea and applies this to the porous medium such that at a given injection rate particles are deposited at distances away from the injector sorting according to their respective sizes with coarser particles deposited closer to the high energy environment of the injector while finer particles are transported deeper into the formation (figure 3. The residence time in this case is the average time it takes a particle to remain in suspension during injection while the critical settling velocity is the minimum velocity required for particles to be transported, hence particles with Stokes' settling velocity equal to or greater than the critical settling velocity will get deposited in the formation (Stabel, 1986).

Model Assumptions

1. Model considers non-reactive flow, that is, the transported particles do not react or form solutions with the filtrate and mechanically induced damage is the main damage mechanism which involves: injection of solids and velocity induced damage (fines migration and settling) mainly for an unconsolidated reservoir (Bennion *et al*, 1994). Damage caused by scales, asphaltenes and wax is not considered.
2. The main mechanism of particle deposition is sedimentation, the effects of other mechanism of capture are not considered. The particles flowing in the streamline of the carrier liquid tend to move in the gravity direction according to Stokes' law. The gravity force acts upwards for light particles and downwards for heavier particles (Civan, 2007).
3. Assumes steady state conditions and Newtonian fluid flow, that is, the solid particles flows along a streamline (Laminar flow) unless acted upon by an unbalancing force.
4. The physics of particle invasion and deposition in the pore space and throat, using fractional flow theory coupled with deep bed filtration theory, is developed, therefore, the sizes of particles invading the formation is assumed to have a diameter smaller than the pore spaces and throats diameter of the formation otherwise the build-up of an external filter

cake (caused by the accumulation of larger particles at the sand face) will occur from the start of injection. This is illustrated in figure 1.

5. Injected particles are assumed to be spherical in shape to simplify the model.
6. The tortuosity (τ) of the formation was assumed to be unity.

.

Deposited Particle Profile Model

Figure 2(a) illustrates an injector injecting through its completed interval into the porous medium. As injection of water begins, flow tends to be radial away from the injector (figure 2 (b)) and this implies that the velocity of the water flood will vary with distance and decreases as the water progresses away from the injector wellbore which encourages the deposition of particles in the porous medium. In order to account for this phenomenon, the radial flow equation was adapted to Buckley-Leverett fractional flow equation as explained in this section. Consider a particle of a specific size flowing in an isolated pore space and throat, in the porous medium, the particle moves on a constant plane of water saturation as illustrated in figure 3(a) and its trajectory as it is transported is always in the gravity direction owing to the density difference between the carrier fluid (water) and that of the particle as shown in figure 3(b). This implies that at a point and time in the formation, it will get deposited and as injection time increases more particles will get deposited (accumulation) initiating the build-up of a damaged zone around the injector which induces the gradual decline in its injectivity (as illustrated in figure 1). The details of the derivation and steps applied to obtain the depositional particle profile model are discussed in appendix C.

Buckley Leverett fractional flow theory was applied considering the mass balance equation of the filtrate flowing through a differential element as shown in figure 2(b). It was used to obtain the distance of a constant plane of saturation away from the injector, the particle speed and its residence time.

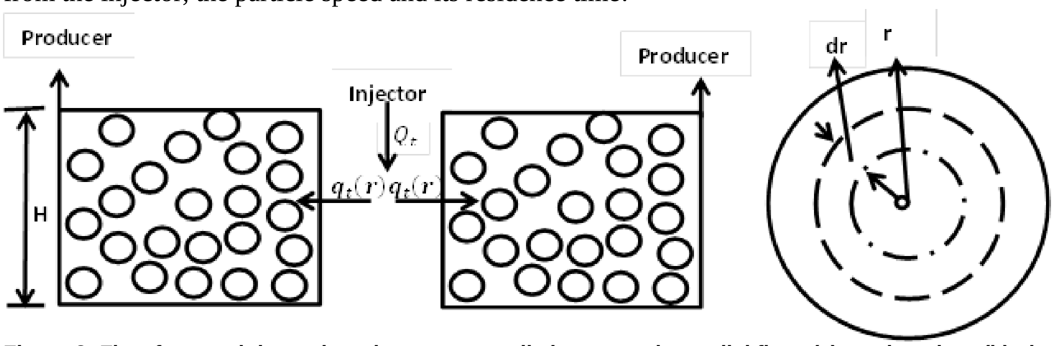

Figure 2: Flow from an injector into the porous media incorporating radial flow: (a) section view, (b) plan view depicting radial flow.

Equation 2 below gives the distance of a constant plane of saturation at any time in the porous medium. Figure 3(a) is a plot of water saturation profile in the formation with distance and also shows different particles flowing on these different planes of saturation.

$$\boldsymbol{r(S_w)} = \sqrt{\frac{Q_t t}{\pi H \phi}\left[\frac{dF_w}{dS_w}\right]_{S_{wx}} + r_w^2} \tag{2}$$

The speed of a particle transported by the flood as a function of the saturation it is flowing in is represented by:

$$\boldsymbol{v} = \frac{Q_t}{2\pi r H \phi}\left[\frac{F_w}{S_w}\right]_{S_{wx}} \tag{3}$$

F_W/S_W is the particles' dimensionless speed in water as obtained from fractional flow theory. It gives the real speed of the particle as it is transported on a constant plain of saturation (figure 3a). Existing models that use the mass balance of the flowing solids assume that the velocity of the solids are equal to the advective velocity of the flood, that is assuming same velocity for all suspended solids which does not tally with reality. The distance of a particle at any instance of time can also be represented by the distance of the saturation stream it is being transported. Therefore, the residence time of the particle as a function of this saturation distance is given by (refer to appendix C for the mathematical details):

$$\boldsymbol{t_c} = \frac{V_{container}}{Q_t} = \frac{\pi[r(S_w)^2 - r_w^2]H\phi}{Q_t}\left[\frac{S_w}{F_w}\right]_{S_{wx}} \tag{4}$$

A pore space or throat in the formation is considered with a particle of a particular size (*Dpi*) and shape flowing through it along a streamline as shown in figure 3(b); the conditions for the particle to settle within the pore space are:

1. Its Stokes' settling velocity must be equal to or greater than the critical settling velocity.
2. It must have traveled through an average vertical distance approximating to the pore radius within a time equal to the residence time in the pore volume.
3. The diameter of the particle must be less than the pore diameter to allow penetration.

The Stokes equation for particle settling velocity for laminar flow ($N_{Re} \ll 1$) is given by:

$$\boldsymbol{v_s} = \frac{g(\rho_s - \rho_l){D_p}^2}{18\mu} \tag{5}$$

This equation accounts mainly for the settling velocity of a particle falling through a still fluid (Cheel *et al*, 2005). Therefore, for a dynamic fluid, in other for particle settling to take place, its Stokes' settling velocity (v_s) has to be greater than the minimum velocity required for its transport which is given by the particles critical settling velocity (v_c) (figure 3b). With this noted a condition for particle transport was developed to determine the transportable particle size of the water flood at any given injection rate and time.

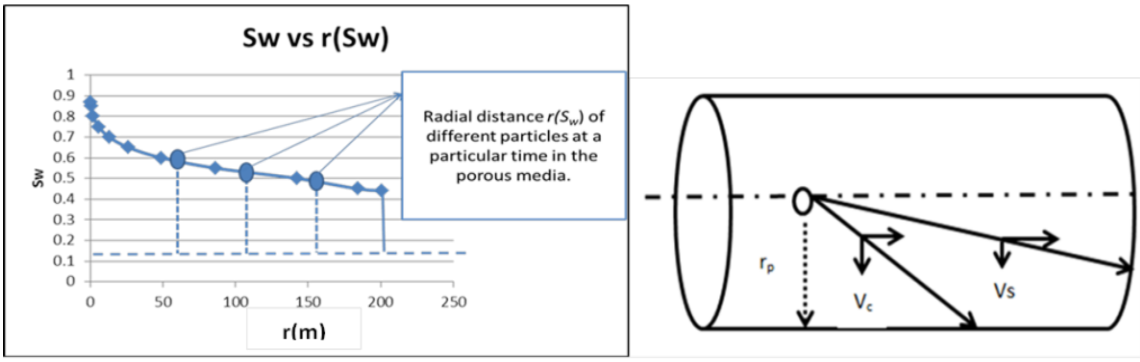

Figure 3: (a) A plot of water saturation against radial distance showing particles flowing on a constant plane of saturation. (b) an isolated pore space in the formation showing a suspended particles trajectory in the formation.

To prevent particle settling: $v_s < v_c$ and for particle to be deposited: $v_s = v_c$ (Stabel, 1986; Coulson and Richardson, 2002). It is worth emphasizing that the resultant trajectory of the particle along the streamline is always inclined downwards in the gravity direction as it is transported (figure 3b); this is due to the influence of gravity and the density difference between the particle and the filtrate. The particle therefore has a critical settling velocity equaling:

$$v_c = \frac{r_p}{t_c} \tag{6}$$

The mean hydraulic tube diameter of the formation as given by Carman-Kozeny equation (Civan, 2007) is:

$$D_h = 4\sqrt{2\tau}\sqrt{\frac{k_0}{\phi_0}} \tag{7}$$

τ is the tortuosity of the formation. The mean radius of the pore and the particles residence time is substituted into equation 6 to obtain the particles critical settling velocity.

$$v_c = \frac{Q_t}{\pi[r(S_w)^2 - r_w^2]H\phi_0}\left[\frac{F_w}{S_w}\right]_{S_{wx}}\sqrt{\frac{8k_0}{\phi_0}} \tag{8}$$

Therefore in order to satisfy particle transport, equation 5 and 8 are equated ($v_s < v_c$) as shown below:

$$\frac{g(\rho_s - \rho_l)D_p{}^2}{18\mu} < \frac{Q_t}{\pi[r(S_w)^2 - r_w^2]H\phi_0}\left[\frac{F_w}{S_w}\right]_{S_{wx}}\sqrt{\frac{8k_0}{\phi_0}} \tag{9}$$

$$D_p < \sqrt{\frac{18Q_t\mu}{\pi\phi_0[r(S_w)^2 - r_w^2](\rho_s - \rho_l)gH}\left[\frac{F_w}{S_w}\right]_{S_{wx}}\sqrt{\frac{8k_0}{\phi_0}}} \tag{10}$$

This equation gives the transportable particle size. Therefore the diameter of deposited particles for radial flow geometry can be obtained thus:

$$D_{pc} = \sqrt{\frac{18Q_t\mu}{\pi\phi_0[r(S_w)^2 - r_w^2](\rho_s - \rho_l)gH}\left[\frac{F_w}{S_w}\right]_{S_{wx}}\sqrt{\frac{8k_0}{\phi_0}}} \tag{11}$$

Equation 11 is the deposited particle profile model that tracks both the spatial and temporal size of deposits during injection of particulate laden water. Figure 4(a) gives the plot of deposited particle diameter against distance as obtained using equation 11. From this plot, a gradual decrease in the deposited particle size with distance away from the injector is observed. The curve ($D_p = D_{pc}$) represents the diameter of particles deposited with time along the path of flow of the flood away from the injectors wellbore. Particles with diameter that fall above this curve cannot be transported by the flood while those with diameter below are transportable. The area below this curve represents the average transportable particle size and can be used to determine the damage volume near-wellbore of the injector during water flood. This model mimics what happens in the sediment size distribution over a shoreline profile as illustrated in figure 4(b) where particles get finer with distance away from the shore. Figure 4(a) confirms that finer particles are deposited deep in the formation away from the high energy environment of the injector well while coarser particles are deposited at the immediate vicinity of the well thereby occupying larger pore space and inducing greater damage; this implies that, high level of impairment is expected close to the near-wellbore region of the injector if the injected water has high concentration of these large solid particulates at declining rates of injection. The realizations from the linear flow model development and model sensitivity analysis to ascertain the robustness of the developed models to typical range of uncertainties in some process and reservoir variables is explained in Appendix C.

A regression curve was fit to the plot of diameter of particles against distance and the realized data points followed a general function in both linear and radial realizations given by:

$$D_p(r) = ar^{-N} \tag{12}$$

Therefore, a power-law distribution (equation 12) of particle size with distance was adopted. “a” and “N” are variables that are obtained from fractional flow analysis. The major drivers of the parameters “a” and “N” will be investigated in the section dealing with model sensitivities. Figure 5 shows different snapshots of the flood front with respective deposited particle profile and confirms that Buckley Leverett fractional flow theory can be used to track the deposited particle profile with time in the porous media. An observation from this figure is that the transport capacity of the flood reduces and finer particles are deposited as the water front moves away from the injector through the porous medium. This drop in transport capacity of the flood as injection time increases is signified by the maximum particle size transported by the flood for each snapshot taken at 50, 100, 160 and 223days which is 8, 5.5, 4.5 and 3.8µm respectively. One of the questions that arise is: how can the change in pore radius, represented by porosity and permeability over time and distance are tracked? This question will be answered in the next section.

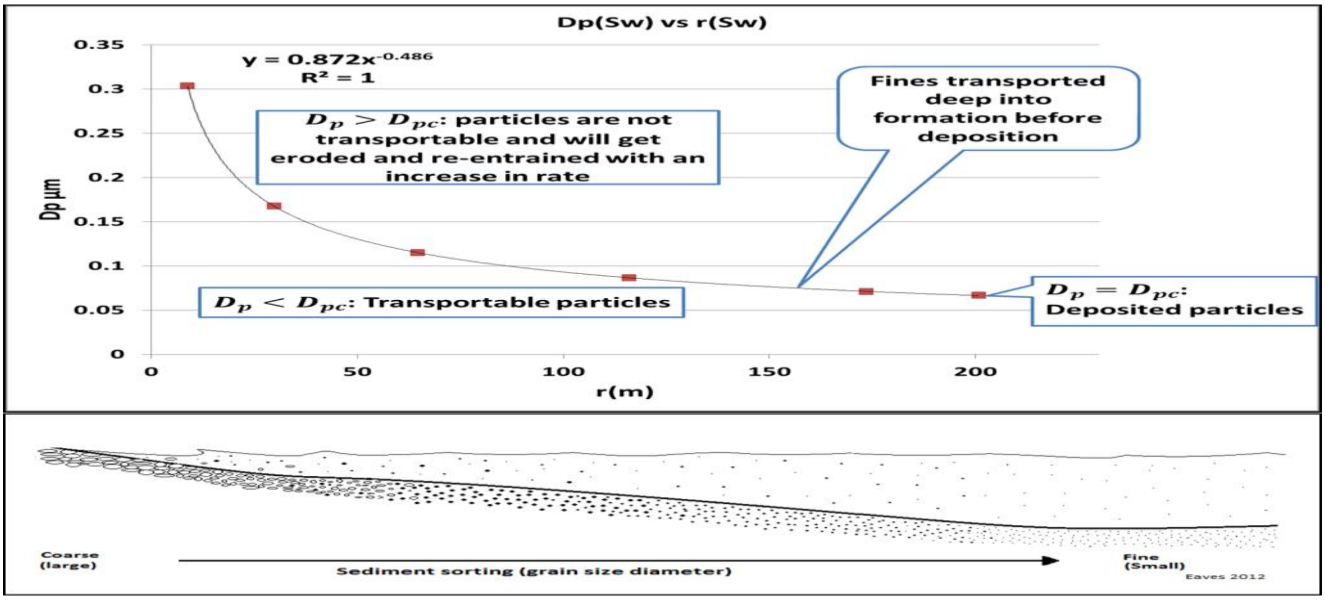

Figure 4: (a) a plot of Deposited/transported particles diameter with distance. (b) Offshore shoreline profile of sediments assuming this mechanism applies in the porous media (below) - (culled from: Eaves, 2012).

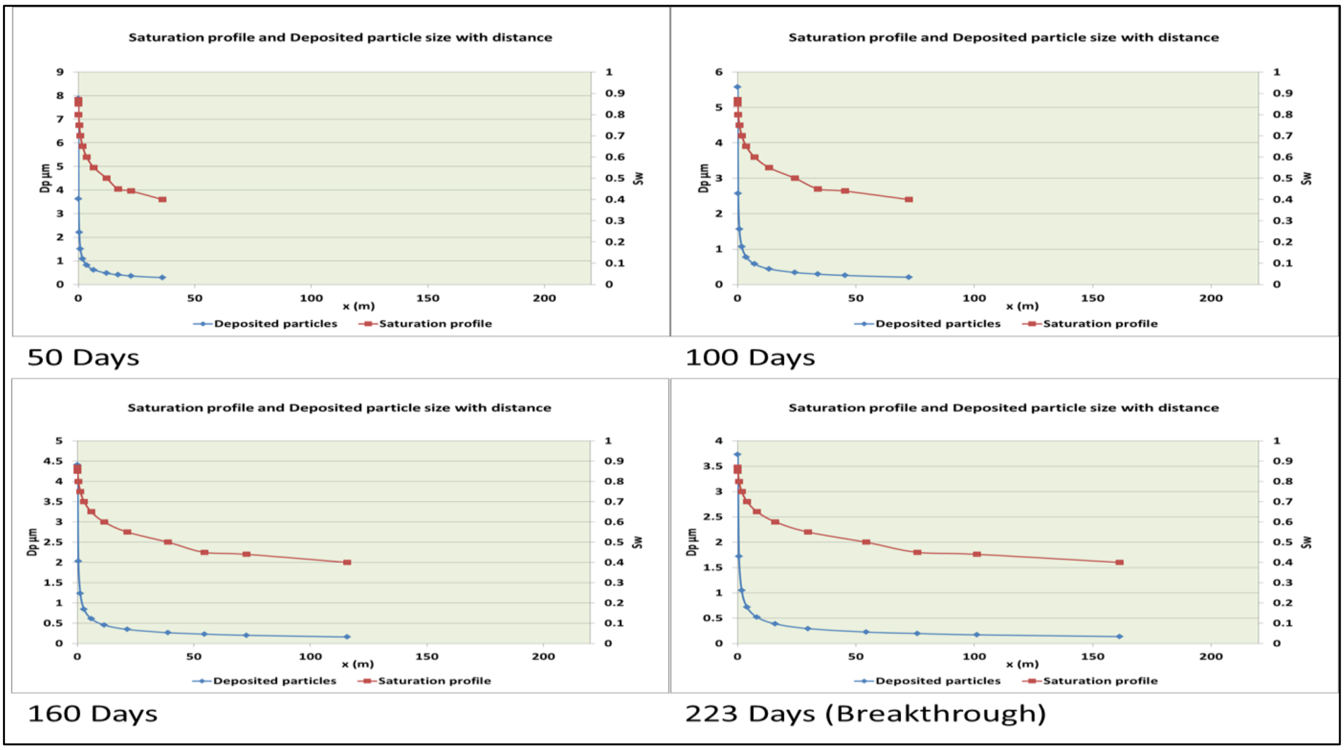

Figure 5: snapshot of the flood front and deposited particles profile with time: (a) 50days (b) 100days (c) 160days (d) 223days.

Injectivity Decline Model Development

The aim of this model is to capture the impact of the accumulation of deposited particles over time in the porous media on the porosity and permeability of the formation which in turn has a great impact on the injectivity performance of an injector. The model assumes the following: (1) the main mechanism of particle deposition is sedimentation and does not consider the effect of particle erosion and re-entrainment due to increased interstitial velocity. (2) The flow of particles in the flood is laminar (N_{Re}<<1). (3) Injected particles are spherical. It incorporates radial flow away from the well in which the Darcy's velocity (q_t) varies with distance. Figure 6(c) below shows the damage porosity contained in a pore, damage in this context refers to the fraction of the pore-space occupied by deposited particles. Once decline in injection commences, particle deposition increases at a higher rate owing to the reduction in pore radius (reduced particle residence time) which leaves a very small fraction of the pore space available for particle transport (reduced permeability). This room left for particle transport is the remaining porosity and it is expected that the smaller the pore radius the lower the volume of particles transported.

From the profile of particles deposited with distance shown in figure 6(a), for the sake of emphasis, it can be inferred that due to the deposition of coarser particles near-wellbore, the volume of deposits at this region will be higher compared to that away from the immediate vicinity of the injector (where the volume is insignificant relative to the near-wellbore damage) and this damage volume/porosity reduces the formation permeability near-wellbore which has a very high impact on the injectivity of the well. The impact of this damage on a wells' injectivity depends on the particle/pore size distribution, the concentration of injected particles, injection rate and the reservoir characteristics (initial formation permeability). It is expected that a well injecting into a low permeability reservoir at high rates with high solid contents will require more work-overs than one injecting into a high permeability reservoir (Furtado *et al*, 2007).

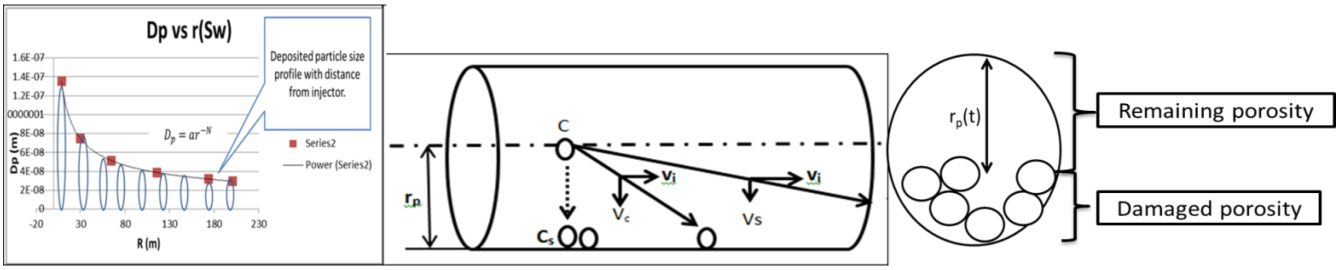

Figure 6: (a) power-law distribution of deposited particles showing the size profile with distance (b) accumulation of deposits in the pore throat (c) pore radius showing damaged porosity occupied by deposits and the remaining porosity available to flow.

In this analysis, the volume of transported particles is obtained using fractional flow theory and it is subtracted from the volume of injected particulates to obtain the volume of deposits in the pores which is used to obtain the damage porosity for later input into an impairment model to quantify formation damage and predict injectivity decline. Details of the mathematical principles, concepts and theories adopted to obtain the developed permeability impairment model are explained in appendix C.

The average transportable particle size at any given time and injection rate can be obtained from the area under the curve in figure 6a and it is given by:

$$\overline{D_p} = \frac{a}{(1-N)[r(S_{wf})-r_w]}\left[r(S_{wf})^{1-N} - r_w^{1-N}\right] \quad ; \qquad For\ r(S_w) \neq r_w \tag{13}$$

In order to obtain the volume of transportable particles, the area occupied by the transported particles flowing in a pore space is determined. A power-law distribution was also adopted to represent the area of transported particles, assuming spherical particles, as a function of radial distance as explained in appendix C. This function, when integrated with respect to distance gives the volume of transportable particles for a given number of pore volumes of water injected.

$$V''_{trans} = \left\{\frac{\alpha}{1-\beta}\right\}\left[r(S_{wf})^{1-\beta} - r_w^{1-\beta}\right] \tag{14}$$

Equation 14 above is the volume of transported particles for a given number of pore volumes of water injected. In order to obtain the transported volume in field scale, an upscale was implemented as explained in appendix C to determine the total volume of transportable particles by the flood at any instance of time. Equation 15 below is the realized volume:

$$V_{trans} = \frac{\pi r_e^2 H\phi_o}{W_{id}}\left\{\frac{\alpha}{1-\beta}\right\}\left[r(S_{wf})^{1-\beta} - r_w^{1-\beta}\right] \tag{15}$$

The volume of injected particles is given by: $V_{pinj} = CQ_t tB_w = CW_{inj}$ **(16)**

The total volume of deposited particulates can then be obtained as:

$$V_{dep} = CQ_t tB_w - \frac{\pi r_e^2 H\phi_o}{W_{id}}\left\{\frac{\alpha}{1-\beta}\right\}\left[r(S_{wf})^{1-\beta} - r_w^{1-\beta}\right] \tag{17}$$

The porosity impairment model (equation C-55) is used to obtain the permeability impairment model by applying the porosity-permeability power-law correlation (equation C-56) as discussed in appendix C**.** Therefore, the permeability impairment model due to deposition of suspended particulates can be represented thus:

$$\frac{k_{rem}}{k_o} = \left(1 - \frac{1}{\phi_o \pi r_e^2 H}\left(CQ_t tB_w - \frac{\pi r_e^2 H\phi_o}{W_{id}}\left\{\frac{\alpha}{1-\beta}\right\}\left[r(S_{wf})^{1-\beta} - r_w^{1-\beta}\right]\right)\right)^n \tag{18}$$

This model (Equation 18) will be validated by history matching to field data, sensitivity analysis will be implemented to ascertain its robustness to uncertainties in reservoir and process variables, and it will then be used as a predicting tool to forecast the expected injectivity of an injector in the subject field.

Model Sensitivity Analysis

A model sensitivity study is performed to find the major drivers of the parameters "a" and "N" in the adopted power-law distribution function of the deposited particle profile model (equation 12). In order to determine this, the response of the model to alterations in reservoir wettability, time, injection rate, particle size, viscosity of the filtrate, and formation permeability was critically studied. This was implemented using the linear flow model realizations (Appendix C).

Sensitivity to Reservoir Wettability and Viscosity of Filtrate (Water)

The effect of reservoir wettability was investigated by generating relative permeability data sets representing a water wet reservoir and an oil wet reservoir using Corey's correlation with assumed Corey's coefficient and end point parameters. The viscosity of the filtrate (water) was varied in both water wet and oil wet case to capture the effect of fluid mobility on the solid carrying capacity of the flood. A summary of the parameters used for the sensitivity, equations, the assumed parameters and results obtained are given in appendix C.

Table 1 summarizes the observations. It can be observed that the mobility of the filtrate in the oil wet system is higher than that of the water wet system; this higher mobility of the water makes its solid carrying capacity high. Physically, in an oil-wet reservoir the water occupies larger pores than the oil ($k_{rw}\ \alpha\ water\ flow\ \alpha\ A_w{}^2$). Larger particles are transported by the water flood in the oil wet reservoir and deposited deep in the porous medium; this can be seen in the value of maximum deposited particle (Dp_{max}) given by 16.3 and 0.7µm for oil and water wet cases respectively when the viscosity of water was set at $1 \times 10^{-3} Nm^{-2}.s$. It can also be observed that an increase in the water viscosity from $0.5\times 10^{-3}\ to\ 1 \times 10^{-3} Nm^{-2}.s$ lead to a corresponding increase in the size of deposited particles in both oil and water wet reservoirs. This increase was from 6.4 to 16.3µm in the oil wet case. This confirms that larger particles will be transported by a highly viscous fluid because the higher the viscosity, the lower the particle settling velocity and the longer the residence time of the particle. A reduction in viscosity of the injected water, could be caused by an increase in its temperature as it migrates into the reservoir causing a corresponding decrease in the residence time (t_c) of transported particles; this leads to their early deposition at the near-wellbore region of the injector and over time could result in severe permeability impairment.

Table 1: Summary of results from the wettability and viscosity sensitivity analysis.

Parameters	Water wet	Oil wet	Water wet	Oil wet
Mobility (M)	1.2	4.25	2.94	10.6
Vwf	1.74	2.62	1.88	3.4
tbt (days)	435	289	403	223
µo (cp)	1	1	5	5
µw (cp)	0.5	0.5	1	1
Dpmax (µm)	**0.3**	**6.4**	**0.7**	**16.3**
Swf	0.78	0.44	0.73	0.35
Fwf	0.92	0.76	0.9	0.68
(Fw/Sw)max	1.23	1.89	1.29	2.05

Table 2: summary of well parameters

Parameters	A-1	A-2	A-3
Wellbore Radius (m)	0.15	0.15	0.15
Drainage Radius (m)	450	450	450
Perforation Height (m)	23.8	14	14.6
Net-to.gross	79	90	86
Particle Concentration (ppm)	28	28	28
Completion	F&P	F&P	F&P
Current Injection Regime	Fracture	Fracture	Fracture
Sump (mah)	67	425	-
Reservoir	A	B	B

Sensitivity to Time and Injection Rate

In appendix C it is shown that the parameters "a" and "N" (equation 12) remain constant with time as long as the injection rate is constant. An increase in injection time only effects the transportation of more fines deep into the porous media towards the producer while larger or coarse particles are dropped close to the near-wellbore region of the injector. Figure 7a shows that the higher the injection rate, the larger is the amount of transportable particles and size of deposited particles (reflected by the movement of the curve upwards or the increase in area below the curve), also, the deeper into the formation is a particle of a given size (Dp_i) transported at a particular time. Change in rate only affects the value of "a", "N" remains constant as observed. Also, it can be inferred that particles deposited when the flow rate was $143\ m^3/day$ becomes eroded and re-entrained by the flood with an increase in injection rate to$318\ m^3/day$. Furthermore, figure 7b is a plot of the particle dimensionless speed against its diameter; it confirms that the transportable particles moving at a particular speed becomes smaller in size with time increase. This further explains the fact that larger particles are dropped while finer particles, which move at higher speed (Bedrikovetsky *et al*, 2009), are transported deep into the formation by the flood as it moves through the porous medium.

As observed from the model sensitivity analysis in appendix C, the parameters: "a" and "N" (equation 12) are only affected by a change in viscosity of the filtrate and wettability of the reservoir. This could be due to the impact of viscosity on fluid mobility. Model sensitivity to formation permeability and residence time of the particle are discussed in appendix C and it was observed from the analysis that there will be an increase in the transport capacity of the flood with particle re-entrainment and transportation deeper into the formation at increased rate and at higher initial formation permeability.

Field Case Study

Pressure-rate history data sets for three (3) injectors were used for analysis, two of which (A-2 and A-3) were drilled in the same reservoir (B) while a third was drilled in another reservoir in the same field which is at 1000m water depth, offshore Niger Delta and deposited in a turbidite environment. Appraisal of the field and the data sets for the analysis are discussed in appendix E. The injectors of concern are frac-packed wells in which proppant filled fractures are used in their completion. They are completed in the oil bearing column of the formation with no underlying aquifer. Table 2 gives a summary of the well parameters used for analysis. Diagnostic analysis to ascertain the cause of injectivity decline in the ailing wells is discussed in appendix F as all the wells analyzed showed severe plugging throughout their injection history. Furthermore, these data sets will be used in the validation of the developed models and in illustrating field applications in subsequent sections.

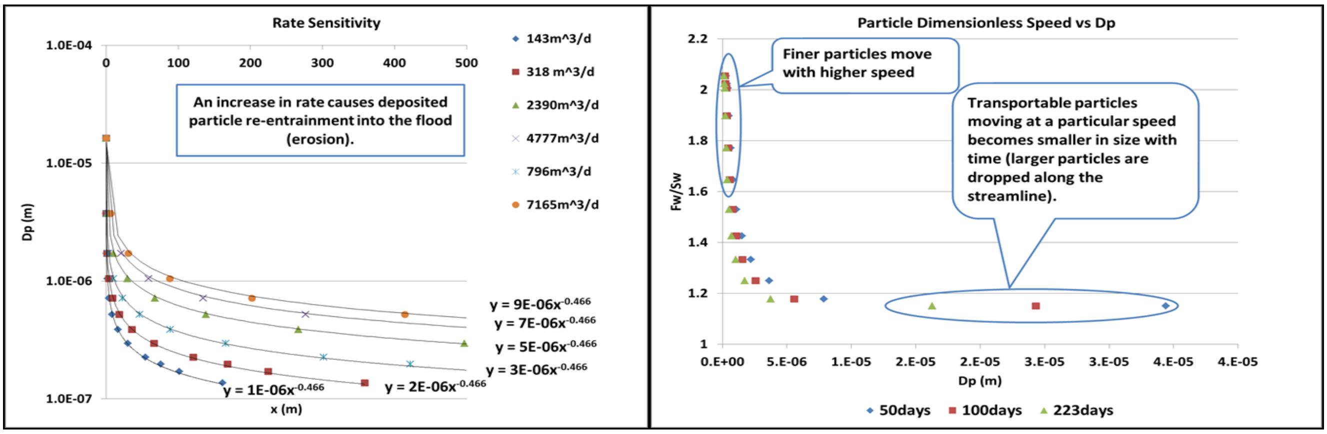

Figure 7: (a) model sensitivity to injection rate; (b) a plot of the particles dimensionless speed against diameter indicating that particles moving at a particular speed become smaller with time increase, larger particles are dropped.

Model Validation and Determination of Empirical Parameter Ranges

The deposited particle profile model (Equation11) was applied to the field to determine where the various sizes of injected particles will settle out, both the linear and radial flow realizations were used for this analysis. Field realized relative – permeability datasets: rock curve and the upscaled pseudo-curve are applied. These relative permeability curves which were generated using different Corey parameters to capture the effects of uncertainties in the extent of reservoir wettability and fluid mobility are shown in appendix D with a detailed explanation of the new methodologies applied to validate the models. A new method for determining the volume filtration coefficient of the formation is also introduced in appendix D.

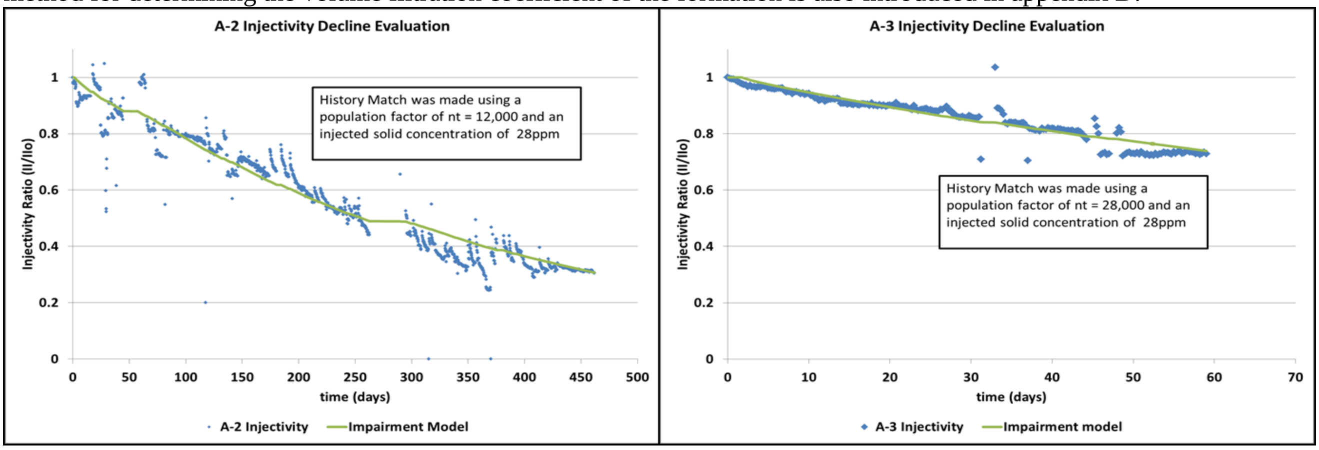

Figure 8: Validation of impairment model: (a) with first decline period of well A-2. (b) Validation of impairment model with first decline period of well A-3.

In order to validate the impairment model using well A-2 and A-3, the first decline period of both wells are selected and used for analysis. From the plot of injectivity against time, of the different wells it was observed that trend lines fit to all the decline period of the wells (A-1, A-2, and A-3) are parallel and this suggest that the same mechanism of impairment is responsible for damage recorded in the field. Figure 8(a) and (b) below shows the history match of the impairment model to the first decline period of well A-2 and A-3 respectively and table 3 gives a summary of the fitting parameter used for matching the model. The matched "*re*" values represent the effective damage radius of the wells.

Figure 9 (a) and (b) is a plot of the average transportable particle size (equation 13) against time for well A-2 and A-3 respectively. It can be observed that the transport capacity of the flood in well A-2 is higher than that in well A-3 which is clearly indicated by maximum particle size which the flood carries at the beginning of the selected decline period of about 12µm and 4.5µm respectively. This implies that if particles greater than 4µm which are not transportable by the flood at the given rate of injection are present in the injection water or are present as loose grains in the formation, they will be deposited either in the wellbore (wellbore fill-up) or trapped by the sand-face of the formation triggering rapid decline in injectivity. This low transport capacity which can be tied to the lower injection rate of this well (A-3), for the selected decline period, is also observed in the volume of transportable particles with well A-2 having a transport capacity of about $1.8mm^3$ while A-3 has a capacity of $1.4mm^3$at the beginning of the analyzed periods. In addition, figure 9(a) shows a period in which significant erosion and re-entrainment of particles into the flood, marked by an increase in the volume of transportable particulates, occurred between 350 to 400days. Figure 10(a) and (b) shows the field scale volume of transportable particles (equation 15) and deposits (equation 17) for both wells and illustrates that the initial transport capacity of the flood is very high, but this declines rapidly in less than 3days signifying severe plugging during this period and also points to the fact that a large concentration of transported particles are deposited in the formation within this period.

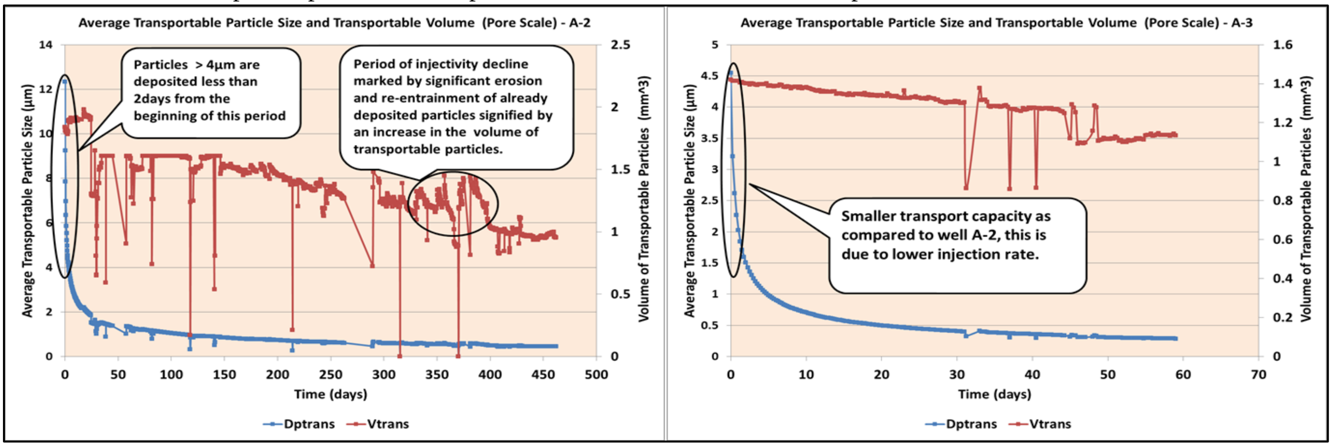

Figure 9: Average transportable particle size and volume of transported particles (pore scale): (a) for Well A-2. (b) For Well A-3.

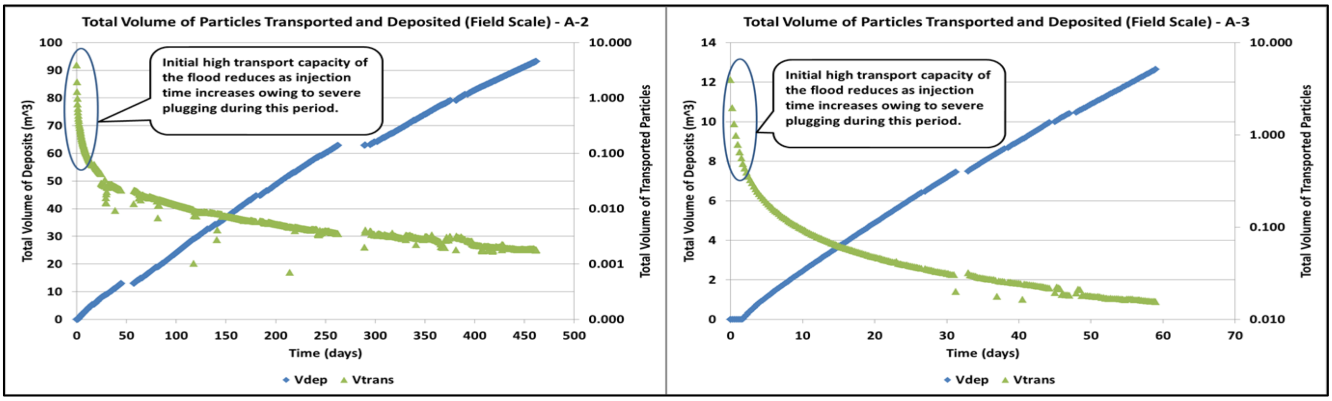

Figure 10: a plot showing the volume of deposits and transportable particles (upscaled): (a) for A-2. (b) For well A-3.

Impairment Model Sensitivity Analysis (Well A-2)

In this analysis, well A-2 with its matched parameter is used as a case study for sensitivity analysis of the impairment model. A faster rate of decline is observed in figure 11(a) when the value of initial porosity is smaller for a given decline period. This faster decline rate at smaller initial porosity is due to a decrease in the volume of transported particles through the porous medium as illustrated in figure 11(b). The impact of initial porosity on the volume of particles deposited is minimal as this is highly dependent on the concentration of injected particles. Also from figure 11(a), the expected half-life (time it takes the injectivity index of the injector to reach 50% of the initial value) of the injector is 130days, 190days, and 240days if the initial porosity at the start of the decline period is 0.18, 0.22, and 0.31 respectively. This can be used as a tool to predict the performance of an injector after a remediation operation has been carried out bearing in mind that the decline trend lines of these well-reservoir systems are parallel. Furthermore, this emphasizes the fact that the volume of particles transported in the formation decreases with time as porosity decreases due to the increase in the amount of deposits in the pore space.

Similarly, the concentration of injected particles was varied to investigate its impact on the injectivity of the wells. Figure 12(a) and (b) illustrates the effect of concentration of injected particles on injectivity and the volume of deposits accumulated over time. Decline in this case is caused by an increase in the concentration of deposits. The model suggest that for an injected solid concentration of 28ppm (the matched concentration), the injector half-life will be 250days and goes on to predict what the resulting decline rates would have been at higher and lower injected solids concentration. This implies that the half-life of the injector would have been 150days for a concentration of 54ppm and negligible for an injected particle concentration of 5ppm. Figure 12(b) shows an increase in the concentration of particles injected leads to a corresponding increase in the volume of deposits, hence, the faster the rate of decline. This indicates that a reasonable Total Suspended Solids (TSS) specification is fundamental to the success of a water flood project. A reasonable TSS could help control fracture growth and prevent fracture breakout into the low permeability seal or inter-bedded shale layer. The impact of the concentration of particles of different sizes on the volume of deposition is further investigated using the dynamics of a closed system in Appendix G.

Field Applications

Prediction of Injectivity Decline (Well A-1)

A forecast was done to determine injectivity performance of well A-1 using the fitted parameters of well A-2 and A-3 and customizing the well geometry, the perforation height thickness in this case, to well A-1. From the trend observed as shown in figure 13, the half-life of the well will be approximately 450days compared to a 250days half-life for well A-2 with an injected particles concentration of 28ppm.

Deposited Particle Profile/ Particle Residence Time Analysis

The injected sea water particles range from **0.04 to 5µm** and the modal particle size is approximately 2μm as shown in the injected sea water particle size distribution in appendix E with detailed analysis. The current injection-water treatment criterion, aims at having over 95% of the particulates in the injection stream below 5 µm diameter, hence, 5% of the particles that would be allowed in the effluent downstream of the water treatment facility could be greater than this threshold particles size. The depositional particle profile model coupled with the residence time of injected particles can be used to recommend an optimum injection water specification for the design of water treatment facilities filtration requirement in the subject field. As illustrated in figure 14(a), particles > 4µm have a particle to pore size ratio > 33% and they get deposited within 4m radius of the near-wellbore region at an injection rate of $5570 m^3/day$ (35000bwpd) and at initial porosity and permeability of formation, hence, these particles are deposited closer with decrease in injection rate and pore radius reduction owing to plugging. Furthermore, figure 14(b) indicates particles with diameter >4µm have a residence time that is less than a day (≈18hours) with that of a 5µm particle approximately < 3hours.

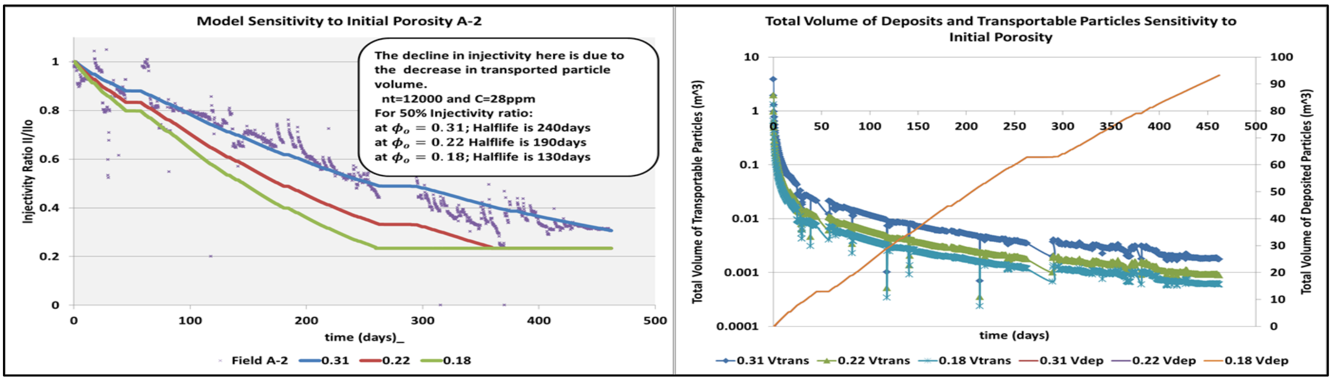

Figure 11: (a) Impairment model sensitivity to initial porosity (b) Impact of initial porosity on the volume of transportable particles.

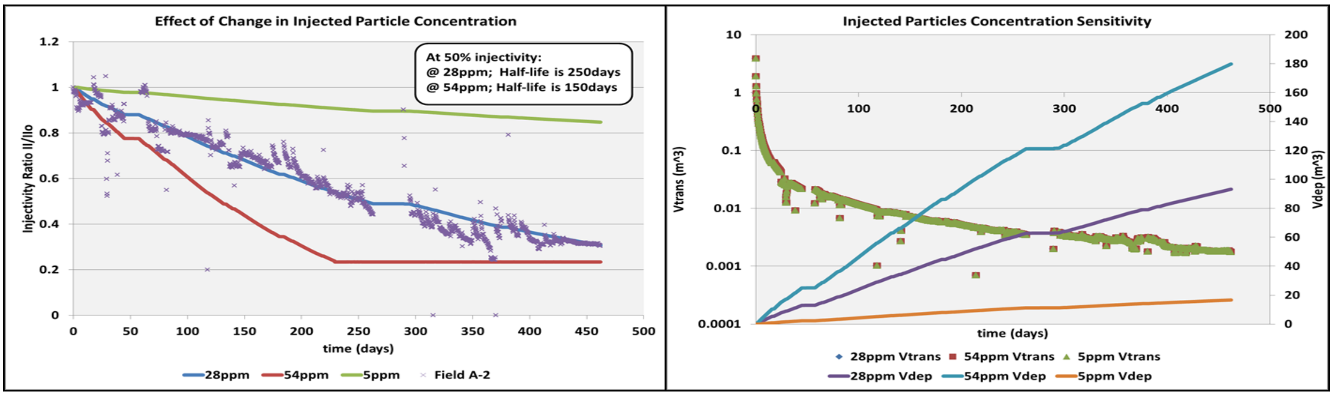

Figure 12: (a) Impairment model sensitivity to Injected Particles Concentration (b) Impact of injected particles concentration on the volume of deposited particles.

Minimum Effective Back flush Rate

Back flush is a remedial technique used in injector wells to clean out trapped particles in the formation (mechanically induced damage). During this process the flow of water through the porous media is reversed. In practice it is mostly carried out by creating a drawdown about the well completion and allowing the well to produce the fluids for a few barrels. In this section a new method to implement an effective and safe back flush operation without compromising the integrity of the cap rock is proposed. The equation of the deposited particle profile model (equation 11) is modified to obtain:

$$Q_c \geq \frac{\pi(r_d^2-r_w^2)(\rho_s-\rho_l)gH\phi_o D_p^2}{18\mu}\sqrt{\frac{\phi_o}{8k_o}} \quad r \neq r_w\,; \qquad v_c = \frac{Q_c}{2\pi r_d H\phi_o} \tag{19}$$

The required pressure drawdown for a corresponding back flush rate given the current injectivity ($II(t)$) of the well is:

$$\Delta P \geq \frac{Q_c}{II(t)} \tag{20}$$

In this modification, since the particle is at rest, the velocity required to erode it is equal to the critical advective velocity of the receding flood. The main purpose of this application is to analyze the back flush rate required to clean out particles of different sizes that pose both internal and external filter cake threat to the formation in this field ($D_p > 4\mu m$). In appendix E, it is shown that the required back flush rate increases with the particle size responsible for damage and also with the radius of damage. Also from figure 15(a), the required back flush rate increases with decline in formation permeability, this simply implies that an intense impaired formation requires a very high back flush rate. As illustrated in this plot, at the initial permeability of the formation, a 5μm particle will require a back flush rate of $1320m^3/day$, these rate becomes $1870m^3/day$ and $5900m^3/day$ at 50% and 5% of the initial permeability respectively.

Conclusively, an effective back flush operation depends on the current permeability of the formation, the size range of the possible particles responsible for damage, the viscosity of the receding flood and the current injectivity of the subject well. A detailed sensitivity analysis of back flush rate is discussed in appendix E in the field case study presented.

Table 3: impairment model matched parameters

	Wells	
	A-2	**A-3**
***II(t)/IIo* (30 days)**	**0.91**	**0.86**
C = 5ppm		
re match (m)	**1.72**	**1.1**
C = 28ppm		
re match (m)	**4.1**	**1.25**

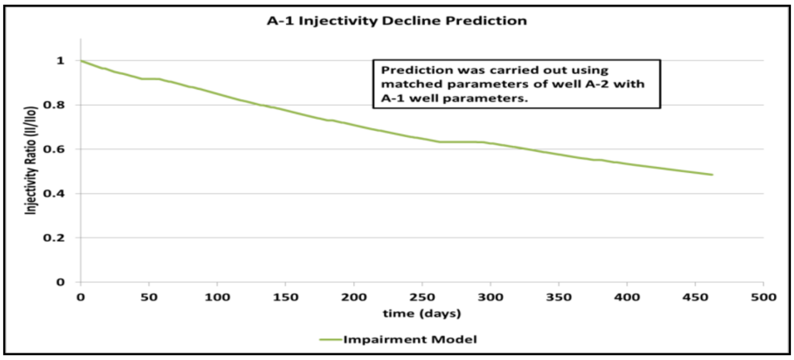

Figure 13: prediction of injectivity performance of well A-1.

Evaluating the impact of formation damage on Hydrocarbon recovery

This is done assuming 100% voidage replacement, that is, the pore volume of oil recovered (PVR) equals the pore volume of water injected (PVI). This analysis is performed on all injectors to evaluate the impact of formation damage, which may be due to the injection of particle-laden sea water, on the injectivity of a well, hydrocarbon recovery which in turn has its own share of impact on the economics of the entire field. It is therefore of high importance to analyze the extent to which damage to the formation will impact the economic delivery of hydrocarbon. Damage in this context refers to the fraction of pore space rendered impermeable due to solid fill-up. In order to implement this, the total volume of deposits obtained by history matching the impairment model to field data can be used to obtain the pore volume of particles deposited which when subtracted from the pore volume of water injected; it will return an estimate of the actual number of pore volumes of hydrocarbon recovered. Figure 15(b) illustrates this for well A-2 in which analysis show that 34% of hydrocarbon was not recovered owing to damage. These plots can be compared overtime to assess the performance of a reservoir. The closer both curves are the lower the damage and the higher the injectivity performance of the injector.

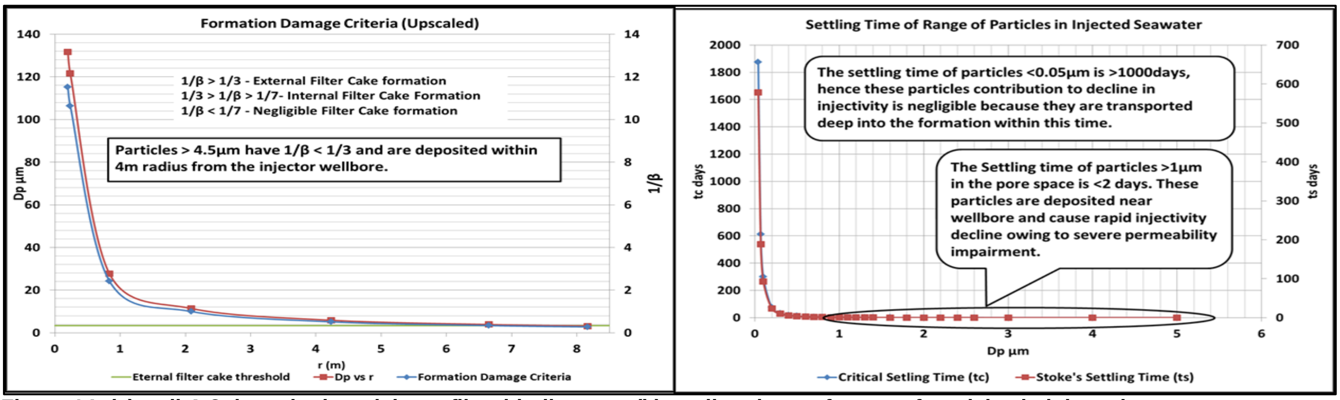

Figure 14: (a) well A-2 deposited particle profile with distance; (b) settling times of range of particles in injected seawater.

Discussion

From the analysis and results obtained, it can be inferred that Buckley Leverett fractional flow theory coupled with deep bed filtration theory can be used to track the spatial and temporal variation in the size of particles deposited in the formation, as the flood front sweeps through the porous medium, which in turn can be used to estimate the amount of deposits in the formation, hence, quantifying formation damage at any given instance of time during production. The developed model clearly indicates that near-wellbore damage is more severe than the expected damage away from the injector due to the deposition of coarser particles in this region at every given injection rate. Model sensitivity analysis implemented show that the realized model is robust and responds to uncertainties and alterations in different reservoir and process variables thereby representing the physics and phenomenon of particle transport and deposition in the porous medium.

Validation exercise of the developed impairment model showed that it rationalized the available field data sets from both wells (A-2 and A-3) with an error of less than 5% in injectivity as can be observed in figure 8a and b. This confirms that it is a very robust model that can respond to alterations in the different process and reservoir variables including the reservoir wettability and mobility of the injected and reservoir fluids as observed from sensitivity analysis. It was then used to predict the injectivity performance of a third well. A new method of determining the volume filtration coefficient of the formation is presented in appendix C and applied in appendix D. Numerical experiments involving new methodologies were developed to validate and apply model to field.

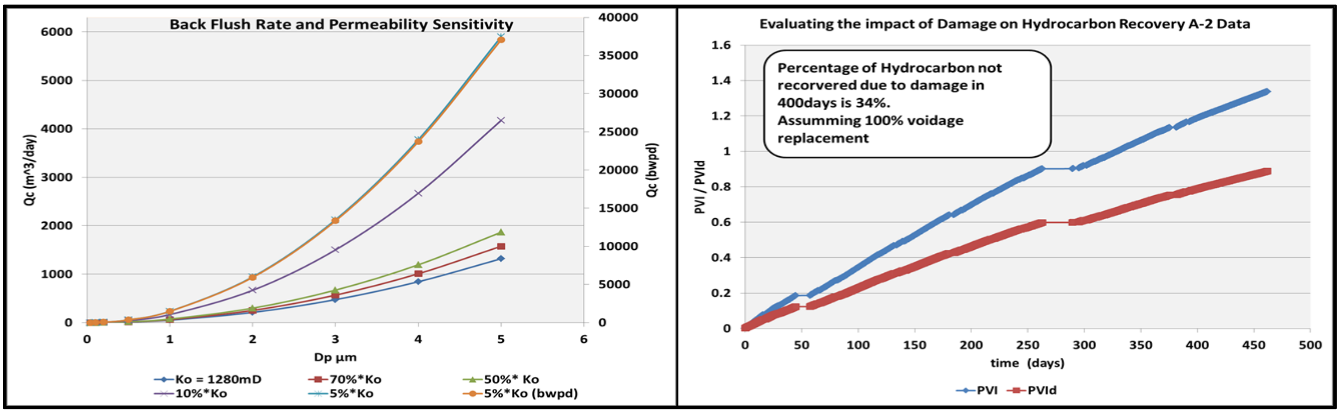

Figure 15: (a) back flush rate sensitivity to formation permeability; (b) the impact of damage on well A-2 on hydrocarbon recovery.

Depending on the injection rate, the deposited particle profile model, when integrated with the particle residence time and formation damage criteria (figure 14a and b) predicts that particles $\leq 0.05\mu m$ have negligible contribution to the injectivity performance of a well as they are transported deeper into the formation while those $> 4\mu m$ with particle-to-pore size ratio $(\beta) > 33\%$ are major threats to a wells' injectivity (Pautz *et al*, 1989) since they are easily trapped by the formation sand face and get deposited in less than 3 hours in the pore and within a radius of 4m from the near-wellbore region for this field (Todd *et al*, 1984). The linear flow model as described in appendix E predicts a smaller radius of deposition of about 30cm. The model confirms that the injection of larger particles induces severe damage closer to the near-wellbore region, but the injection of particles from 0 - 3µm can cause damage though out the entire length of the formation (Vetter *et al*, 1987). Physically, due to reservoir heterogeneities and the presence of other mechanism of particle capture, particles will get deposited closer to the wellbore than predicted by this model, hence the model gives an insight of the maximum distance a particle will travel in the formation before deposition at any given injection rate. These analyses can be applied in the design of an optimized water treatment facility to enhance reservoir performance.

Figure 9a and b gives the average transportable particle size of the flood and shows an initial high transport capacity for both wells (A-2 and A-3) which reduces rapidly within the first 2days from about 12.5µm to 4µm for well A-2. This high transport capacity recorded initially is re-emphasized in figure 10a and b which is a plot of the field scale volume of transportable particles and the volume of deposits over time. This rapid decreases in the transport capacity of the flood within the first two days suggest the occurrence of severe plugging after which a gradual decrease in the volume of transported particles is noted due to the reduced fraction of pores available for particle transport (reduced particle residence time) denoting decline in formation permeability (figure C-8b). Physically, during particle invasion into the pore reduced residence time of the particles causes them to get deposited closer to the injector leading to a rise in the bottom-hole pressure which induces rapid decline in the wells' injectivity. It represents solely the physics of internal filter cake formation (figure 1) due to particle invasion of the pores (Pang and Sharma, 1997).

The concentration of injected particles have a very strong impact on the amount of deposits collected over time in the pore space, as illustrated in figure 12a and b, but this depends on the relative size of particles present in the injected water as the effect of concentration is negligible if a high amount of small particles (< 0.1µm) are present (Pang and Sharma, 1997). This phenomenon is confirmed in appendix G where the impact of injected particle concentration and the size of the particle on the volume of deposits were investigated using the dynamics of a closed system with results obtained shown in figure G-3 for a 0.05, 0.1, 0.5 and 5µm. The results show that the effect of concentration on the transportation of particle <0.05µm is negligible. Sharma *et al*, (2000) in their work showed that the injection particles within the range of 1-5µm and a concentration range of 0.5-2ppm still resulted in significant decline in injectivity for all the injectors they studied (this was a case of un-fractured injectors).

A new method to implement an effective and safe back flush operation to ensure cap rock integrity has been proposed by modifying the depositional particle profile model. It shows that an effective back flush operation depends on the current permeability of the formation, the size range of the particles responsible for damage, the viscosity of the receding flood, the current injectivity of the well and the radius of the damage zone. Furthermore, a new method of evaluating the impact of formation damage on hydrocarbon recovery which could help in the assessment of reservoir performance was also presented.

Conclusions

1. Buckley Leverett fractional flow theory coupled with deep bed filtration theory can be used to track the spatial and temporal variation in the size of particles deposited in the formation which in turn was used to estimate the amount of deposits in the porous medium.
2. A new impairment model has been developed and has being validated and used for predicting the performance of other wells showing its robustness in simulating the physics of particle capture in the porous medium and alterations in different reservoir and process variables .
3. The injection history of the wells suggest severe formation and fracture face plugging which could be as a result of the current specification of the injected water or it may be caused by fluidized loose grains from the formation.
4. The deposited particle profile model can be used to implement a safe back flush operation to ensure cap rock seal integrity. Back flush operation is recommended to clear out mechanical plugging for the understudied field (due to injected solids).
5. For the analyzed field, particles >4µm with a particle to pore size ratio >33% settle out of suspension in less than a day (≈3hours) from the start of injection at a distance within 4m ($4000m^3/d$) of the near-wellbore region of the injector while particles <0.05µm settle out in >1000days hence they have negligible contribution to near-wellbore permeability impairment. This analysis can be used for an optimized water treatment specification.

Recommendations and Further Work

The following recommendations can be drawn from application of the new models to the field:

1. Further analysis should be carried out to investigate the effect of injected particle concentration on the volume of transportable particles.
2. The deposited particle profile model can be calibrated using field data by analyzing the particle distribution of produced water following the breakthrough of injected water. This can be compared against breakthrough particle size predicted by the model.
3. Improvement efforts should focus on incorporating other relevant mechanisms of particle capture to enhance the robustness of the model and derivative analyses.
4. Analysis and methodologies formulated here should be implemented alongside impairment core flood tests to have a broad overview of the impacts of different factors on injectivity decline in specific well-reservoir systems.
5. Particle residence time analysis can be used in the design of an optimal water treatment facility.
6. Analysis of retrieved solids during coil tubing intervention to know the class and size of solids responsible for wells' damage. Cycles of such retrieval would depend on sump depth.
7. A new method to implement an effective and safe back flush operation to remove mechanically induced damage.
8. The developed models should be applied considering the pore distribution in the field to factor in some required uncertainties in the results.
9. Well sump should be deep enough below perforation interval to allow larger accommodation space for particulates in the wellbore.
10. Effective pump pressure distribution to the injectors will help sustain high injection rates in order to push damage zones or regions where solids will settle out deeper into the formation away from the near-wellbore region of the well.

Acknowledgements

My profound gratitude goes to the Shell Petroleum Development Company of Nigeria for sponsoring my MSc in Petroleum Engineering course at Imperial College London. I would also like to thank my supervisors Fidelis Tendo, Kazeem A. Lawal (both of Shell Nigeria Exploration and Production Company), and Prof. Martin Blunt (Imperial College London), for their support and direction during this research work.

Nomenclature

a = coefficient of power-law distribution of particle sizes
B_w = water formation volume factor, m^3/sm^3
C = injected solids concentration, volume fraction
C_s = volumes of particles in suspension per unit pore volume
D_h = hydraulic tube diameter, L, m
D_p = transported particle diameter, L, m
F_w= water fractional flow
H = perforation height thickness, L, m
II = injectivity index, $m^3/d/(kgms^{-2}/\ m^2)$
k = permeability, L^2, mD
n = intrinsic flow coefficient, dimensionless
N = exponent of power-law distribution of particle sizes
N_{Re} = Reynolds's number, dimensionless
n_t = population factor, dimensionless

Unit Conversion Factors

B x 1.589 873 E – 01 = m^3
cp x 1.0* E-03 Pa·s
ft x 3.048* E -01 = m
°F (°F – 32)/1.8 = °C
psi x 6.894 757 E + 00 = kPa
mD x 9.87xE-16 = m^2

q_t = Darcy velocity, ms^{-1}
Q_t = total injection rate, m^3/d
Q_c = back flush rate, m^3/d
r = radial distance, m
r_p = mean pore radius, μm
S_w = water saturation, fraction
t_c = particle residence time, d
t_s = Stokes' settling time, d
v = particle speed, ms^{-1}
v_c = critical settling velocity, ms^{-1}
v_s = Stokes' settling velocity, ms^{-1}
x = linear distance, m
ϕ = porosity, fraction
λ = Volume filtration coefficient, m^{-1}
α = power-law distribution coefficient for area of transported particles, $\alpha = \pi a^2$
β = power-law distribution exponent for area of transported particles, $\beta = 2N$
ρ = density, kg/m^3
τ = tortuosity of formation, fraction
μ_w = water viscosity, $Pa.s$
Subscript
0 = initial condition
f = front

References

1. Adler, P. M., Jacquin, C. G. and Quiblier, J. A.: "Flow in Simulated Porous Media," *Int. J. Multiphase Flow*, Vol. 16, (1990) 691-712.
2. Barkman and Davidson: "Measuring Water Quality and Predicting Well Impairment," paper presented at the 1971 SPE 46th Annual Fall Meeting, New-Orleans, October 3-6.
3. Bedrikovetsky, P.; Marchesin,D.; Shecaira,F.; Serra,A.L.; Marchesin,A.; Rezende,E.& Hime,G.: "Well Impairment During Sea/Produced Water Flooding: Treatment of Laboratory data," paper SPE 69546 presented at the 2001 SPE Latin American and Caribbean Petroleum Engineering Conference, Buenos Aires, Argentina, March 25-28.
4. Bedrikovetsky, P. G.; Santos,P. M., Neto,A. M. and Riente,A. F.: "Fractional Flow Theory for Suspension Flow in Petroleum Reservoirs," paper SPE 121822 presented at the 2003 Latin American and Caribbean Petroleum Engineering Conference, Cartagena, Columbia, May 31 - June 3.
5. Bennion, D. B., Bennion, D. W., Thomas,.F. B. and Bietz, R. F.: "Injection Water Quality - A Key Factor to Successful Waterflooding," paper presented at the 1994 Annual Technical Meeting of the Petroleum Society of CIM, Jun 12 - 15.
6. Blunt, M. J & Muggeridge, A.: *Reservoir Performance Predictors*. Imperial College London Course Notes (2012).
7. Civan, F. *Reservoir Formation Damage.* Burlington, Elsevier (2007) 82, 142.
8. Cheel, R. J.: *Introduction to Clastic Sedimentology,* Brock University Course Notes, (2005).
9. Coulson and Richardson: *Chemical Engineering, Particle Technology and Separation Process*, Volume 2, Fifth Edition, Butterworth-Heinemann (2002) 300.
10. David, A. S., David, W.R., Richard, C. E., Richard, C. J. and Glen, L.: "Improved Water Injector Performance in a Gulf of Mexico Deepwater Development using an Openhole Frac Pack Completion and Downhole Filter System: Case Study," paper SPE 84416 presented at the 2003 SPE Annual Technical Conference and Exhibition held in Denver, Colorado, U.S.A., October 5-8.
11. Davidson H. D.: "Invasion and Impairment of Formations by Particulates," paper SPE 8210 presented at the 1979 *SPE* Annual Technical Conference and Exhibition, Nevada, September 23-26.
12. Furtado, C. J., Souza,A. and Araujo,C.: "Evaluation of Different Models for Injectivity Decline Prediction," paper SPE 108055 presented at the 2007 Latin American & Caribbean Petroleum Engineering Conference, April 15-18.
13. Izgec, B. and Shah, K. C.: "Real Time Performance Analysis of Water-Injection Wells," paper SPE 109876 presented at the 2007 SPE Annual Technical Conference and Exhibition, California, November 11-14.
14. Khatib, Z. I.: "Prediction of Formation Damage Due to Suspended Solids: Modeling Approach of Filter Cake Buildup in Injectors," paper presented SPE 28488 at the 1994 *SPE* Annual Technical Conference and Exhibition, Louisiana, September 25-28.
15. Khodaverdian, M. et al.: "Injectivity And Fracturing In Unconsolidated Sand Reservoirs:Waterflooding Case Study, Offshore Nigeria," paper ARMA 10-139 presented at the 2010 US-Canada Rock Mechanics Symposium, Salt Lake City, UT, June 27-30.
16. Kumar, T.:"Formation Damage Resulting from Particle Invasion," paper SPE 23561 presented to the society of petroleum of engineers for distribution and publication, June 24, 1991.
17. Lawal, K. A., Vesovic, V. and Boek, E. S.: "Modeling of Asphaltene Formation Damage in Closed Systems," paper SPE 138497 presented at the 2010 International Petroleum Exhibition and Conference, Abu Dhabi, November 1-4.
18. Ojukwu, K. I. & Van den Hoek,P.J.: "A New Way to Diagnose Injectivity Decline during Fractured Water Injection by Modifying Conventional Hall Analysis," paper SPE 89376 presented at the 2004 SPE/DOE Symposium on Improved Oil Recovery, Oklahoma, April 17-21.
19. Oort, E. V., van Velzen,J.F.G. and Leerlooijer,K.: "Impairment by Suspended Solids Invasion: Testing and Prediction," SPEPF (Sept. 1992)178-184.
20. Pang, S. and Sharma, M.: "Predicting Injectivity Decline in Water Injection Wells," Paper published in SPE Formation Evaluation 194-201, September 1997.
21. Pang, S. and Sharma, M.: "Evaluating the Performance of Open-Hole, Perforated and Fractured Water Injection Wells," paper 30127 presented at the 1995 *SPE European Formation Damage Conference," May 15-16.*

22. Pautz, J.F., Crocker, M. E. and Walton, C. G.: "Relating Water Quality and Formation Permeability to Loss of Injectivity," paper SPE 18888 presented at the 1989 SPE Production Operations Symposium, Oklahoma, March 13-14.
23. Stabel, H.: *Settling velocity and residence time of particles in Lake Constance,(1986)*
24. Todd, J. E., Somerville, J. F. and Scott, G.: "The Application of Depth of Formation Damage Measurements in Predicting Water Injectivity Decline," paper SPE 12498 presented at the 1984 SPE Formation Damage Control Symposium, February 13-14.
25. Vetter O. J., Kandarpa, V., Stratton, M and Veith, E.: "Particle Invasion into Porous Medium and Related Injectivity Problems," paper presented at the 1987 *SPE* International Symposium on Oilfield Chemistry, San Antonio, Texas, February 4-6.
26. Wennberg, K. E. and Sharma, M.: "Determination of the Filtration Coefficient and the Transition Time for Water Injection Wells," paper SPE 38182 presented at the 1997 SPE European Formation Damage Conference. June 2-3.

Appendices

Appendix A Milestone Study of Injectivity Decline

SPE Paper n°	Year	Title	Authors	Contribution
3453	1972	"Measuring Water Quality and Predicting Well Impairment"	Barkman, J.H.; Davidson, D.H.	1. Introduced the first comprehensive theory for predicting the behaviour of injector wells. 2. First to come up with a proposal on how to measure the quality of injection water using water quality ratio (WQR)
8210	1979	"Invasion And Impairment Of Formations By Particulates"	H.,Davidson, Donald	1.First paper to point out that there is a relationship between linear flow velocity and particle movement through porous media. 2.First to indicate the inverse relationship between particle size and velocity required to prevent particle deposition.
11332	1985	"The Effect of Thermoelastic Stresses on Injection Well Fracturing"	K,Perkins, T.; A,Gonzalez, J.	Determined thermoelastic stresses for cooled regions of fixed thickness and of elliptical cross section and developed a theory of hydraulic fracturing of injection wells. They also developed a correlation for analysing formation face damage resulting from injection of suspended solids.
17146	1988	"A One-Dimensional Formation Damage Simulator for Damage Due to Fines Migration"	S. Vitthal,; M,Sharma, M.; K.,Sepehrnoori,	First to propose a network model to predict permeability impairment owing to fines migration or injection.
18461	1990	"Injection-Water Salinity, Formation Pretreatment, and Well-Operations Fluid-Selection Guidelines"	F.,Scheuerman, Ronald; M.,Bergersen, Barbara	First to develop the injection water and formation clay compatibility criteria to determine when the pre-treatment of injection water is required to prevent permeability impairment.
28488	1994	"Prediction of Formation Damage Due to Suspended Solids: Modelling Approach for Filter Cake Buildup in Injectors"	Z. I. Khatib	First to introduce a new model for calculating the combined matrix and filter cake resistances in perforations and fractures by using the electrical analogy theory.
23822	1993	"Impairment by Suspended Solids Invasion: Testing and Prediction"	Oort,Eric van; van Velzen,J.F.G.; Leerlooijer ,Klaas	1.Proposed a model for predicting injectivity decline owing to internal filter cakes only. 2. First to introduce two new parameters: the damage factor and the volume filter coefficient.
28489	1994	"A Model for Predicting Injectivity Decline in Water-Injection Wells"	Pang,Shutong; Sharma,M. M.	First to build a model to predict injectivity decline considering both internal and external cake filtrators using the transition time concept.
30127	1995	"Evaluating the Performance of Open-Hole, Perforated and Fractured Water Injection Wells"	Shutong,Pang,; M.,Sharm a, Mukul	1.First to present equations that allowed for the modelling of open hole, perforated completions and fractured wells. 2.First to develop methods using a simulator to calculate model parameters when core flow data is not available.

38181	1997	"Determination of the Filtration Coefficient and the Transition Time for Water Injection Wells"	E,Wennberg, K.; M,Sharma, M.	First to present a new method of determining the development of the filtration coefficient with time, utilizing the concept of critical porosity.
60901	1997	"Injectivity Decline in Water Injection Wells: An Offshore Gulf of Mexico Case Study"	M.,Sharma, Mukul; Shutong,Pang,; Er ik,Wennberg, Kjell; Lee,Morgenthaler,	Conducted studies to determine the optimum water requirement needed to design the surface facilities required for water treatment and for maintaining a specified injection rate.
69546	2001	"Well Impairment during Sea/Produced Water Flooding: Treatment of Laboratory Data"	Bedrikovetsky,P.; Marche sin,D.; Shecaira,F.; Serra, A.L.; Marchesin,A.; Reze nde,E.; Hime,G.	presented the first inverse problem for the determination of functions of the filtration coefficient and permeability versus deposited concentration from lab test on Deep Bed Filtration
83673	2002	"Damage Characterization of Deep Bed Filtration from Pressure Measurements"	Bedrikovetsky,P.; Marche sin,D.; Shecaira,F.; Serra, A.L.; Marchesin,A.; Reze nde,E.; Hime,G.	They proposed a new method for the simultaneous determination of the Filtration Coefficient and the Formation Damage Coefficient using pressure data at an intermediate core point, supplementing pressure measurements at the core inlet and outlet.
86524	2004	"Formation Damage due to Scale Formation in Porous Media Resulting from Water Injection"	Moghadasi,J.; Jamialahm adi,M.; Müller-Steinhagen,H.; Sharif,A.	The paper presented both experimental and theoretical results of permeability impairment caused by scaling in porous media.
89376	2004	"A New Way to Diagnose Injectivity Decline During Fractured Water Injection By Modifying Conventional Hall Analysis"	Ojukwu,K.I.; Van den Hoek,P.J.	First paper to modify Hall's technique by using it to quantify damage skin
109876	2007	Real-Time Performance Analysis of Water-Injection Wells	Izgec,Bulent; Shah Kabir,C.	Introduced an analytic derivative method, a new formulation of the Hall analysis, to ascertain variables such as radial distance of the injection bank and pressure at the water/oil interface.
108055	2007	Evaluation of Different Models for Injectivity Decline Prediction	Furtado,Claudio Jose Alves; Souza,Antonio Luiz Serra de; Araujo,Carlos Henrique Vieira	Evaluated three injectivity decline models, compared their results, pointed out their limitations and finally adjusted them to fit historical data from injector wells
121822	2009	Fractional Flow Theory for Suspension Flow in Petroleum Reservoirs	Bedrikovetsky,Pavel G.; Santos,Peter Monteiro; Neto,Adelina Mouta Moreira; Riente,Aliel Faria	They introduced a method that uses a close system of equations for mono-dispersed suspension transport in porous media.

Appendix B. Critical Literature Review

SPE 3543-PA (1972)

Measuring Water Quality and Predicting Well Impairment

Authors: Barkman, J.H., Shell Oil Co.; Davidson, D.H., Shell Development Co.

Contribution

1. Introduced the first comprehensive theory for predicting the behaviour of injector wells.
2. First to come up with a proposal on how to measure the quality of injection water using the Water Quality Ratio which can be obtained from membrane filter test and core data, and in turn use this to predict rate of formation impairment caused by suspended solids.
3. Provided a means of estimating the half-life of an injector, which is an easy way to predict how long an injector will be in use before stimulation.

Objective of the paper

It proposes methods and a theory that can be used to interpret water quality data used to predict well impairment caused by suspended solids.

Methodology used

Four basic impairment mechanisms were modelled for a constant pressure drop process. With the time derived constant-pressure-drop filtration test using core and membrane filter data to measure the water quality and from filtration theory was able to distinguish invasion from filter cake build-up and make a valid calculation of cake permeability.

Conclusion

1. The Water Quality Ratio can be obtained from filtration test and used to predict rate of well impairment.
2. The half-life of the injector, which is derived for the four basic models of which an injector well can get impaired by solids, is a direct function of the Water Quality Ratio in most cases.
3. The theory presented can be used in evaluating the performance of an existing water treating project or in planning the degree of water treating required.

Comments

1. The results hold for constant pressure process only, the equations were not applied to process control (did not consider rates).
2. The filter cake permeability obtained from membrane filter test is far from reality since the pore morphology of the membrane filter differs from that of a porous rock.
3. He did not consider the compressibility of the solids when determining the filter cake parameters knowing that the cake porosity and permeability depends on the average particle size and compressibility.

SPE 8430 (1982)

Entrainment and Deposition of Fine Particles in Porous Media

Authors Gruesbeck,C.; Collins,R.E.

Contribution

The paper describes the result of studies conducted to determine the factors affecting the entrainment and deposition of fine particles in porous media. Discovered a critical velocity below which entrainment of fines does not occur and above which the rate of entrainment increases linearly with flow rate.

Objective

The paper sought to determine local laws of deposition and entrainment that can be used to determine where fines are entrained and deposited in the formation as a basis for remedial treatment.

Methodology

1. They used a sequence of experiments using fines and un-consolidated sands of large grains to identify fundamental processes and to provide guidelines for a phenomenological description.
2. Two types of experiments were carried out:
   - With an dirty fluid flowed through an initially clean column
   - An initially clean fluid flowed through a dirty column filled with fines deposit.
3. A theoretical description of the deposition and entrainment process was constructed.
4. Field cores and naturally occurring fines were used in controlled laboratory experiments to verify results of earlier studies on the topic.

Conclusion

Comments

SPE 11332 (1985)

The Effect of Thermoelastic Stresses on Injection Well Fracturing

Authors K,Perkins, T.; A,Gonzalez, J.

Contribution

Determined thermoelastic stresses for cooled regions of fixed thickness and of elliptical cross section and developed a theory of hydraulic fracturing of injection wells. They also developed a correlation for analysing formation face damage resulting from injection of suspended solids.

Objective

1. The paper considered thermoelastic stress which results from cooled regions of fixed thickness and of elliptical cross section of the flood front.
2. Deduced the stress for an infinitely thick reservoir using information from public literature.
3. Developed a numerical method to calculate the thermoelastic stress induced within elliptically shaped regions of finite thickness.
4. Used the two approaches to develop empirical correlations for the estimation of induced stress.

Methodology

1. They saturated laboratory test core plugs with brine that have the same saturation as the test water and used this to establish stable permeability of the core before test water is injected.
2. The total pressure drop from the core was taken as the pressure drop through the initial core plus an additional resistance due to filtration of solids from the injected water.
3. Used a resistance term (R_s) which can be determined from correlation to represent the flow resistance.

Conclusion

1. They successfully showed, using examples, that the injection of cool water can reduce each stress around injection wells substantially, causing them to fracture at pressures considerably lower than would be expected under conditions in which the thermoelastic effect is absent.
2. They discovered that short fractures which form as a result of low injection rate, high permeability, or low reservoir pressure do not change the shape of the waterflood front from the circular shape that will be expected for an unfractured well. Noticeable elliptical shape of the waterflooded region can be observed as a result of high injection rates, low permeability, high reservoir pressure or poor water quality.

Comments

The paper did not consider the effect of resistance due to completions on the formation damage.

SPE 28488 (1994)

Prediction of Formation Damage Due to Suspended Solids: Modelling Approach for Filter Cake Buildup in Injectors.

Author Z. I. Khatib

Contribution

The paper introduced a new model for calculating the combined matrix and filter cake resistances in perforations and fractures by using the electrical analogy theory.

Objective

1. Used results from experiments to show the significant effect that the types pf solids and the presence of oil has on the brine permeability through a thin filter cake in the wellbore.
2. Presented and discussed the permeability/porosity correlations used in predicting injectivity decline rates as a function of different types of solids.
3. Demonstrated the effective use of electrical circuit analogy to simulate flow resistances of thin filter cakes formed in perforations and fractures.
4. Presented a modelling approach for prediction of filter cake buidup and injector half-life for different well completions.

Methodology

1. Used capillary pressure data to determine pore size distribution.
2. The average total porosity, thickness and permeability of various filter cakes were determined experimentally using a Compression-Permeability (C-P) cell.
3. An electrical analogy of a flow resistance model was then used to represent the flow resistance of a filter cake assumed to buildup homogenously in a cylindrical geometry.

Conclusion

1. The type of solids and the presence of oil have a significant effect on the brine permeability of a thin filter cake that builds up in the wellbore.
2. The cake porosity is not constant and varies with applied pressure, particularly *for* compressible particles such in iron hydroxide.
3. The filter cake characteristics of the solids can be defined by developing empirical permeability/porosity correlations.
4. The permeability reduction due to solids in a Berea core can be predicted closely using the permeability/ porosity correlation.
5. The use of the electrical circuit analog was effective in simulating filter cake resistances in perforations and fractures.

Comments

The model can only determine the end effect of the injected solids since a time factor was not included in its prediction. It does not consider the internal damage step.

SPE 28489 (1994)

A Model for Predicting Injectivity Decline in Water-Injection Wells

Authors Pang,Shutong; Sharma,M.M.

Contribution

The first to model both internal and external filter cakes for the prediction of well impairments using the transition time concept.

Objective:

Develop a model that properly accounts for both the infiltration of particles and the buildup of an external filter cake at the rock surface.

Methodology

- Water Quality type curves were used to determine the mechanism of injectivity decline caused by suspended particles (External, Internal or both).
- Curve fit core flow test data which were used to determine the cake properties.
- Used resulting model to predict injector well performance.

Conclusion

The new model derived to predict injectivity decline considering both external and internal filtration showed excellent results with data available from literature.

Comments

- Method can only be used when core data is available.
- Model is only applicable to open-hole geometries.
- Model did not consider the effect of the injected and resident fluid mobility on a well’s injectivity.

SPE 30127 (1995)

Evaluating the Performance of Open-Hole, Perforated and Fractured Water Injection Wells

Authors Shutong,Pang,; M.,Sharma, Mukul

Contribution

First to present a simulator used to predict the injectivity decline of water injection wells using equations derived that allowed for the modelling of open hole and perforated completions as well as hydraulically fractured wells.

Objective

This provided a reliable and user friendly simulator for predicting injectivity decline in water injection wells. The simulator considers both external and internal filter cake formation for various well completions, such as open-hole, cased/perforated and hydraulically fractured wells.

Methodology

1. Used equations from linear geometry for parameter estimation using data from core flow experiments.
2. A model for perforated wells was created by considering a perforation as an ellipse that is rotated about its axis.
3. The model for hydraulically fractured well was made considering three filtration cases: internal damage in rock, External damage on rock faces and internal damage in the fracture.
4. Simulator used two types of input data to predict injectivity: The required and the optional data.
5. The required data included well geometry. It estimates the values of optional data whose values are not available based on empirical correlations obtained from literature.

Conclusion

1. Found out that the injectivity decline to a fractured well is primarily due to internal damage to the fracture, the effects of other damage mechanisms are minimal.
2. The use of smaller filtration parameter values will lead to a slow decrease in injectivity in agreement with the expected behaviour in practice due to the high flow velocity in fracture.
3. The equations derived were incorporated into the simulator for the prediction of injectivity decline and each model parameters could be obtained using either experimental core flow data or from empirical correlations.

Comments

The paper did not consider the effect of fluid rate and velocity on the filtration coefficient.

SPE 38181 (1997)

Determination of the Filtration Coefficient and the Transition Time for Water Injection Wells

Authors E,Wennberg, K.; M,Sharma, M.

Contribution

First to present a new method of determining the development of the filtration coefficient with time, utilizing the concept of critical porosity.

Objective

To determine the downhole filtration of the formation to correctly predict the injectivity decline.

Methodology

1. They determined the solution of the mass conservation equation by considering two scenarios: non-changing filtration coefficient and changing filtration coefficient.
2. Used the concept of critical porosity to determine the transition time.

Conclusion

1. A filtration coefficient that varies with time can be used to adequately describe the downhole filtration of injection water.
2. The initial filtration coefficient can be determined within a reasonable accuracy from correlations derived under conditions in which the forces acting between formation grains and injection particles are attractive.
3. Available experimental data shows large scatter when it comes to the regression of filtration coefficient with time.
4. Suggested that if experimental data are not available a constant filtration coefficient should be used.

Comments

The correlations available to determine the evolution of the filtration coefficient with time are not regarded as generally applicable.

SPE 60901 (1997)

Injectivity Decline in Water Injection Wells: An Offshore Gulf of Mexico Case Study

Authors M.,Sharma, Mukul; Shutong,Pang,; Erik,Wennberg, Kjell; Lee,Morgenthaler,

Contribution

The paper presented a field case study on the impact of water quality on unfractured wells.

Objective

The paper applied some injectivity decline models to five injector wells in an offshore environment to clearly point out the need of such analysis in determining the optimal water quality requirements which dictate the surface facilities needed to maintain a specific injection rate.

Methodology

A simulator was used to predict well injectivity decline with well parameters as input.

Conclusion

1. Injection half-life between 30 and 90 days may be expected in situations where relatively clean water is injected into unfractured cased-hole or open hole injected wells.
2. The injection half-life can be improved by a factor of 2 to 5 by significantly improving the injection water quality.
3. Fractured wells are more tolerant to poor injector water quality; as such they have half-lives that are order of magnitude greater than that of unfractured wells.
4. Conducting “what if” study on the performance of an injector well can be used to determine the economic impact of the project.

Comments

Filtration requirement is very important in the preservation of injectivity in unfractured wells. The initial skin of an injection well has a very high impact on its rate of decline.

SPE 89376 (2004)

A New Way to Diagnose Injectivity Decline During Fractured Water Injection By Modifying Conventional Hall Analysis

Authors Ojukwu,K.I.; Van den Hoek,P.J.

Contribution

This is the first paper to modify Hall's technique by using it to quantify the damage skin.

Objective

The main objective of this paper was to investigate water quality required for matrix and controlled fracturing injection, evaluate the subsurface aspects of the injectivity decline mechanism and to provide guidance for well remediation and water treatment facility design.

Methodology

1. The paper uses the modified hall analysis equation and the Bottomhole pressure versus rate plot to study the performance of 5 injectors using historical data.
2. Bottomhole pressure versus rate plot was used to provide evidence of wellbore plugging and/or fracture plugging.
3. Modified Hall plot equation was used with field data for diagnosing matrix/fracturing regimes, quantifying the degree of damage and determining the location of the damage.

Conclusion

1. The modified hall analysis was useful in characterizing matrix, plugging matrix, initial fracture, plugging fracture, stimulation and fracture growth events.
2. The Bottomhole pressure versus rate plot was useful in predicting location of damage either at wellbore or fracture, from which recommendations can be made for the well.
3. The extent of damage was determined for all injectors using the modified Hall plot analysis.

Comments

SPE 86524 (2004)

Formation Damage due to Scale Formation in Porous Media Resulting from Water Injection

Authors Moghadasi,J.; Jamialahmadi,M.; Müller-Steinhagen,H.; Sharif,A.

Contribution

The paper presented both experimental and theoretical results of permeability impairment caused by scaling in porous media.

Objective

The objective of the paper is to investigate the formation of scale minerals, kinetics of calcium sulphate scale formation, and transformation of one hydrate to another for the determination of the nature of the scale formed under field conditions as a function of both temperature and ionic strength.

Methodology

1. Experiments were carried out using a test rig.
2. The scale formation experiments were performed with aqueous solutions of $NaSO_4.CaNO_3.4H_2O$ and Na_2CO_3. The solubility of the salts and the valency of their respective ions were the criteria used in selecting the solution.
3. The permeability reduction by calcium sulphate and calcium carbonate scales deposition on the porous media were studied by considering a wide range of flow velocities, bulk temperatures, and fluid bulk concentrations recording the pressure drop across the test section continuously.

Conclusion

1. The decline in permeability due to scale formation in the porous bed ranged from less than 30% to more than 90% of the initial permeability and depended on the solution composition, the initial permeability, temperature, flow rate and solution injection period.
2. The scaling due to calcium sulphate and calcium carbonate increase at higher temperature due to their solubility which decreases with increasing temperature.
3. Brines of higher degree of supersaturation produced a more rapid decline in permeability. This behaviour was expected as a high degree of supersaturation means a high rate of precipitation.
4. It was observed that the rate of permeability decline increased as the flow rate is increased, this is due to the fact that at higher flow rates the more calcium and sulphate ions will enter the formation in a given instant of time , hence providing more materials for deposition and increased precipitation.

Comments

In order to implement an efficient water injection project the chemical composition of the injection water most be ascertained to determine if there is a possibility of scale formation.

SPE 109876 (2007)

Real-Time Performance Analysis of Water-Injection Wells

Authors Izgec,Bulent; Shah Kabir,C.

Contribution

The paper introduced an analytic derivative method, a new formulation of the Hall analysis, to ascertain variables such as radial distance of the injection bank and pressure at the water/oil interface.

Objective

The main aim of the paper was to provide a proper application of the original Hall formulation by updating the outer-bank pressure at every time step.

Methodology

1. They used coupled geomechanical/fluid-flow simulations to present synthetic cases showing fracturing, non-fracturing and plugging of the formation in order to develop the diagnostic signatures of waterflooding situations.
2. They used both the Hall integral and its derivative was used to diagnose the status of injection.
3. Used a variable oil/water interface pressure to obtain the Hearn or reciprocal in injectivity plot.
4. A pseudo-steady state (PSS) solution is used to carry out the derivative calculations.

Conclusion

1. PSS solution can be used to approximate transient behaviour as long as skin is obtained from transient formulation.
2. Superposition principle can be used to account for change in injection rate.
3. The original Hall formulation works best in cases where steady state conditions prevail (post-breakthrough situation) when the change in the oil/water interface pressure changes minimally.
4. The new variable-Pe analytical formulation works at all times and holds both for Hearn and Hall plot, thereby proving its suitability for real time monitoring.
5. The re-formulated Hall approach is superior to the Hearn method because when the derivative curve is used in tandem with the Hall integral, it provides unambiguous diagnosis of a well’s performance status.
6. The Hall’s derivative is applicable to wells injecting water in various formations and is equally effective in monitoring matrix acidizing.

Comments

The use of the Pressure-rate plot, Hearn plot, Hall integral and its derivative used in tandem have proven to be very useful diagnostic tools in isolating the main cause of injectivity decline in reservoir-well systems.

SPE 69546 (2001)

Well Impairment during Sea/Produced Water Flooding: Treatment of Laboratory Data

Authors Bedrikovetsky,P.; Marchesin,D.; Shecaira,F.; Serra,A.L.; Marchesin,A.; Rezende,E.; Hime,G.

Contribution

The paper presented the first inverse problem for the determination of functions of the filtration coefficient and permeability versus deposited concentration from lab test on Deep Bed Filtration.

Objective

The paper formulated a well posed and stable sequence of two procedures for the determination of a filtration function and of formation damage function from the outlet concentration and pressure drop measurements.

Methodology

The characteristics of the Deep Bed Filtration were determined by:

1. Firstly, determining the filtration coefficient from the concentration history of the core outlet using the solution of a first inverse problem.
2. Secondly, the formation damage function was determined from the pressure drop on the core using the solution of a second inverse problem.

Conclusion

1. The first inverse problem of determination of the filtration function from the particle concentration on the core outlet is well-posed and always allows for the unique solution which is stable with respect to small perturbation of measured concentration.
2. The formation damage function can be determined from the pressure drop data assuming that the filtration coefficient is a known function.

Comments

1. Results obtained from core-flood data are not fully representative of the filtration coefficient of the formation.
2. The Filtration Coefficient of the formation is not constant but varies exponentially with time.

SPE 83673 (2002)

Damage Characterization of Deep Bed Filtration from Pressure Measurements

Authors

Bedrikovetsky,P.; Marchesin,D.; Shecaira,F.; Serra,A.L.; Marchesin,A.; Rezende,E.; Hime,G.

Contribution

They proposed a new method (the Mathematical Recovery Method) for the simultaneous determination of the Filtration Coefficient and the Formation Damage Coefficient using pressure data at an intermediate core point, supplementing pressure measurements at the core inlet and outlet (the Three Point Pressure Method).

Objective

1. The main objective was to determine statistical relationship between the filtration and formation damage coefficient and the ratio of pore radius to particle size.
2. They used the proposed method for the analysis of laboratory test data on Deep Bed Filtration and investigated the effect of particle type and porous media wettability on permeability decline analysis using different cores.

Methodology

1. They analysed the results of 34 laboratory test using the three point method.
2. They carried out three types of test: coreflood with injection of water with solid particles, with liquid particles, and with both kinds of particles.
3. The particle to pore radius ratio was used to determine the effect of straining mechanism on formation damage.

Conclusion

1. The average formation damage coefficient (β) is higher for solids than that for solid-liquid mixtures, and that for solid –liquid mixture is higher than that for water injected with liquid particles.
2. The filtration coefficient for solid particles is higher than that for liquid particles because of oil droplets penetration through pore throats, decreasing the effective capture for liquid particles.
3. An external cake does not form from oily water injection.

Comments

Measuring concentration of particles in the effluent of the stream to determine the Filtration coefficient is a very difficult and uneconomical process to carry out because of the expensive equipment required. Authors tried to mitigate this difficulty by the determination of the required constants from the total pressure drop along the core measured at different times during flow.

SPE 108055 (2007)

Evaluation of Different Models for Injectivity Decline Prediction

Authors Furtado,Claudio Jose Alves; Souza,Antonio Luiz Serra de; Araujo,Carlos Henrique Vieira

Contribution

Evaluated three injectivity decline models, compared their results and finally adjusted them to fit historical data from injector wells.

Objective

1. The paper compared some injectivity decline models, using historical data from an injector previously reported.

Methodology

1. Predicted well behaviour using three models of injectivity decline with parameters found in literature. The aim was to show how to predict injectivity decline using parameters measured from analogous conditions.
2. The differences in the result of the three models were ascertained by running a set of 80 different injection conditions and simulating them using the available models and parameters obtained from literature.

Conclusion

1. All models show good results but they may have better results.
2. In several cases, special care needs to be taken in predicting conditions when water with good quality is injected with low flow rate in a rock with high permeability as the model used in Reveal cannot show the effects of internal damage; hence it predicts worst decline than would be expected.
3. Phenomenological model also shows good results. The advantage of this model when compared with others is that it considers two kinds of damage mechanism: internal damage and cake formation. Its disadvantage is the high number of empirical parameters needed to be determined to use this model.
4. The best model that fit historical well data is the empirical model (Perkins and Gonzalez work) as it involves the determination of one empirical constant. Its limitation is the absence of temperature and mobility effects and the consideration of only one kind of damage.

Comments

The evaluated models do not have skin as an input so they predict lower injectivity decline than well data. It was proposed that the models should be upgraded by including temperature and mobility effects.

SPE 121822 (2009)

Fractional Flow Theory for Suspension Flow in Petroleum Reservoirs

Authors Bedrikovetsky,Pavel G.; Santos,Peter Monteiro; Neto,Adelina Mouta Moreira; Riente,Aliel Faria

Contribution

1. They introduced a method that uses close system of equations for mono-dispersed suspension transport in porous media and uses the fractional flow function as the flux-reduction factor.
2. The paper introduced a new small parameter that describes cases of low concentration and low retained suspensions. There model differed significantly from classical filtration model.

Objective

1. Calculated the forms of filtration function for different pore size distribution for the fractional flow model.
2. Introduced a new small parameter that describes cases of low concentration and low retained suspensions that allows predicting filtration coefficient distribution from initial pore size distribution data.

Methodology

1. They used closed system of equation for monodispersed suspensions to represent transport in porous media.
2. The microscale system for mono dispersed suspension flow was averaged and resulted in a modified deep bed filtration model.
3. They used fractional flow nature of the derived model to explain particle acceleration or slowing down when compared with the carrier water velocity.
4. Two sets of laboratory data on injectivity decline were treated and assumed that pore size distribution does not change significantly under the test condition.

Conclusion

1. The effect of particle storage introduced in cut off accessible pores lead to the loss of conservation form for averaged particle balance equation.
2. The generalized model shows that in particular case of pure particle straining, the retention rate is proportional to inaccessible pores.
3. The generalized model has a fractional flow form.
4. The breakthrough time in bundle of capillaries is less than unity and this is explained by velocity enhancement and pore accessibility.

Comments

1. Ahead of the water front the suspended and retained particle concentrations are zero.
2. Correctly analysed the speed of the suspension front using the saturation dependent speed (F/S).

Appendix C: Model Development

The concept of retention time will be used to determine the critical settling velocity of the particles in the suspension. The retention time is the average time it takes a particle to remain in suspension while the critical settling velocity is the minimum velocity required for particles to be transported, hence particles with settling velocity equal to or greater than the critical settling velocity will get deposited in the formation.

Model Assumptions

1. Non-reactive flow
2. Main mechanism of particle deposition is sedimentation.
3. Assumes steady state conditions and Newtonian fluid flow, that is, the solid particles flows along a streamline (Laminar flow) unless acted upon by an unbalancing force.
4. The sizes of particles are smaller than the pore throat of the formation if not external filter cake buildup will occur from start of injection.
5. Injected particles are assumed to be spherical in shape.
6. Assumes free settling of particles, hindered settling due to Brownian motion (collision of particles) is not considered.
7. The tortuosity (τ) of the formation was assumed to be unity.
8. Model development considered both linear and radial flow

Deposited Particle Profile Model

As injection of water begins, flow tends to be radial away from the injector (figure C-1) and this implies that the total injection rate will vary with distance, also, the velocity of the water front decreases as the water progresses away from the injector wellbore and this encourages the deposition of particles in the porous media. In order to account for this, the radial flow equation was adapted to Buckley-Leverett fractional flow equation as explained in this section.

From the mass balance equation for the filtrate:

Volume entering the element – Volume leaving the element = change in fluid volume **C- 1**

Consider a circular differential element *dr* of the porous media, with an area *A*, and porosity ϕ with water flowing in and out of it as shown in figure C-1a. (Ahmed, 2000; Blunt and Muggeridge, 2012)

The volume of water entering the element is: $\boldsymbol{Q_t F_w dt}$ **C- 2**

The volume of water leaving the element which will now have smaller water cut is:

$$\boldsymbol{Q_t(F_w - dF_w)dt} \quad \textbf{C- 3}$$

The accumulation of water within this differential element is given by:

$$\boldsymbol{A\phi dr dS_w} \quad \textbf{C- 4}$$

Substituting into the mass balance equation (Equation C-1) we have:

$$Q_t F_w dt - Q_t(F_w - dF_w)dt = A\phi dr dS_w$$

For radial flow, the surface flow area is given by: $A = 2\pi rH$

$$Q_t F_w dt - Q_t(F_w - dF_w)dt = 2\pi rH\phi dr dS_w \quad \text{C- 5}$$

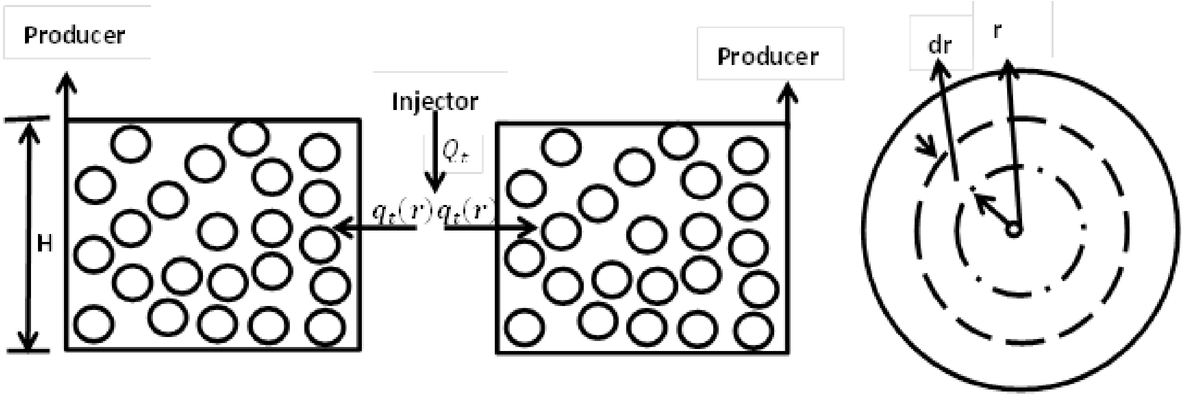

Figure C- 1: Flow from an injector into the porous media incorporating radial flow: (a) sectional view (b) plan view showing radial flow

This implies that the speed of a constant plane of saturation (S_w) is:

$$\left(\frac{dr}{dt}\right)_{S_w} = \frac{Q_t}{2\pi rH\phi}\left[\frac{dF_w}{dS_w}\right]_{S_w} \quad \text{C- 6}$$

Darcy's velocity, $\boldsymbol{q_t} = \frac{Q_t}{2\pi rH}$ **C- 7**

Similarly it can be inferred that the speed of a particle transported by the flood will be:

$$\boldsymbol{v} = \frac{Q_t}{2\pi rH\phi}\left[\frac{F_w}{S_w}\right]_{S_{wx}} \quad \text{C- 8}$$

F_w/S_w is the particles dimensionless speed in water as obtained from fractional flow theory.

$$Q_t = q_t(r).2\pi rH$$

$$q_t(r) = \frac{Q_t}{2\pi rH}; \qquad dr = \frac{q_t(r)}{\phi}dt$$

The distance covered by the particle at a particular time is:

$$\boldsymbol{dr} = \frac{Q_t}{2\pi rH\phi}\left[\frac{F_w}{S_w}\right]_{S_{wx}} \boldsymbol{dt} \quad \text{C- 9}$$

Integrating both sides of equation C-9 we have:

$$\int_{r_w}^{r} \frac{2\pi rH\phi}{Q_t}\left[\frac{S_w}{F_w}\right]_{S_{wx}} \boldsymbol{dr} = \int_0^{t_c} \boldsymbol{dt} \quad \text{C- 10}$$

The residence time of the particle in the porous media will then be:

$$t_c = \frac{\pi(r^2 - r_w^2)H\phi}{Q_t}\left[\frac{S_w}{F_w}\right]_{S_{wx}} \qquad \text{C- 11}$$

Where t_c is the residence time, r is the radial distance covered by particle away from the injector well, H is the injection interval and Q_t is the injection rate.

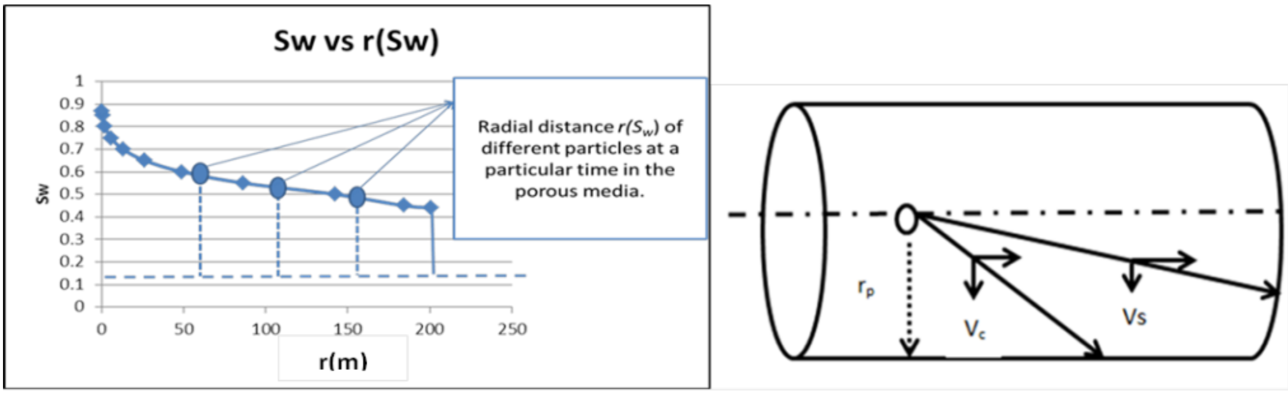

Figure C- 2: (a) A plot of water saturation against radial distance showing particles flowing on a constant plane of saturation; (b) an isolated pore space in the formation showing a suspended particles trajectory in the formation.

Since the particle speed is a function of a constant plane of saturation of the flood as shown in figure C-2a, the distance covered by a particle as a function of saturation it flows in if a snapshot of the porous media is taken at an instant of time is obtained by integrating both sides of equation C-6:

$$\int_{r_w}^{r} r.dr = \frac{Q_t}{2\pi H\phi}\left[\frac{dF_w}{dS_w}\right]_{S_{wx}} \int_0^t dt \qquad \text{C- 12}$$

$$r^2 - r_w^2 = \frac{Q_t}{\pi H\phi}\left[\frac{dF_w}{dS_w}\right]_{S_{wx}} .t$$

$$r = \sqrt{\frac{Q_t t}{\pi H\phi}\left[\frac{dF_w}{dS_w}\right]_{S_{wx}} + r_w^2}$$

This implies that, the distance of a constant plane of saturation can be given by:

$$r(S_w) = \sqrt{\frac{Q_t t}{\pi H\phi}\left[\frac{dF_w}{dS_w}\right]_{S_{wx}} + r_w^2} \qquad \text{C- 13}$$

The residence time of a particle transported as a function of this distance is:

$$t_c = \frac{V_{container}}{Q_t} = \frac{\pi[r(S_w)^2 - r_w^2]H\phi}{Q_t}\left[\frac{S_w}{F_w}\right]_{S_{wx}} \qquad \text{C- 14}$$

Considering a pore space or throat in the formation with a particle of a particular size (Dpi) and shape flowing through it along a streamline as shown in figure C-2(b); the conditions for the particle to settle within the pore space are:

4. Its settling velocity must be equal to or greater than the critical settling velocity.

5. It must have traveled through an average vertical distance approximating to the pore radius within a time equal to the residence time in the pore volume.
6. The diameter of the particle must be less than the pore space diameter.

It is worth noting that the resultant trajectory of the particle along the streamline is always inclined downwards in the gravity direction as it is transported; this is due to the influence of gravity and the density difference between the particle and the filtrate. The particle therefore has a critical settling velocity equaling:

$$\boldsymbol{V_c = \frac{r_p}{t_c}} \qquad \text{C- 15}$$

The mean hydraulic tube diameter of the formation is given by Carman-Kozeny equation (Civan, 2007):

$$\boldsymbol{D_h = 4\sqrt{2\tau}\sqrt{\frac{k_0}{\phi_0}}} \qquad \text{C- 16}$$

τ is the tortuosity of the formation. This implies that the approximate radius of the pore can be represented by Equation C-17, assuming tortuosity equals unity for this analysis:

$$\boldsymbol{r_p \approx \sqrt{\frac{8k_0}{\phi_0}}} \qquad \text{C- 17}$$

$$\boldsymbol{v_c = \frac{1}{t_c}\sqrt{\frac{8k_0}{\phi_0}}} \qquad \text{C- 18}$$

Substituting for the residence time from Equation C-14 into C-15, critical settling velocity of the transported particle for radial flow can then be obtained as:

$$\boldsymbol{v_c = \frac{Q_t}{\pi[r(S_w)^2 - r_w^2]H\phi_0}\left[\frac{F_w}{S_w}\right]_{S_{wx}}\sqrt{\frac{8k_0}{\phi_0}}} \qquad \text{C- 19}$$

The Stokes equation for particle settling velocity for laminar flow is given by:

$$\boldsymbol{v_s = \frac{g(\rho_s - \rho_l){D_p}^2}{18\mu}} \qquad \text{C- 20}$$

The Stokes equation represents the settling velocity of a particle falling through a still fluid. Therefore, for a dynamic fluid, in other for particle settling to take place its Stokes velocity has to be greater than the minimum velocity required for its transport which is given by the particles critical settling velocity (Equation C-19). With this noted a condition for particle transport was developed to determine the transportable particle size of the water flood at any given injection rate and time.

To prevent particle settling: $v_s < v_c$ and for particle to be deposited: $v_s = v_c$

$$\boldsymbol{\frac{g(\rho_s - \rho_l){D_p}^2}{18\mu} < \frac{Q_t}{\pi[r(S_w)^2 - r_w^2]H\phi_0}\left[\frac{F_w}{S_w}\right]_{S_{wx}}\sqrt{\frac{8k_0}{\phi_0}}} \qquad \text{C- 21}$$

$$D_p < \sqrt{\frac{18Q_t\mu}{\pi\phi_0[r(S_w)^2 - r_w^2](\rho_s - \rho_l)gH}\left[\frac{F_w}{S_w}\right]_{S_{wx}}\sqrt{\frac{8k_0}{\phi_0}}} \quad \text{C- 22}$$

This equation gives the transportable particle size. Therefore the diameter of deposited particles for radial flow geometry can be obtained thus:

$$D_{pc} = \sqrt{\frac{18Q_t\mu}{\pi\phi_0[r(S_w)^2 - r_w^2](\rho_s - \rho_l)gH}\left[\frac{F_w}{S_w}\right]_{S_{wx}}\sqrt{\frac{8k_0}{\phi_0}}} \quad \text{C- 23}$$

A power-law distribution of particle size in the formation was adopted after sensitivity analysis.

$$D_p(r) = ar^{-N} \quad \text{C- 24}$$

Injectivity Decline Model Development

The aim of this model is to capture the impact of the accumulation of deposited particles over time in the porous media on the porosity and permeability of the formation which has a great impact on the injectivity performance of an injector. The model assumes the following: (1) the main mechanism of particle deposition is sedimentation and does not consider the effect of particle erosion and re-entrainment due to increased interstitial velocity. (2) The flow of particles in the filtrate is laminar (N_{Re}<<1). (3) Injected particles are spherical. It incorporates radial flow away from the well in which the Darcy's velocity (q_t) varies with distance. The area under the curve in figure 6(a) represents the average transportable particle size at a given time.

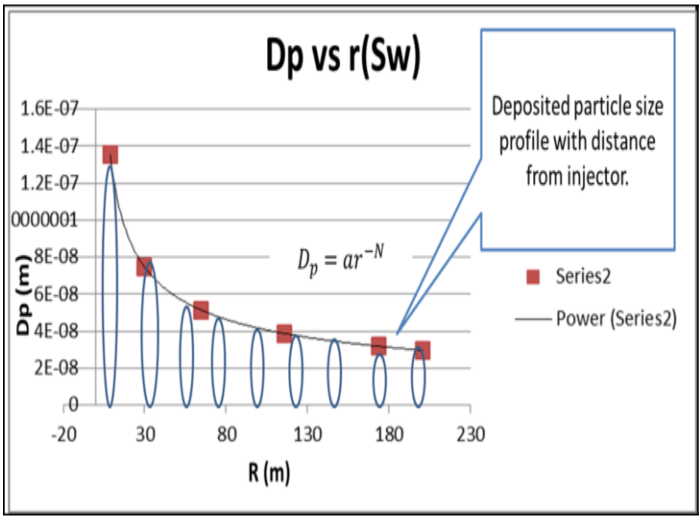

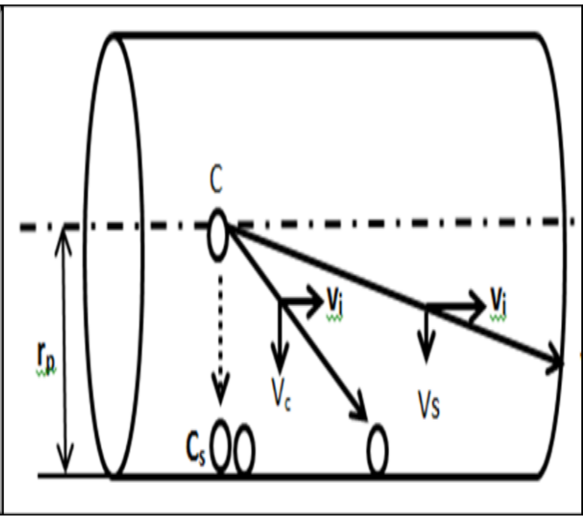

Figure C- 3: (a) Profile of transported/deposited particles with distance. (b) the accumulation of injected particles in a pore space

Volume of each particle transported: $V'_{trans} = \frac{\pi D_{pti}^3}{6}$ **C- 25**

The total volume of Transported particulates: $V_{trans} = n_s V'_{trans}$ **C- 26**

n_s is the population of suspended particles of size D_{pti}.

The average transportable particle diameter is gotten by integrating along the curve of deposited particles' diameter (Equation C-24) with respect to radial distance as shown below:

$$\overline{D_p} = \frac{1}{r(S_{wf})-r_w}\int_{rw}^{r(S_{wf})} D_p(r)dr \qquad \text{C- 27}$$

Put Equation C-24 into C-27:

$$\overline{D_p} = \frac{1}{r(S_{wf})-r_w}\int_{r_w}^{r(S_{wf})} ar^{-N}dr$$

$$\overline{D_p} = \frac{1}{r(S_{wf})-r_w}\left[\frac{a[r]^{1-N}}{1-N}\right]_{r_w}^{r(S_{wf})}$$

$$\overline{D_p} = \frac{a}{(1-N)[r(S_{wf})-r_w]}\left[r(S_{wf})^{1-N} - r_w^{1-N}\right] \; ; \qquad For\ r(S_w) \neq r_w \qquad \text{C- 28}$$

r(S $r(S_{wf})$ is the distance of the shock front from the injector at a particular time during water flooding.

$$r(S_{wf}) = \sqrt{\frac{Q_t t}{\pi H \phi}\left[\frac{dF_w}{dS_w}\right]_{S_{wf}} + r_w^2} \qquad \text{C- 29}$$

For an approximate solution, N can be taken to be approximately equal to **1.0** as observed from different sensitivities runs carried out on model considering radial flow geometry. With this noted, our function of deposited particles (Equation C-24) with distance will become: $D_p(r) = ar^{-1}$. The average transportable particle at an instant of time will then be given by:

$$\overline{D_p} = \frac{1}{r(S_{wf})-r_w}\int_{r_w}^{r(S_{wf})} ar^{-1}dr$$

$$\overline{D_p} = \frac{a}{r(S_{wf})-r_w} ln\left(\frac{r(S_{wf})}{r_w}\right) \qquad For\ r(S_w) \neq r_w \qquad \text{C- 30}$$

In order to obtain the volume of transportable particles, the area occupied by the transported particles flowing in a pore space is determined. A power-law distribution was also adopted to represent the area of transported particles, assuming spherical particles, as a function of radial distance as illustrated in figure C-4a and b. This function, when integrated with respect to distance gives the volume of transportable particles for a given number of pore volumes of water injected.

$$A_{trans} = \pi D_p(r)^2 \qquad \text{C- 31}$$

$$A_{trans} = \pi(ar^{-N})^2 = \pi a^2 r^{-2N}$$

$$A_{trans} = \alpha r^{-\beta} \qquad \text{C- 32}$$

$$\alpha = \pi a^2 \; ; \qquad \beta = 2N \qquad \text{C- 33}$$

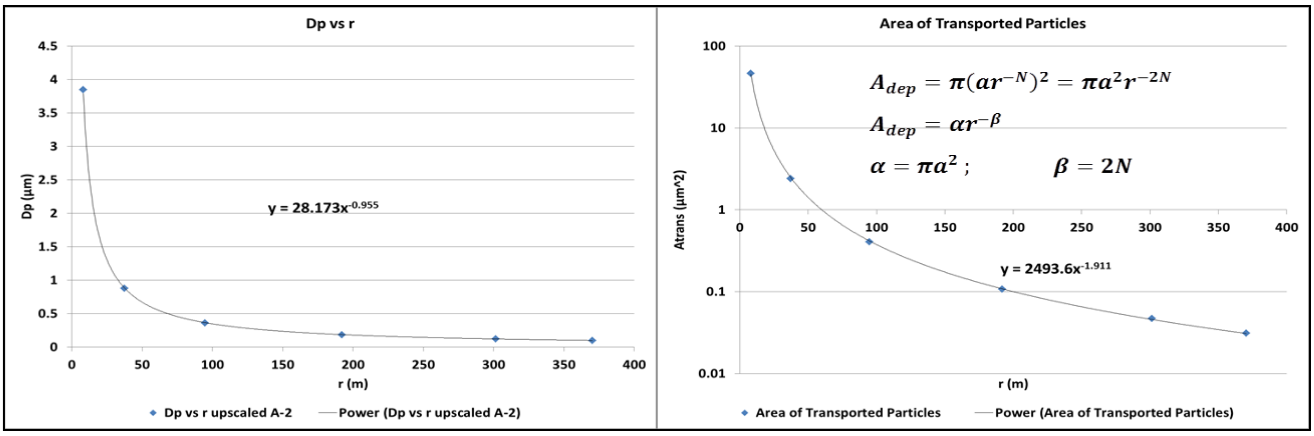

Figure C- 4: (a) size of transported particles against distance. (b) Area of transported particles against distance

The volume of transported particles can be obtained by integrating the area of transported particles (equation C-32) with respect to radial distance:

$$V''_{trans} = \alpha \int_{r_w}^{r(S_{wf})} r^{-\beta} dr$$

$$V''_{trans} = \alpha \left[\frac{r^{1-\beta}}{1-\beta}\right]_{r_w}^{r(S_{wf})}$$

$$V''_{trans} = \left\{\frac{\alpha}{1-\beta}\right\} \left[r(S_{wf})^{1-\beta} - r_w^{1-\beta}\right] \quad \text{C- 34}$$

Equation C-34 above gives the volume of transported particles for a given number of pore volumes of water injected.

$$W_{inj} = W_{id} V_p; \qquad W_{id} = \frac{W_{inj}}{V_p} \quad \text{C- 35}$$

W_{id} is the dimensionless number of pore volume of water injected (PVI), W_{inj} is the cumulative water injected and V_p is the pore volume. For radial flow:

$$1PV = V_p = \pi r_e^2 H \phi_o \quad \text{C- 36}$$

Therefore, the volume of particles transported in a pore volume (1PV) of water injected can be obtained using the following simple conversion:

$$(W_{inj} = W_{id} V_p) \equiv V''_{trans}$$

$$\therefore \left(1PV = V_p\right) \equiv \frac{V''_{trans}}{W_{id} V_p} \times V_p = \frac{V''_{trans}}{W_{id}} \quad \text{C- 37}$$

Putting equation C-34 for V''_{trans} into equation C-43 we have:

$$V_{tid} = \frac{1}{W_{id}} \left\{\frac{\alpha}{1-\beta}\right\} \left[r(S_{wf})^{1-\beta} - r_w^{1-\beta}\right] \quad \text{C- 38}$$

V_{tid} is the dimensionless number of transported particles. This implies that the total transportable solids in suspension can be obtained thus:

$$V_{trans} = V_{tid} V_p \quad \text{C- 39}$$

$$V_{trans} = \frac{\pi r_e^2 H\phi_o}{W_{id}}\left\{\frac{\alpha}{1-\beta}\right\}\left[r\left(S_{wf}\right)^{1-\beta} - r_w^{1-\beta}\right] \quad \text{C- 40}$$

Similarly the volume of deposit of a particular size D_{pi} is: $V'_{dep} = \frac{\pi D_{pi}^3}{6}$ C- 41

The total volume of deposited particulates:

$$V_{dep} = n_t V'_{dep} = \left(V_{pinj} - V_{trans}\right) \quad \text{C- 42}$$

The cumulative water injection: $W_{inj} = Q_t t B_w$ C- 43

The injected particle volume: $V_{pinj} = CQ_t t B_w$ C- 44

$$V_{pinj} = CW_{inj} \quad \text{C- 45}$$

C is the volume fraction of injected particles in the filtrate and n_t is the population of each deposits of specific diameter (D_{pi})

The dimensionless number of pore volumes of injected particles:

$$V_{pid} = CW_{id} = \frac{CQ_t t B_w}{\pi re^2 H\phi} \qquad in\ m^3/PV \quad \text{C- 46}$$

The dimensionless number of deposits can be obtained thus:

$$V_{did} = V_{pid} - V_{tid} \quad \text{C- 47}$$

$$V_{dep} = V_{did} V_p \quad \text{C- 48}$$

Subtracting equation C-44 from equation C-51, the volume of deposits can be obtained thus:

$$V_{dep} = CQ_t t B_w - \frac{\pi r_e^2 H\phi_o}{W_{id}}\left\{\frac{\alpha}{1-\beta}\right\}\left[r\left(S_{wf}\right)^{1-\beta} - r_w^{1-\beta}\right] \qquad m^3 \quad \text{C- 49}$$

But porosity is given by: $\phi = \frac{PV}{Bulk\ volume} = \frac{V_p}{V_b}$ C- 50

For radial flow geometry: $V_b = \pi r_e^2 H$ C- 51

Remaining porosity: $\phi_{rem} = \phi_o - \phi_{dep} = \left[1 - \frac{\phi_{dep}}{\phi_o}\right]\phi_o$ C- 52

$$\frac{\phi_{rem}}{\phi_o} = \left[1 - \frac{\phi_{dep}}{\phi_o}\right] \quad \text{C- 53}$$

$\O_{dep}$ is the fraction of pore space occupied by deposits.

$$\phi_{dep} = \frac{V_{dep}}{V_b} \quad \text{C- 54}$$

$$\frac{\phi_{rem}}{\phi_o} = 1 - \frac{1}{\phi_o \pi r_e^2 H}\left(CQ_t t B_w - \frac{\pi r_e^2 H\phi_o}{W_{id}}\left\{\frac{\alpha}{1-\beta}\right\}\left[r\left(S_{wf}\right)^{1-\beta} - r_w^{1-\beta}\right]\right) \quad \text{C- 55}$$

The porosity and permeability of a given formation can be reasonably correlated using the power law (Adler et al, 1990) (Lawal et al, 2011) given as:

$$k\ \alpha\ \phi^n \quad \text{C- 56}$$

This implies that Permeability impairment due to deposition of suspended particulates can be represented thus:

$$\frac{k_{rem}}{k_o} = \left(1 - \frac{1}{\phi_o \pi r_e^2 H}\left(CQ_t t B_w - \frac{\pi r_e^2 H \phi_o}{W_{id}}\left\{\frac{\alpha}{1-\beta}\right\}\left[r\left(S_{wf}\right)^{1-\beta} - r_w^{1-\beta}\right]\right)\right)^n \qquad \text{C- 57}$$

Determination of Volume Filter Coefficient of the Formation

The volume filtration coefficient will be determined by coupling Buckley leveret fractional flow theory to deep bed filtration (DBF) theory using the mass balance equation of the flowing solids. In this application the porous media is conceptualized as a homogenous filter bed with a capability of trapping and retaining transported particles. The filtration coefficient is referred to as the rate constant for particle deposition in the formation and it is a dynamic quantity that changes with the amount of previously deposited particles (Wennberg and Sharma, 1997).

The form of the mass balance equation for the flowing solids is as given below:

$$\phi_o \frac{\partial C_s}{\partial t} + q_t(r)\frac{\partial C_s}{\partial r} = -\frac{\partial C_p}{\partial t} \qquad \textbf{C- 58}$$

$$\frac{\partial C_p}{\partial t} = \lambda \mathbf{q}_t(r) C_s \qquad \textbf{C- 59}$$

Equation C-59 is obtained from deep bed filtration theory.

C_s is the volume concentration of the injected suspended solids (vol/vol), C_p is the concentration of deposits per unit bulk volume and λ is the volume filtration coefficient, L^{-1}.

Equation C-59 becomes:

$$\phi_o \frac{\partial C_s}{\partial t} + q_t(r)\frac{\partial C_s}{\partial r} = -\lambda \mathbf{q}_t(r) C_s \qquad \textbf{C- 60}$$

The filtration coefficient varies with the concentration of deposited particles and is a function of the fluid velocity. This implies that it depends on the concentration of injected particle. A rise in the concentration of injected particles causes a corresponding rise in the amount of deposited particles. For this analysis, this coefficient will be taken as a fitting parameter representing the rate of particle capture of the formation.

The boundary conditions and solution to equation C-60 are given by:

$$C_s(r) = 0; \quad r \leq 0 \qquad \text{C- 61}$$

$$C_s(r) = C_0 e^{-\lambda r}; \quad r > 0 \qquad \text{C- 62}$$

Equation C-61 and C-62 above explains that the concentration of the flowing solids (suspension), from deep bed filtration theory, is zero in front of the water front and decays exponentially behind the front respectively.

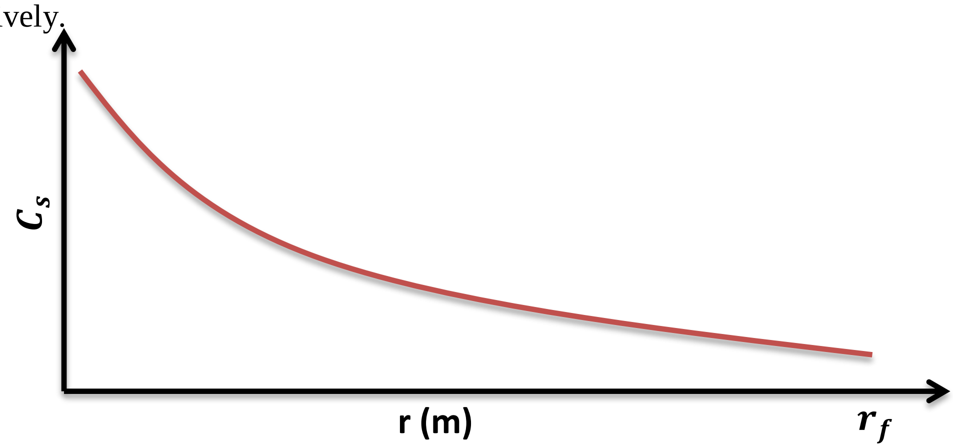

Figure C- 5: a plot showing the profile of concentration of suspended particles with distance.

With this noted, the average concentration of particles behind the front at any time can be obtained by performing a simple integral of equation C-62 with respect to distance:

$$\overline{C_s} = \frac{C_o}{r_f - r_w} \int_{r_w}^{r_f} C_0 e^{-\lambda r} dr \qquad \text{C- 63}$$

$$\overline{C_s} = \frac{-C_o}{\lambda(r_f - r_w)} \left\{ e^{-\lambda r} \right\}_{r_w}^{r_f} \qquad \text{C- 64}$$

$$\overline{C_s} = \frac{C_o}{\lambda(r_f - r_w)} \left\{ e^{-\lambda r_w} - e^{-\lambda r_f} \right\} \qquad \text{C- 65}$$

C_s gives the volume of particles in suspension per unit pore volume (Pang and Sharma, 1997), therefore equation C-65 gives the average volume of particles in suspension per unit pore volume.

In order to determine the filtration coefficient, the average volume of particles in suspension per unit pore volume behind the front will be matched to the volume of transportable particles per unit pore volume (equation C-38) obtained from fractional flow theory described in the previous section given by:

$$V_{tid} = \frac{1}{W_{id}} \left\{ \frac{\alpha}{1 - \beta} \right\} \left[r(S_{wf})^{1-\beta} - r_w^{1-\beta} \right]$$

As observed from both equations, λ is the only unknown which cannot be determined directly, hence it is determined using iteration as a matching parameter of both equations. This method will be applied using well A-2 data sets in appendix D.

Linear Flow Model Development and Model Sensitivities

The assumptions made for linear flow model development is same as that made for radial, the difference is that this model considers the flow of fluid at constant total flow rate, constant surface area of flow and pore scale displacement. Taking a snapshot of the porous media at a particular time t_c and considering different particles moving at different speeds across each plane of saturation behind the shock front as shown in figure C-6, Equation C-66 gives the particle speed as a function of a constant plane of saturation.

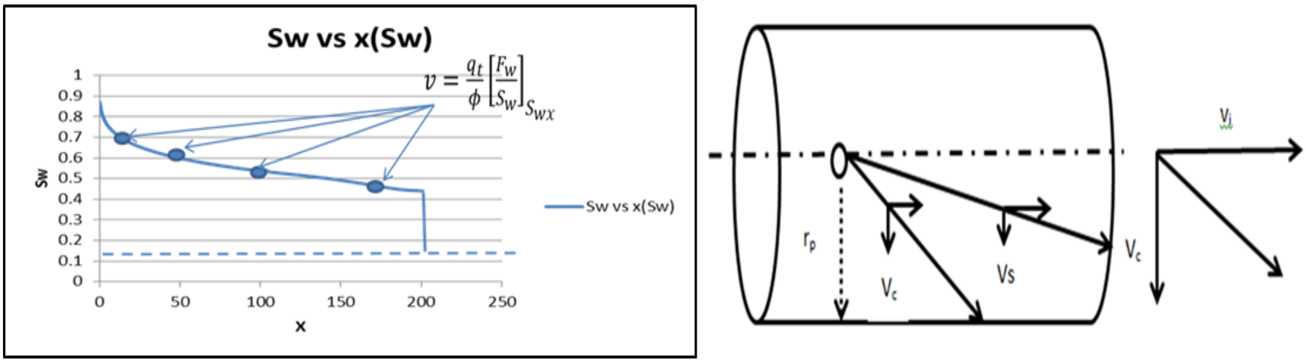

Figure C- 6: (a) Particle distribution on a constant plane of saturation (left). (b) Particle trajectory in a pore space

$$v = \frac{q_t}{\phi}\left[\frac{F_w}{S_w}\right]_{S_{wx}} \qquad \text{C- 66}$$

q_t is the Darcy velocity.

This implies distance of the particles at any point and time is: $x(S_w) = \frac{q_t t}{\phi}\left(\frac{\partial F_w}{\partial S_w}\right)_{S_{wx}}$ **C- 67**

The residence time of the particle can be obtained thus:

$$t_c = \frac{x(S_w)}{v} = \frac{\phi x(S_w)}{q_t}\left[\frac{S_w}{F_w}\right]_{S_{wx}} \qquad \text{C- 68}$$

Considering a particle moving in a pore space, the critical settling velocity (v_c) is the constant vertical component of the velocity it takes the particle to get deposited within the residence time t_c. The diameter of the particle is less than the formation pore diameter. Assuming for deposition to occur particle has to move through distance approximately equal to the pore radius r_p.

The critical settling velocity can be represented by:

$$v_c = \frac{r_p}{t_c} \qquad \text{C- 69}$$

The hydraulic tube pore diameter as suggested by Carman-Kozeny is:

$$\boldsymbol{D_h = 4\sqrt{2\tau}\sqrt{\frac{k_0}{\phi_0}}} \qquad \text{C- 70}$$

This implies that the approximate pore radius is:

$$\boldsymbol{r_p \approx \sqrt{\frac{8k_0}{\phi_0}}} \qquad \text{C- 71}$$

$$\boldsymbol{v_c = \frac{1}{t_c}\sqrt{\frac{8k_0}{\phi_0}}} \qquad \text{C- 72}$$

Substituting equation C-68 into equation C-72 we have:

$$\boldsymbol{v_c = \frac{q_t}{\phi x(S_w)}\left[\frac{F_w}{S_w}\right]_{S_{wx}}\sqrt{\frac{8k_0}{\phi_0}}} \qquad \text{C- 73}$$

The Stokes settling velocity for laminar flow (N_{Re}<<1) is given by:

$$\boldsymbol{v_s = \frac{g(\rho_s-\rho_l)D_p{}^2}{18\mu}} \qquad \text{C- 74}$$

The condition for particle transportation is: $v_s < v_c$ and for particle deposition: $v_s = v_c$

Particles with $v_s > v_c$ are not transportable by the waterflood at a given injection rate and injection pressure. These particles, if present in the formation as loose grains or in the injected water, will constitute a very high resistance flow during injection.

This implies for particle transportation equation C-73 and C-74 can be equated to give:

$$\boldsymbol{\frac{g(\rho_s-\rho_l)D_{pc}{}^2}{18\mu} < \frac{q_t}{\phi x(S_w)}\left[\frac{F_w}{S_w}\right]_{S_{wx}}\sqrt{\frac{8k_0}{\phi_0}}} \qquad \text{C- 75}$$

$$\boldsymbol{D_{pc} < \sqrt{\frac{18q_t\mu}{\phi_o x(S_w)g(\rho_s-\rho_l)}\left[\frac{F_w}{S_w}\right]_{S_{wx}}\sqrt{\frac{8k_0}{\phi_0}}}} \qquad \text{C- 76}$$

Generally it can be represented as:

$$\boldsymbol{D_{pc} < \sqrt{\frac{18q_t\mu}{t_c g(\rho_s-\rho_l)}r_p}} \qquad \text{C- 77}$$

D_{pc} gives the size of the particles that will be deposited at different distances from the injector well in the porous media at any given instant of time. From this it can be inferred that the deposited particle profile for any given flow rate and time can be estimated using the equation:

$$D_{pc} = \sqrt{\frac{18q_t\mu}{\phi_o x(S_w) g(\rho_s - \rho_l)} \left[\frac{F_w}{S_w}\right]_{S_{wx}} \sqrt{\frac{8k_0}{\phi_0}}} \quad \text{C- 78}$$

This equation holds true for constant flow rate and constant surface area of flow.

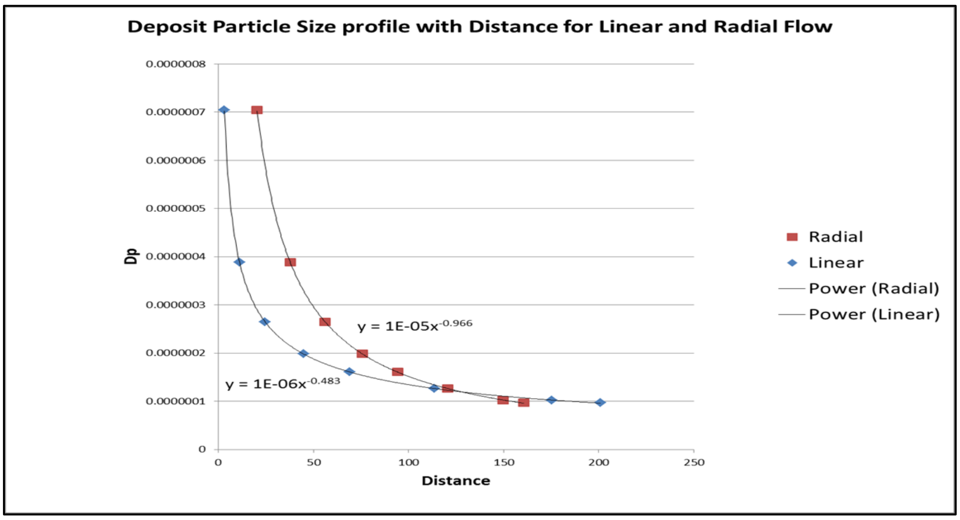

Figure C- 7: Comparison Linear and radial realization of the deposited particle profile model.

Comparison (figure C-7) is carried out under same condition of injection rate, viscosity, time and for a water wet reservoir. As can be observed from the figure above the radial flow model predicts particles to be displaced further into the formation. This could be owing to the fact that in radial flow geometry the interstitial velocity of the filtrate is a function of the radial distance covered by the front and different planes of constant saturation. This velocity is usually high at the immediate vicinity of the injector wellbore region but decreases rapidly as we move away from this region. This tends to push particles further away from the injector at the start of injection. In conclusion from both model realizations and sensitivity analysis carried out on them the profile of transported/deposited particles with distance in the porous media can be represented with a general function for both radial and linear flow geometry given by:

$$D_p(r) = ar^{-N} \quad \textbf{C- 79}$$

Linear Flow Permeability Impairment Model

Permeability impairment model equations will be summarized for linear flow models using similar assumptions and steps used in the radial flow geometry.

The average transportable particle diameter:

$$\overline{D_p} = \frac{1}{x_f}\int_0^{x_f} D_p(x)dx \quad \textbf{C- 80}$$

$$D_p(x) = ax^{-N}$$

$$\overline{D_p} = \frac{1}{x_f}\int_0^{x_f} ax^{-N}dx$$

$$\overline{D_p} = \frac{1}{x_f}\left[\frac{ax_f^{\,1-N}}{1-N}\right]$$

$$\overline{D_p} = \frac{a}{1-N}\,x_f^{\,-N}; \qquad N \neq 1 \qquad \text{C- 81}$$

x_f is the distance of the shock front from the injector at a particular time during water flooding.

Similar to the radial flow model:

$$A_{trans} = \alpha x^{-\beta} \qquad \text{C- 82}$$

$$V''_{trans} = \frac{\alpha}{1-\beta}x_f^{1-\beta} \qquad \text{C- 83}$$

Therefore the volume transported per unit pore volume is:

$$V_{tid} = \frac{\alpha}{W_{id}(1-\beta)}x_f^{1-\beta} \qquad \text{C- 84}$$

Total volume of transported particles (field scale): $V_{trans} = V_{tid}V_p$

For linear flow geometry: $V_p = AL\phi_o$

$$Vtrans = \frac{AL\phi_o}{W_{id}(1-\beta)}x_f^{1-\beta} \qquad \text{C- 85}$$

This implies that the volume of deposits for linear flow geometry will be:

$$V_{dep} = CQ_t tB_w - \frac{AL\phi_o}{W_{id}(1-\beta)}x_f^{1-\beta} \qquad \text{C- 86}$$

The volume of deposits can now be used to obtain the fraction of permeability available to flow; therefore, the permeability impairment model for linear flow geometry is thus:

$$\frac{k_{rem}}{k_o} = \left(1 - \frac{1}{\phi_o AL}\left(CQ_t tB_w - \frac{AL\phi_o}{W_{id}(1-\beta)}x_f^{1-\beta}\right)\right)^n \qquad \text{C- 87}$$

Equation C-87 gives the permeability impairment model for linear flow geometry.

Model Sensitivity

Relative permeability curves were generated considering an oil-wet and water-wet reservoir using Corey's correlation for sensitivity analysis to ascertain the robustness of the developed models to typical range of uncertainties in some process and reservoir variables. Furthermore, model sensitivity was attempted to determine the major drivers of the parameters "a" and "N" in the general function of the deposited particle profile model given by equation C-24 above which was obtained by fitting a regression curve to the plot of deposited particle diameter against distance.

Table C-1: summary of assumed relative permeability data and sensitivity data.

Assumed Rel-Perm Data			General Data	
Parameters	**Water-wet**	**Oil-Wet**	***Qt (m^3/day)***	143.2
Swc	0.25	0.15	***Øo***	0.22
Sor	0.1	0.13	***A (m^2)***	2454
no	2	3	***L (m)***	201
nw	5	2	***h (m)***	6.1
Krow	0.85	0.4	***Ko (mD)***	1000
krw	0.5	0.85	***g (m/s^2)***	9.81
uo	1	1	***ρl (kg/m^3)***	900
uw	0.5	0.5	***ρs (kg/m^3)***	2900
M	1.18	4.25	***Bw***	1

A summary of the parameters used for the sensitivity and the assumed parameters are given in table C-1.

$$k_{rw} = k_{rw}(S_{or})\left[\frac{S_w - S_{wc}}{1 - S_{wc} - S_{or}}\right]^{n_w} \qquad \textbf{C-88}$$

$$k_{ro} = k_{ro}(S_{wc})\left[\frac{1 - S_w - S_{or}}{1 - S_{wc} - S_{or}}\right]^{n_o} \qquad \textbf{C-89}$$

$$F_w = \frac{1}{1 + \frac{Kro\,\mu_w}{\mu_o\,Krw}} \quad ; \qquad M = \frac{\mu_o\,Krw_{max}}{Kro_{max}\,\mu_w} \qquad \textbf{C-90}$$

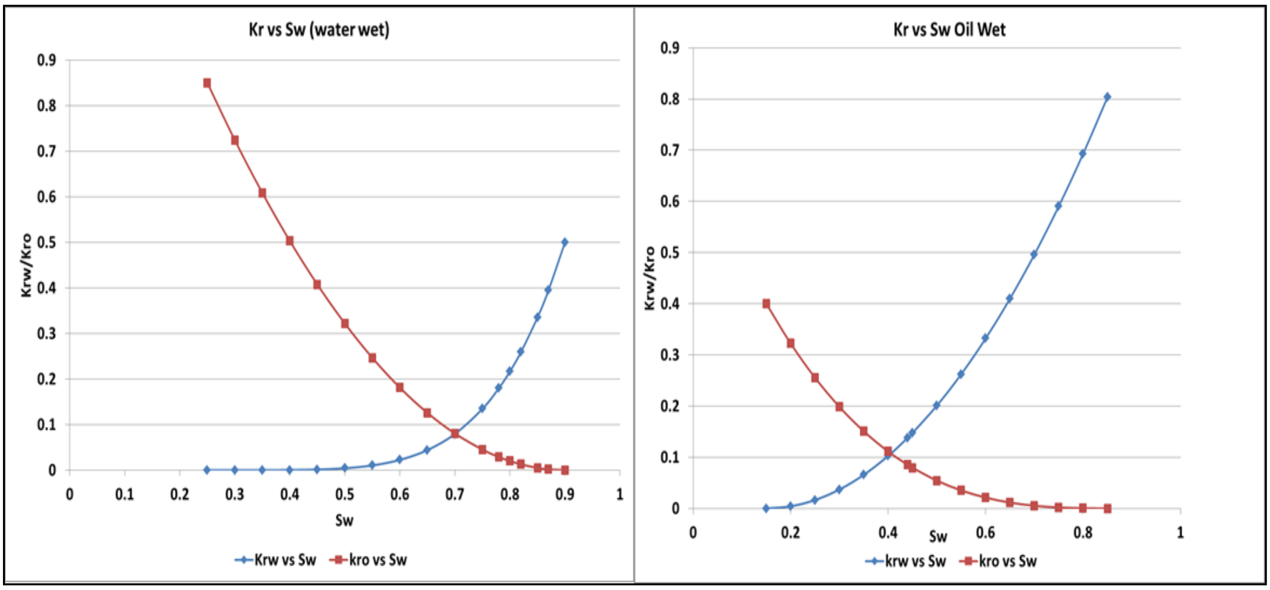

Figure C- 8: Relative permeability curves generated for sensitivities. (a) Water-wet (left). (b) Oil-wet (right)

In order to determine this, the response of the model to reservoir wettability, time, injection rate, particle size, viscosity of the filtrate, and formation permeability was critically studied. The sensitivity study was carried out using the linear flow model.

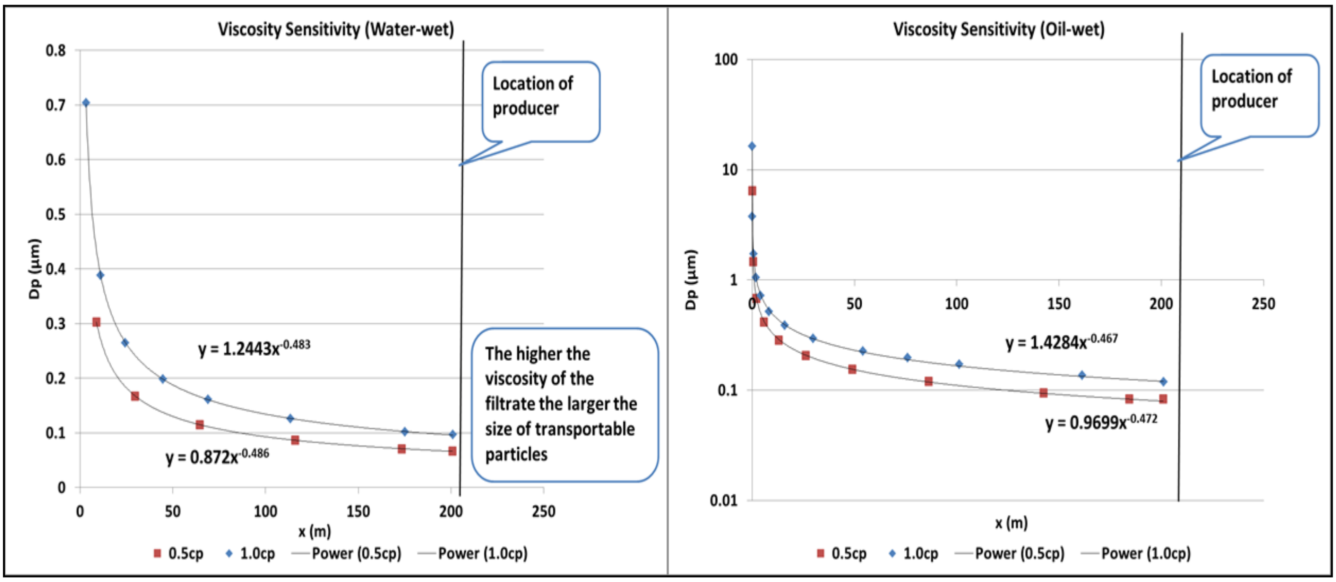

Figure C- 9: results from the wettability and viscosity sensitivity analysis. (a) water-wet (left) (b) Oil-wet (right)

Sensitivity on Formation Permeability

From the plot in figure 13 (b), the higher the permeability of the formation, the higher the injectivity of the injectors and the greater the flood solid carrying capacity. This can be visualized as a movement in the curve upwards with increase in formation permeability from 100 – 10,000mD. This is marked by a corresponding increase in the amount of transportable particle (signified by an increase in the area under the curve. As observed from the regression curves fit to the data, the value of "N" does not change with change in formation permeability, a change only affects the value of "a" which sweeps the curve up when permeability increases and down when there is permeability impairment or reduction.

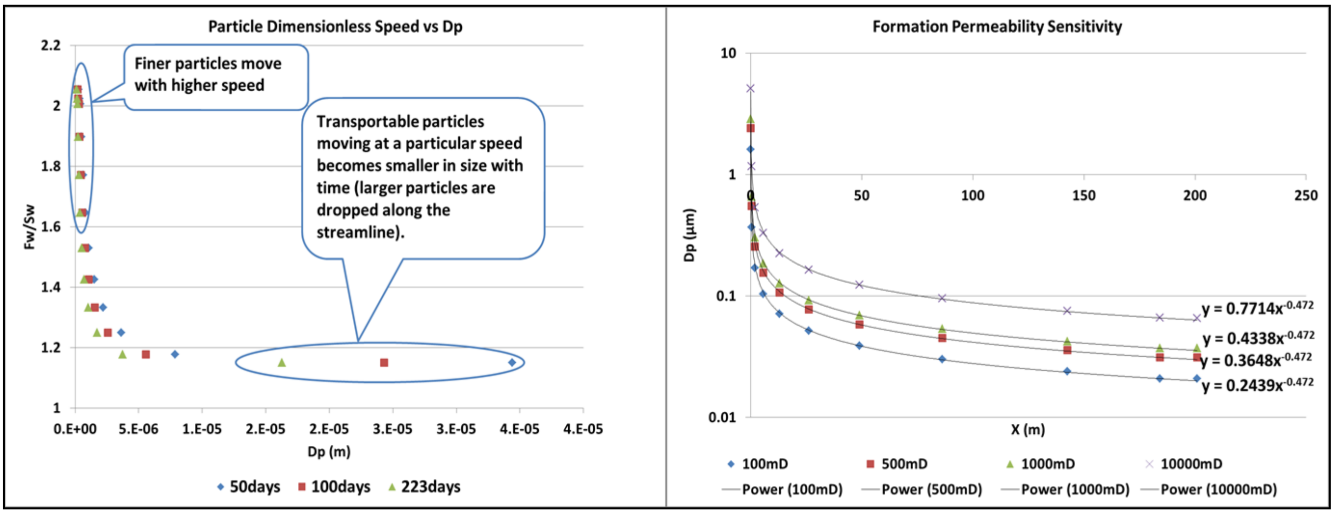

Figure C- 10*: (a) Particle dimensionless speed against diameter (left). (b) Formation Permeability Sensitivity (right)*

Sensitivity on Particle Residence Time

The residence time of a particle does not change with time but depends on the particle size, speed, density and injection rate. It changes with alteration of the system's volume (pore radius) and a change in the viscosity of the injected water. This effect will be investigated in this section using the field relative permeability data sets.

From figure C-11 (a), it can be observed that a reduction in viscosity of the injected water, which could be due to an increase in its temperature as it migrates into the reservoir, causes a corresponding decrease in the residence time (t_c) of transported particles; this leads to their early deposition at the near-wellbore region of the injector resulting in severe permeability impairment. It is noted that the residence time of a 0.05µm particle is 1047days, 1076days, and 2095days at injected water viscosities of 0.5cp, 0.8cp and 1.0cp respectively. The effect of temperature on the viscosity of the injected water is not considered in this analysis.

Additionally, a decrease in formation permeability (reduction in pore radius) owing to accumulation of deposits in the porous media over time leads to a corresponding decrease in particles' residence time, as a result of this, particles accumulate closer to the near-wellbore region of the injector inducing rapid decline in injectivity. This is illustrated in figure C-11 (b), the residence time of a 0.05µm particle is 655days, 926days, and 1048days at formation permeability of 500mD, 1000mD and 1280mD respectively.

Conclusively, the residence time of a particle is a very important factor that determines how far into the formation the particle will travel before it gets deposited, hence it should be determined for an optimized design of water treatment facilities in the planning of a water flood project considering the pore distribution in the formation to know the range of suspended particles which if injected into the porous media will have negligible contribution to permeability impairment and the injectivity performance of an injector.

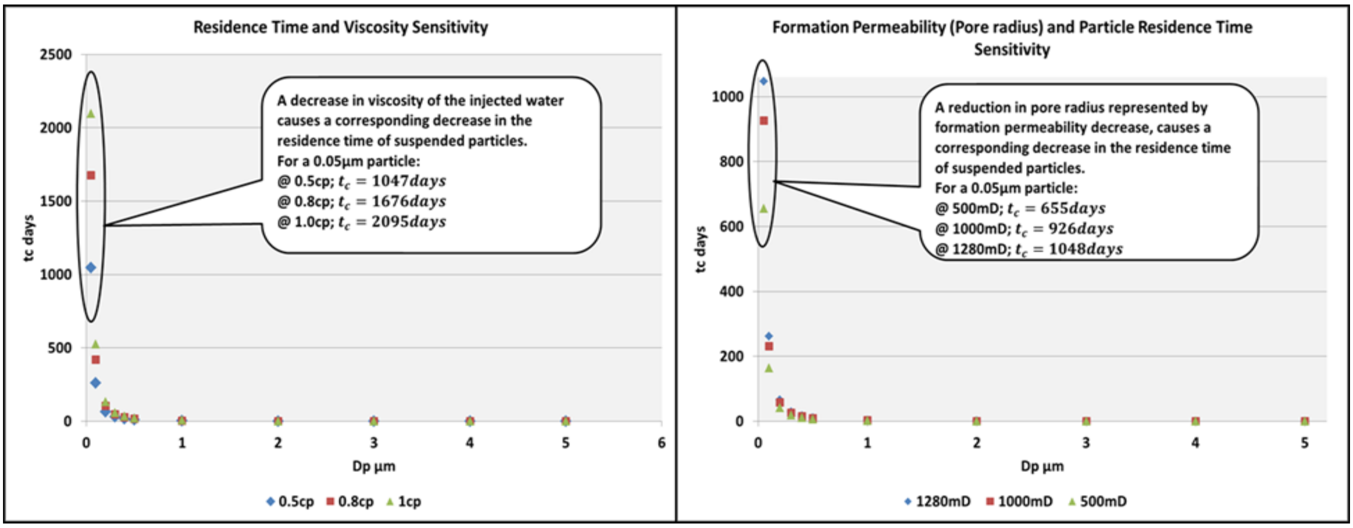

Figure C- 11: (a) particle residence time to viscosity of injected water sensitivity. (b) Particle residence time to formation permeability sensitivity.

Appendix D: Model Validation

The deposited particle profile model (Equation11) was applied to the field to determine where the various sizes of injected particles will settle out, both the linear and radial realizations were used for this analysis. They were both used to predict the transportable solids and the expected particle sizes that will be deposited at different points in the porous medium away from the injector using the field realized relative –permeability datasets: rock curve and the upscaled pseudo-curve. These relative permeability curves which were generated using different Corey parameters to capture the effects of uncertainties in the extent of reservoir wettability and fluid mobility as shown in figure E-2 and table E-1.

The methodology used for the validation exercise is listed below:

1. The values of the variables "a" and "N" from equation 12 are determined from fractional flow analysis using the field's relative permeability data set. For the validation done in this section, the field's upscaled rel- perm curve (figure E-2) will be adopted.

2. A correlation for "a" (figure D-1a) as a function of Q_t was obtained using the rate window (Q_{tmin} - Q_{tmax}) of the extracted decline period of the well. This function for well A-2 (Equation D-1) generated values of "a" within less than 1% error.

$$\boldsymbol{a = 7 \times 10^{-7} Q_t^{0.4782}} \qquad \text{(D- 1)}$$

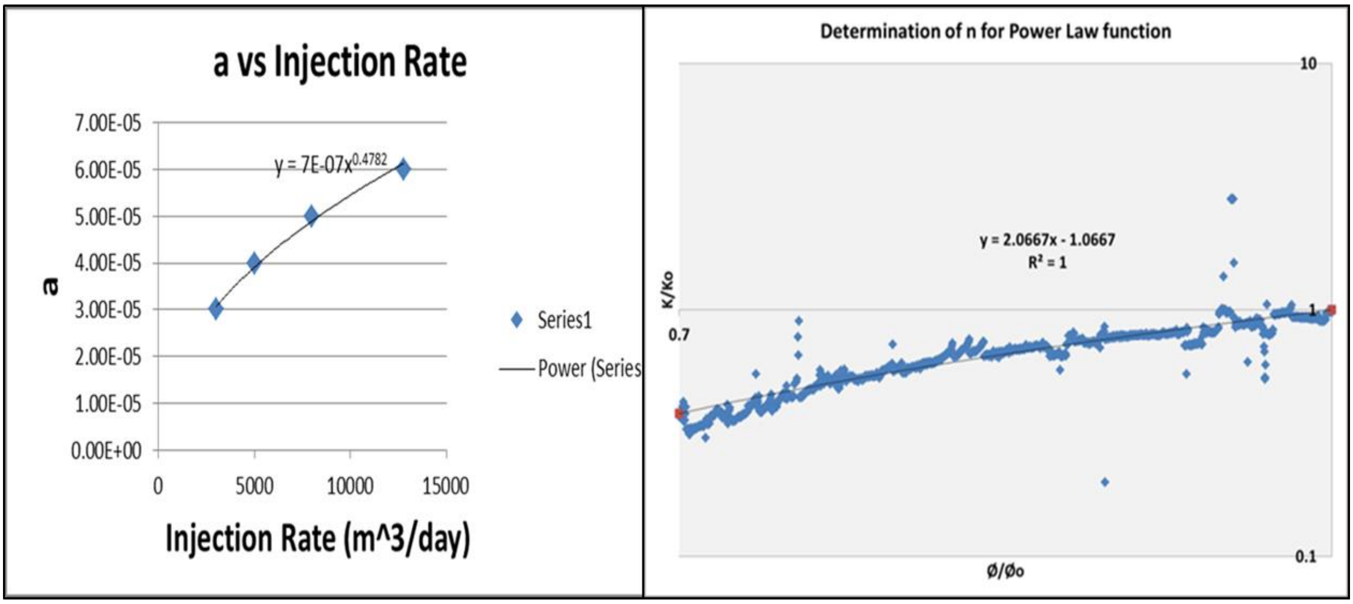

Figure D- 1: (a) correlation for a as a function of injection rate; (b) Determination of exponential coefficient for impairment model power law exponent

3. $\alpha = a^2$ while β is obtained from fractional flow analysis using the field's rel-perm data set. ($\beta = 2N$). α and β are used to obtain the volume of particles transported and the volume deposited (Eq. 15 and 17 respectively).

4. These volumes are now substituted into the impairment model equation (Equation 18) to obtain the fractional porosity remaining of the formation.

5. The porosity-permeability power-law correlation exponent from Equation C-56 is determined by fitting a regression line to the log-log plot of the ratio of permeability against ratio of porosity.

6. A history match to the injectivity ratio data of an injector in the field is then implemented to validate the impairment model (Equation 18).

$$\boldsymbol{II(t)} = \frac{\boldsymbol{k(t)H}}{\boldsymbol{B_w \mu\left[\ln\left(\frac{r_e}{r_w}\right)+S\right]}} \qquad \textbf{(D- 2)}$$

$$\frac{\boldsymbol{II(t)}}{\boldsymbol{II_o}} = \frac{\boldsymbol{k(t)}}{\boldsymbol{k_o}} \qquad \textbf{(D- 3)}$$

7. Different parameters are used for history matching to capture the required uncertainties in the analysis, assuming constant injected particle concentration.

8. A decline period from the well history is used for analysis.

In order to validate the impairment model using well A-2 and A-3, the first decline period of both wells are selected and used for analysis. From figure D-2 on the plot of injectivity against time, it can be observed that the trend line fit to the decline period of all the wells (A-1, A-2, and A-3) are parallel and suggesting the same mechanism of impairment is responsible for damage. Results obtained from model validation, sensitivity analysis and field application are reported in the main body of this work.

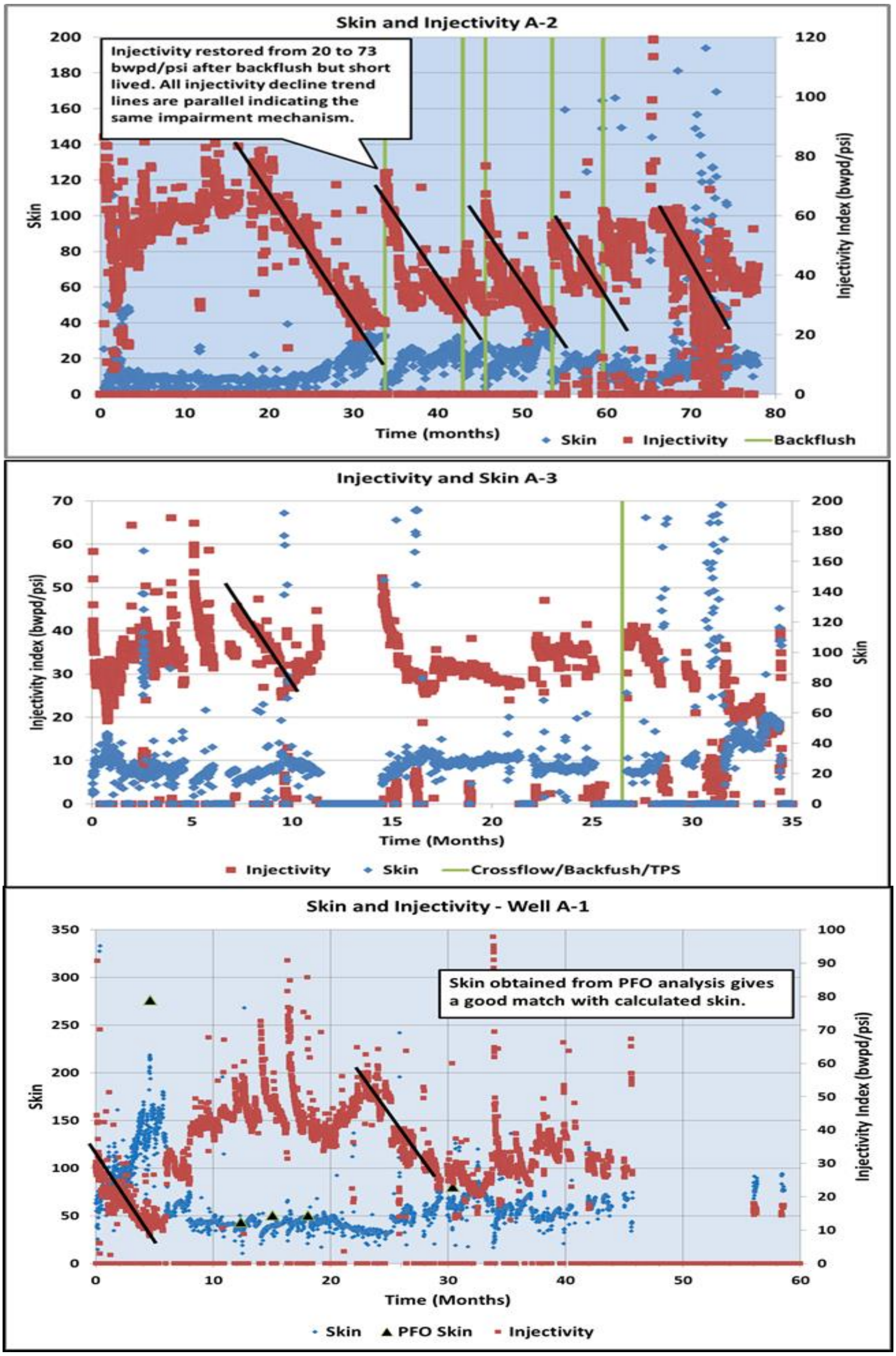

Figure D- 2: Comparison of injectivity decline trend line of wells A-2 (top), A-3, and A-1 (bottom); all trend lines are parallel suggesting the same mechanism of impairment in both reservoirs

Determination of Volume Filtration Coefficient (Field case)

The determination of the formations' filtration coefficient which represents the rate of deposition of particles is applied using data sets from well A-2. The methods applied are as introduced in appendix C. Results obtained are discussed below:

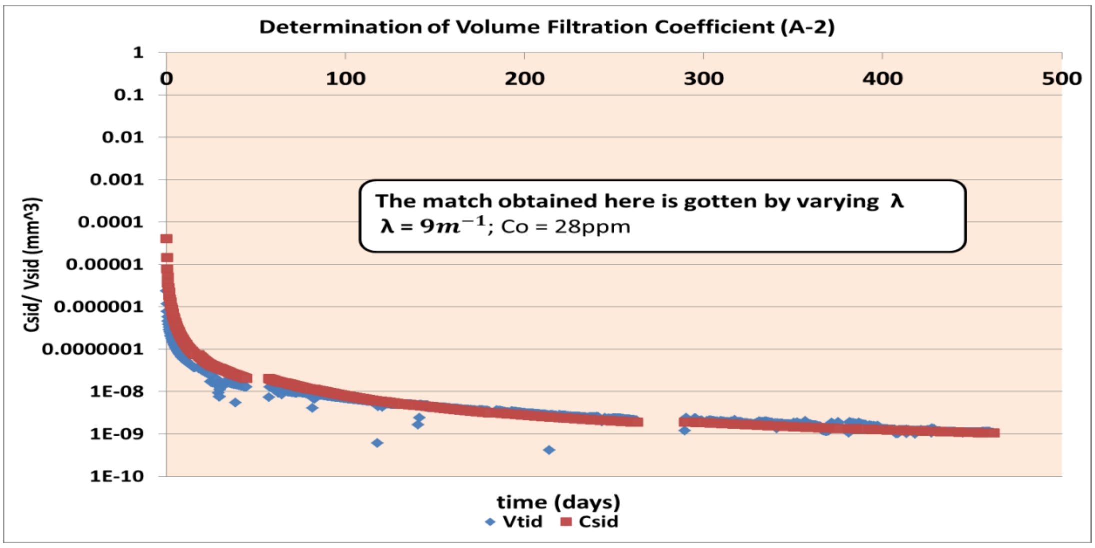

Figure D- 3: a plot showing the obtained match between the volume of transportable as obtained from fractional flow theory and the volume of particles in suspension as obtained from DBF theory.

C_{sid} is obtained from equation C-65 and it is the average volume of particles in suspension per unit pore volume obtained from deep bed filtration theory.

The match obtained from this plot confirms that the volume of transportable particles per unit pore volume obtained from fractional flow analysis can be used to determine the volume filtration coefficient. The result above is for an injected particle concentration of 28ppm. Table D-1 and figure D-4 shows the value of λ obtained for other injected particles concentration (C) for the field. It scan be observed that a higher filtration coefficient will be required to match both curves. This implies that the higher the concentration of injected particles, the higher the rate of particle deposition.

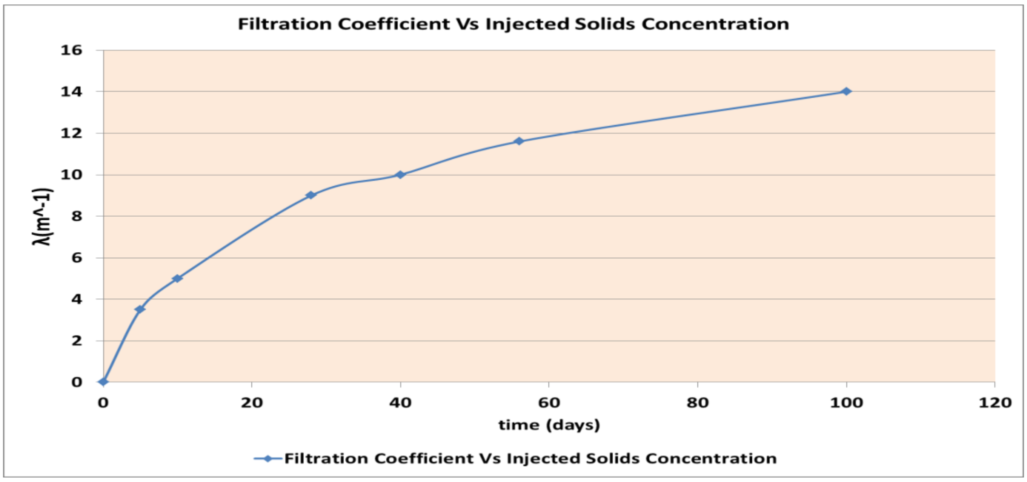

Figure D- 4: plot showing the matched volume filtration coefficient against the injected particles concentration.

Appendix E: Field Case Study

The reservoir being studied is a deepwater reservoir, offshore Niger Delta at a water depth of about 1000m and deposited in a turbidite environment (fine grained mud rich turbidites). Turbidites are clastic sediments transported beyond the continental shelf edge into deep water by sediment gravity flow processes where it is deposited on the continental slope of the basin. It is of Miocene geological age. Refer to table E-1 for the summary of the reservoir characteristics.

It is made up of unconsolidated sandstones which make it difficult to maintain water injectors because injection into this kind of formation is not only used for hydrocarbon recovery and pressure support; it is also used to avoid compaction caused by shear failure of the formation grains. One of the major challenges facing the maintenance of water injectors in unconsolidated reservoirs is sand failure. Although, these sands are multi-Darcy sands they turn loose when injection is performed above their critical velocities. These loose sands present in the formation, over time migrate into pores and throats where they combine with solids from injected water to plug these pores. In order to maintain good injectivity in low permeability reservoirs that are un-fractured, the water quality specification is fundamental. Khodaverdian *et al*, (2010) stated in their work that in order to maintain injectivity in unconsolidated and poorly consolidated sand the injection must be performed under a fracturing regime. It was also pointed out that fracture propagation in unconsolidated sands is associated with multiple branching, channeling and out-of-plane propagation, rather than a single plane of propagation as obtained in consolidated and low permeability reservoirs. Sanding problems induces fracture face skin in unconsolidated reservoirs and this enhances fracture growth and propagation.

In the field under study, the injectors were completed in the hydrocarbon leg of the formation with frac-pack completions. Sea water injection is the secondary recovery method as produced water is not re-injected. This injected seawater contains suspended particulates (sand) and salts which settle out or precipitate in the formation when injected if the water is not properly treated. The impact of scale formation on injectivity is not investigated in this work; only mechanical induced damage is studied.

Diagnostic test performed on the wells (appendix F) indicate that they underwent severe plugging throughout their injection history. The possible cause of this plugging and possible remediation will be proffered in the cause of this study.

Table E- 3: Field relative Permeability data sets		
Parameters	**Rock Curve**	**Upscaled**
Swc	0.1	0.1
Sor	0.1	0.35
no	2	4
nw	4	3
Krow	0.9	0.9
krw	0.6	0.6
uo (cp)	1	1
uw (cp)	0.5	0.5
M	1.3333333	1.333333

TABLE E- 1: STATIC RESERVOIR PROPERTIES	
Fluid Properties	
Gas Gravity (S.G) (air = 1)	0.68
Oil Gravity (°API)	33
Solution Gas-oil Ratio (scf/stb)	737
Bubble Point Pressure (Mpa)	28.9
Original Reservoir Pressure (Mpa)	29.6
Reservoir Temperature (°C)	81
Rock Properties	
Rock Type	Unconsolidated Sandstone
Stratigraphic Unit	Turbidite Systems
Geological Age	Lower Upper Miocene
Porosity Range (fraction)	0.26-0.31
Permeability Range (md)	1000-2000

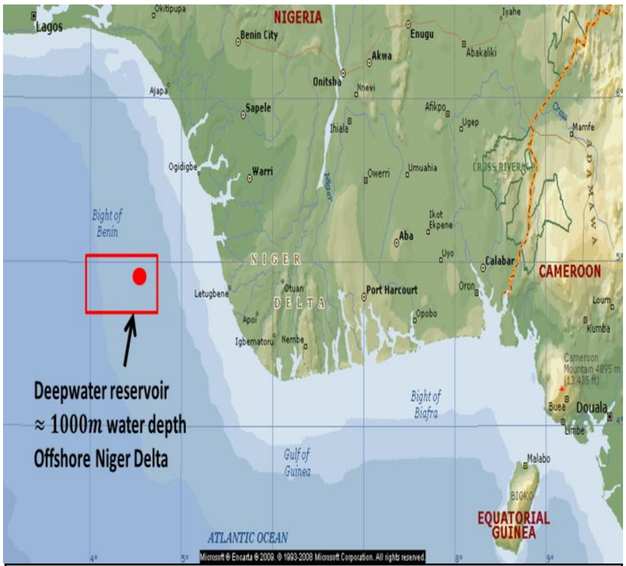

Injector A-1 Completion Interval

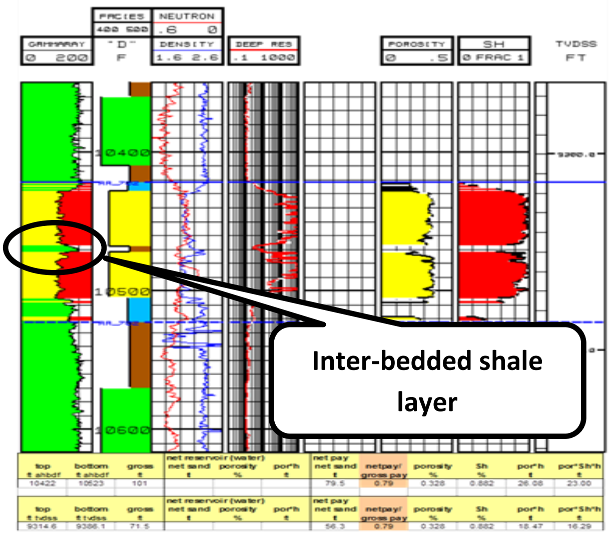

Table E-2: summary of well parameters			
Parameters	A-1	A-2	A-3
Wellbore Radius (m)	0.15	0.15	0.15
Drainage Radius (m)	450	450	450
Perforation Height (m)	23.8	14	14.6
Net-to.gross	79	90	86
Particle Concentration (ppm)	28	28	28
Completion	F&P	F&P	F&P
Current Injection Regime	Fracture	Fracture	Fracture
Sump (mah)	67	425	-
Reservoir	A	B	B

Figure E- 1: Data appraisal: (a) static reservoir properties (Reservoir B; top-left) (b) Field location (top-right). (c) Injector A-1 log and completion interval. (d) summary of well parameters used for analysis.

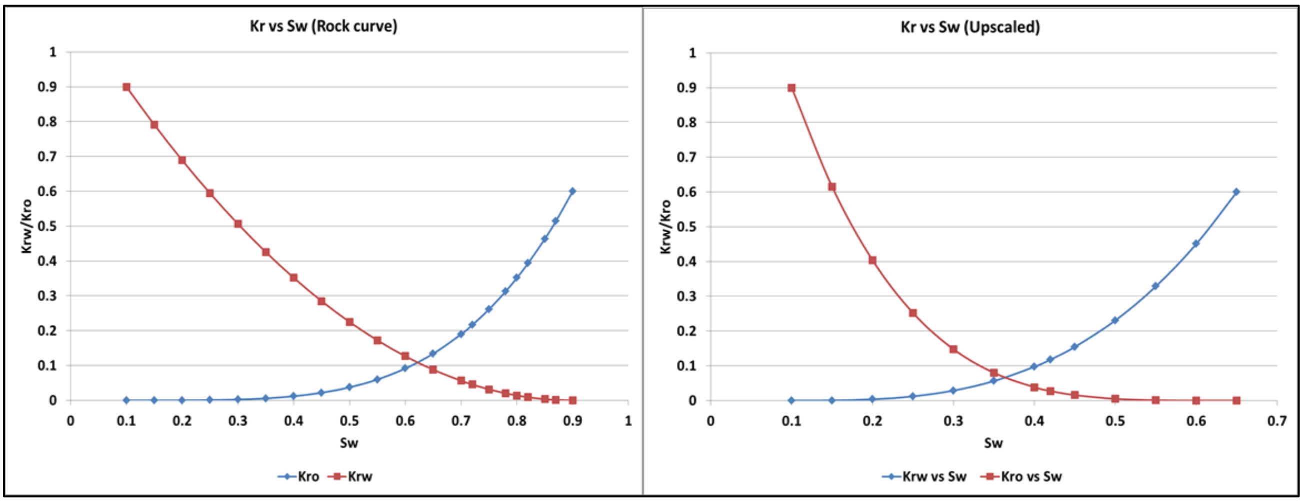

Figure E- 2: field realized relative permeabilty data sets. (a) Rock curve (b) Upscaled pseudo-curve (right)

Field Injectivity Decline Analysis

The deposited particle profile model and the permeability impairment model were applied to the field in order to identify the main mechanism of impairment and proffer some useful recommendations for an optimized operation to reduce the general decline in injectivity recorded.

Back Flush Rate Sensitivity Analysis

Back flush is a remedial technique used in injector wells to clean out trapped particles in the formation (mechanically induced damage). Mechanically induced damage includes: injection of solids and velocity induced damage, that is, fines migration and settling (Bennion et al, 1994). During this process the flow of water through the porous media is reversed. In practice it is mostly carried out by creating a drawdown of about 1000psi about the well completion and allowing the well to produce the fluids for a few barrels. In this section a method to implement an effective and safe back flush operation without compromising the integrity of the cap rock is implemented. The equation of the deposited particle profile model (Equation 11) is modified to obtain a critical rate which could be used for optimized back flush operations.

$$\boldsymbol{Q_c \geq \frac{\pi(r_d^2 - r_w^2)(\rho_s - \rho_l) g H \phi_o D_p^2}{18\mu}\sqrt{\frac{\phi_o}{8k_o}} \qquad r \neq r_w\,; \qquad v_c = \frac{Q_c}{2\pi r_d H \phi_o}} \qquad \textbf{E- 1}$$

The required pressure drawdown for a corresponding back flush rate given the current injectivity (II(t)) of the well is: $\Delta \boldsymbol{P} \geq \frac{\boldsymbol{Q_c}}{\boldsymbol{II(t)}}$ E- 2

Where r_d represents the estimated damage collar radius, Q_c is the critical advective rate (the minimum rate required to transport a particle of sizeD_p) and v_c is the required advective velocity.

In this modification, the particle is at rest and the velocity required to transport it is equal to the critical advective velocity of the receding flood. The main purpose of this application is to analyze the back flush rate required to clean out particles of different sizes that pose an external filter cake threat to the formation in this field ($D_p > 4\mu m$). From figure E-3(a) and b, it can be observed that the required back flush rate increases with the particle size responsible for damage and also with the damage radius. A sensitivity analysis was also done to investigate the impact of viscosity of the receding flood and formation permeability. Figure E-4 (a) shows that the higher the viscosity of the flood, the lower the value of rate required for back flushing. For a 5µm particle, the required back flush rate at an injection water viscosity of 0.5cp is $680m^3/day$ (4000bwpd) and for 1.0cp it is $1300m^3/day$ (8500bwpd). Also from figure E-4 (b), back flush rate increases with decline in formation permeability, this simply implies that a highly impaired formation requires a very high back flush rate. As illustrated, at the initial permeability of the formation, a 5µm particle will require a back flush rate of $1320m^3/day$, these rate becomes $1870m^3/day$ and $5900m^3/day$ at 50% and 5% of the initial permeability respectively.

Conclusively, an effective back flush depends on the current permeability of the formation, the size range of the particles responsible for damage, the viscosity of the receding flood and the current injectvity of the damaged well. A back flush operation could greatly improve the state of the reservoir or worsen it; hence, extra care must be taken when performing this technique.

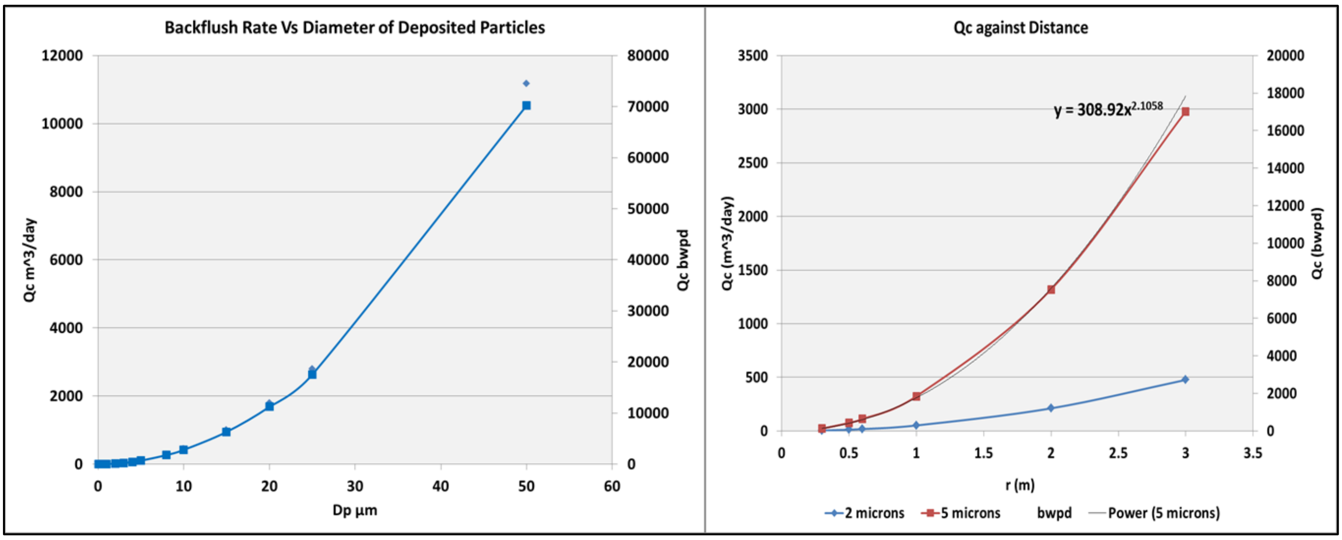

Figure E- 3: (a) Back flush rate versus diameter of deposited particles. (b) Back flush rate against distance

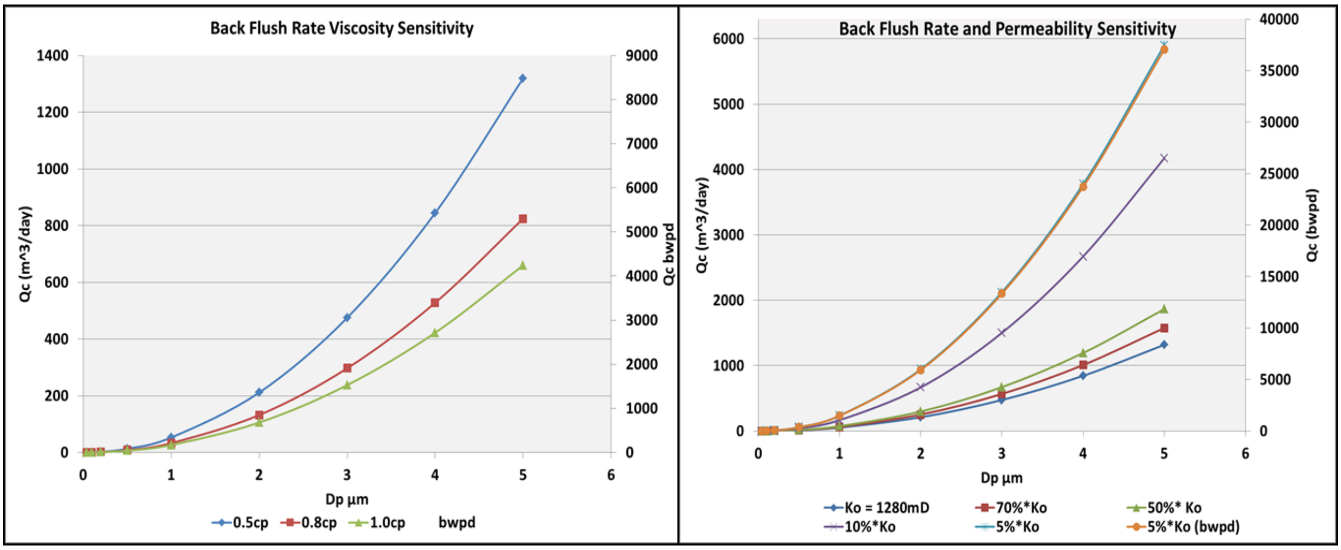

Figure E- 4: (a) back flush rate and water viscosity Sensitivity. (b) Back flush rate and formation permeability sensitivity.

Particle Residence Time Analysis

The injected sea water particles range from **0.04 to 5µm** and the modal particle size is approximately $2\mu m$ as shown in the particle size distribution (figure E-5a). Current injection-water treatment criterion, as illustrated in figure E-5b, aims at having over 95% of the particulates in the injection stream below 5 µm diameter, hence, 5% of the particles in the effluent downstream of the water treatment facility could be greater than this threshold particles size. The impact of these different sizes of particles on injectivity will now be investigated using their residence time in the porous media.

The residence time of the particles is obtained using fractional flow theory and fitting a regression line through a plot of $t_c \; vs \; D_p$ as shown in figure E-6. This analysis can be used to create a tighter water treatment specification which transposes into an optimized water treatment facility design.

The condition for particle deposition and accumulation is: $t_s \leq t_c$. The Stokes settling time is the time it takes a particle to settle in a still fluid, that is, the fluid is assumed to be at rest in a pore as given by equation E-4 (Cheel et al, 2005).

$$t_c = \frac{\pi(r(S_w)^2 - r_w^2)H\phi}{Q_t}\left[\frac{S_w}{F_w}\right]_{S_{wx}} \qquad \text{E- 3}$$

$$t_s = \frac{18\mu_w}{(\rho_s - \rho_l)gD_p^2}\sqrt{\frac{k_o}{\phi_o}} \qquad \text{E- 4}$$

For a 5µm Particle, which is the threshold particle size of the injected sea water, the critical settling time (t_c) equals 0.12 days while its Stokes Settling time (t_s) is 0.04 days. Figure E-7 shows the settling time of the range of particles contained in the injected sea water and predicts that the settling time of particles <0.05µm is >1000days, hence these particles' contribution to injectivity decline is negligible because they are transported deep into the formation within this time while the Settling time of particles

>1μm is <3 days signifying that they are deposited near wellbore where they induce a rapid rate of injectivity decline owing to the build-up of an external filter cake.

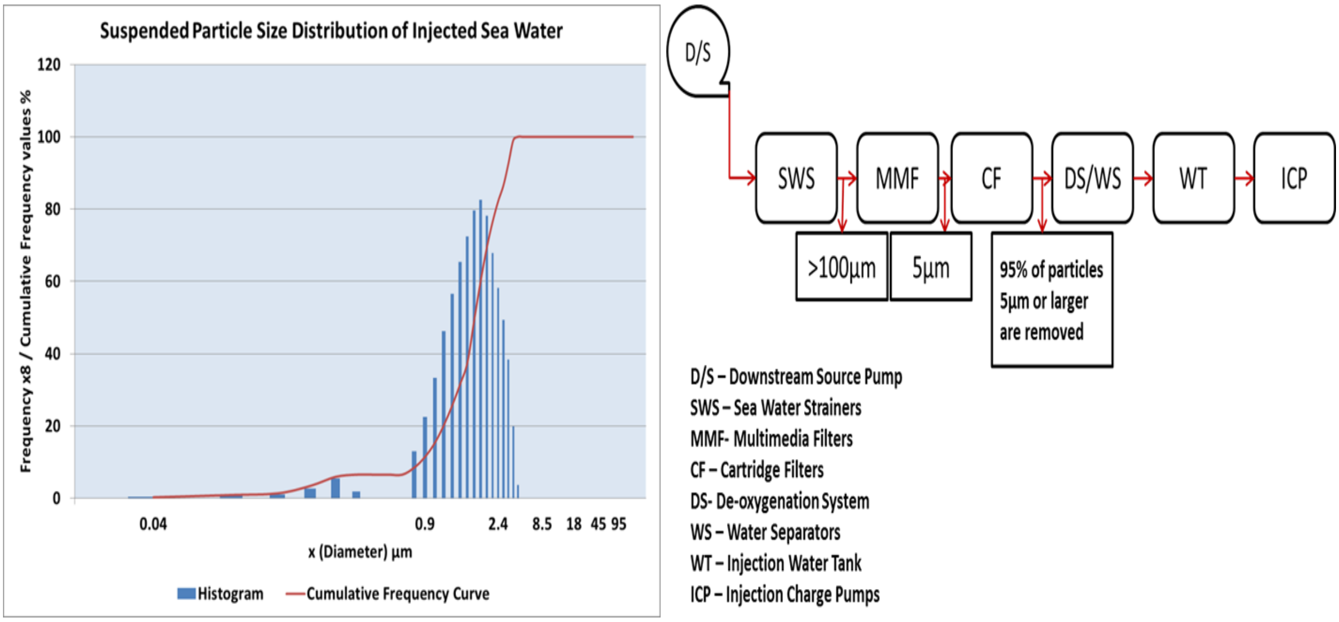

Figure E- 5: (a) a plot showing the particle size distribution of injection water; (b) a diagram showing the Injection water treatment process and criteria.

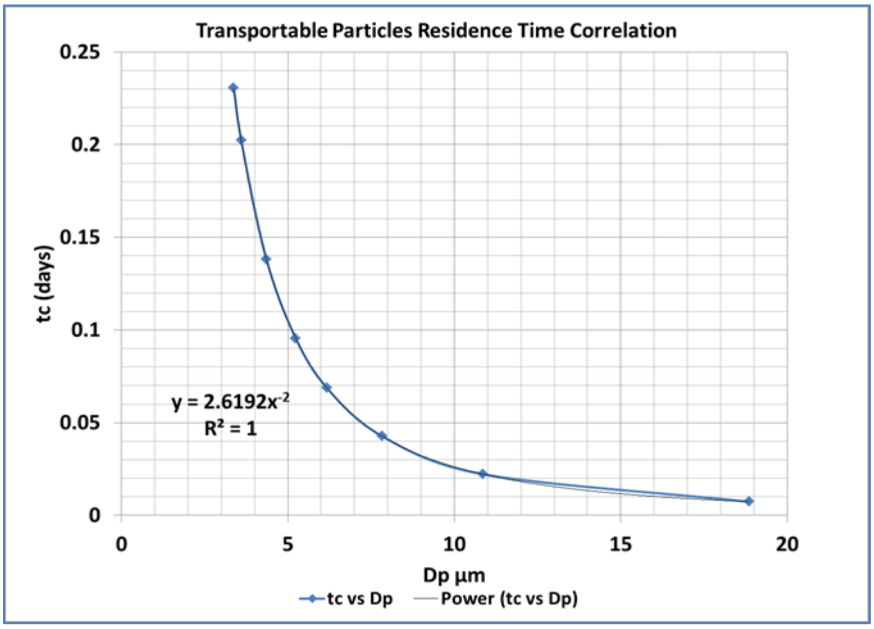

Figure E- 6: a plot showing the particle residence time correlation from fractional flow analysis

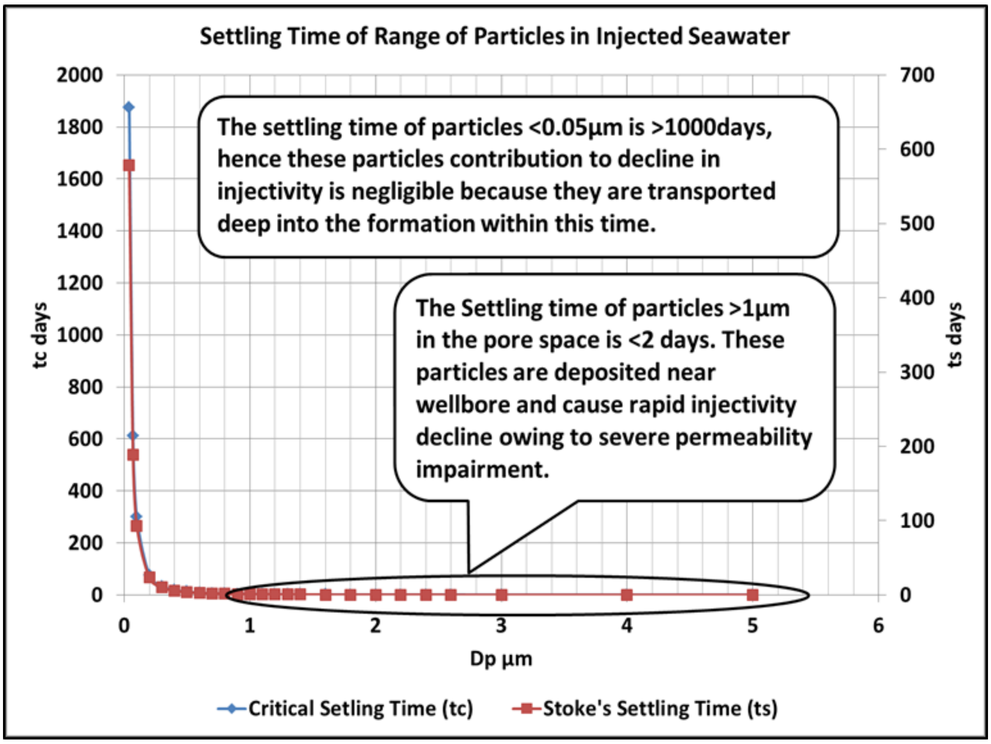

Figure E- 7: Settling times of range of particles in injected seawater

Deposited particle Profile/ Formation Damage Criteria

In this section, the deposited particle profile model is used to obtain an estimate of the distance in which particles of a given size from the injected water, unconsolidated formation and other sources are deposited over time. This is now tied to the 1/3 to 1/7 rule-of-thumb, controlling the bridging phenomenon in the porous media, to determine regions (radius) around the injector wellbore that are prone to external and internal filter cake formation threat. The 1/3 to 1/7 rule-of thumb of particle to pore space diameter ratio can be used to determine the principal mechanism of impairment (either external or internal cake formation) due to different particles deposited at various points away from the injector. The pore space diameter used for this analysis is an approximate one from Carman-Kozeny hydraulic tube model assuming the formation tortuosity equals unity given by:

$$\boldsymbol{\beta} = \frac{\textbf{\textit{Pore throat diameter}}}{\textbf{\textit{Transported Particle diameter}}} = \frac{D_t}{D_p}; \qquad D_h = 4\sqrt{2\tau}\sqrt{\frac{k_0}{\phi_0}} \qquad \text{E- 5}$$

The conditions that will be tested are: $1/\beta > 1/3$ - External Filter Cake formation; $1/3 > 1/\beta > 1/7$- Internal Filter Cake Formation; $1/\beta < 1/7$ - Negligible Filter Cake formation; and Particles with $1/\beta = 1$ cannot penetrate the pore**.**

Figure 19(a) to (d) are different plots of the transportable particles diameter against distance considering both linear and radial flow models and the two relative permeability data sets of the field, that is, the rock curve and the pseudo curve. It can be observed from these plots that particles > 4.5µm have a value of

1/β < 1/3 and are deposited within 4m radius from the injector wellbore at the initial porosity and permeability of the formation, considering an injection rate of $4000 m^3/day$. However, with decline in injection rate and porosity reduction, these particles will get deposited closer to the near-wellbore region where they will get strained or bridge the formation pore throats (internal filter cake formation) while the larger ones get trapped by the formation sand face. Furthermore, the radial flow geometry model predicts particles to be deposited deeper in the formation than that of linear flow geometry. 0.2m in the linear case as compared to 4m in the radial case for particles >4μm as recorded in figure E-8 (c) and (d). This could be because in the radial flow geometry, the interstitial velocity of the flood is a function of the radial distance covered by the front and different planes of constant saturation. This velocity is usually high at the immediate vicinity of the injector wellbore region but decreases rapidly as we move away from this region. Also, the pseudo- curve which is more oil wet predicts a higher particle transport capacity of the flood.

Fines Migration Consideration

The deposited particle profile model is applied here to determine how far away from the wellbore are loose formation grains, due to the unconsolidated nature of the formation, transported. Migration of fines is severe in unconsolidated sandstone formations that contain higher fraction of loosely attached and mobile clays which get detached at injection velocities above their critical interstitial velocity. These fines also turn loose when new fractures are created. The formation grain particle size distribution from the field is shown in figure E-9. Fines (4 - 125μm) get dislodged into the flowing stream at high injection velocities above their critical velocities. The propagation of fines in the porous media is more prominent when the wetting phase of the formation is mobile (Gruesbeck and Collins, 1982; Bennion *et al*, 1994). This implies that fines propagation will be highly imminent the more water wet the reservoir. The particles in the formation can also get fluidized and flushed back towards the water injector during shut-in as a result of water hammer effect at pressures >400psi. Water hammer is a phenomenon that occurs during shut-in or well trip due to a sudden change in fluid velocity which induces pressure transients at the bottom-hole and is recorded and monitored using pressure gauges. They could be used to study the condition of the formation as high recorded water hammer pressures denote a highly impaired formation. These high water hammer pressures causes increased damage to the porous media as illustrated in figure E-10 below where it is observed that higher water hammer pressures are recorded during intense impairment periods. Owing to this fluidization of near-wellbore grains, clays and fines get swabbed past completion screen into the wellbore and accumulate over time leading to the blockage of the completed interval and loss of injectivity. They may also move to pores where they combine with injected solids in plugging these pores leading to injectivity decline.

Also, as discovered in the previous section, these fines are >4µm with a residence time less than a day and their particle-to pore size ratio (β) is greater than 33%, hence, they are major contributors to wellbore/sump fill-up, near-wellbore damage (they get mostly trapped by the formation sand-face), or if they penetrate the pore space they get strained and bridge the pore throat promoting the creation of an internal filter cake which is more damaging and mostly inaccessible by most remediation techniques. Finally, these fines in addition to the injected particles are one of the major contributors to internal fracture damage experienced in the analyzed field.

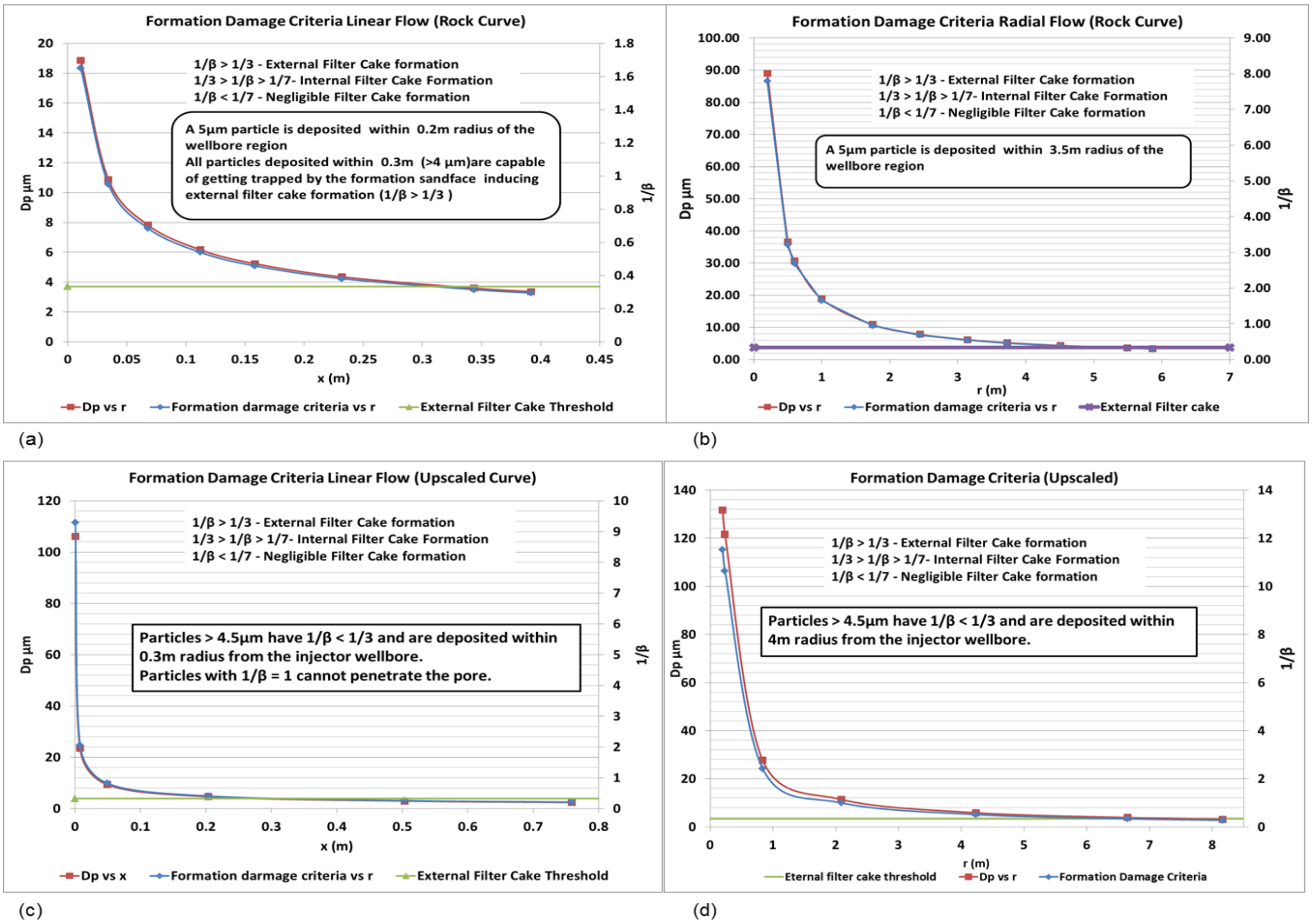

Figure E- 8: plots showing depositional profile of particles transported in the flood. (a) using linear flow model and rock curve. (b) using radial flow model and rock curve. (c) using linear flow model and upscaled curve. (d) using radial flow model and upscaled curve.

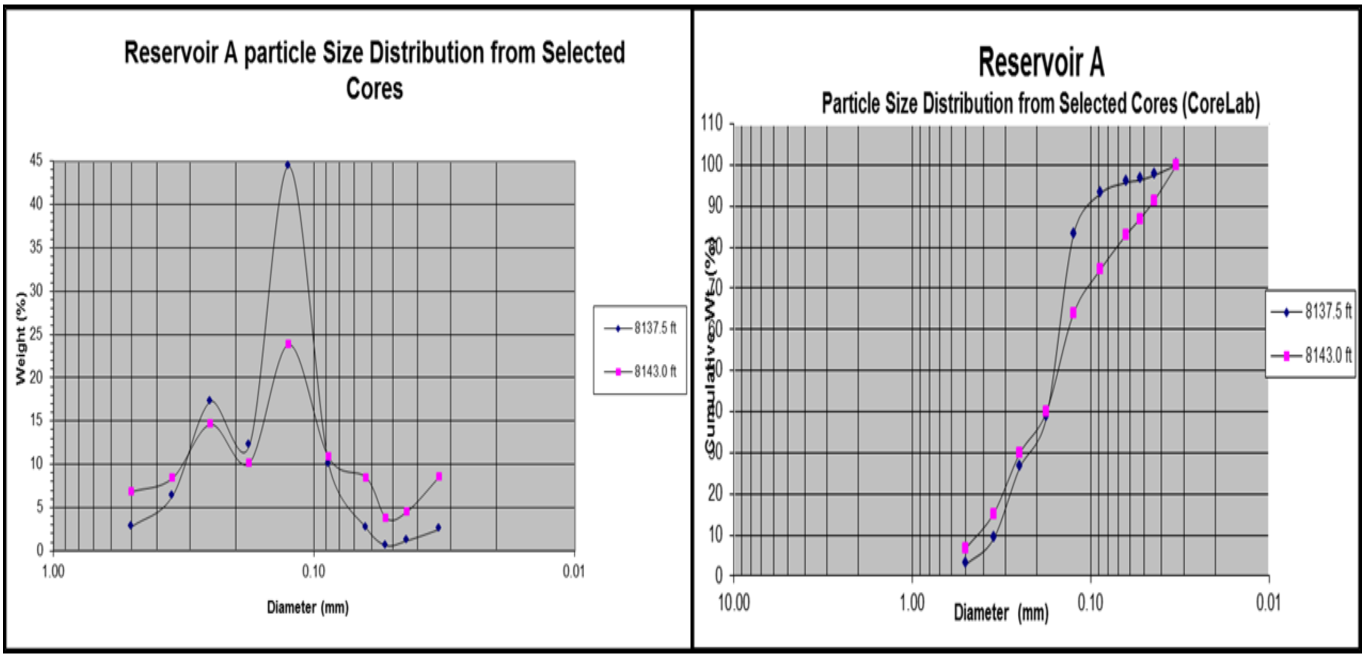

Figure E- 9: Reservoir A particle size distribution

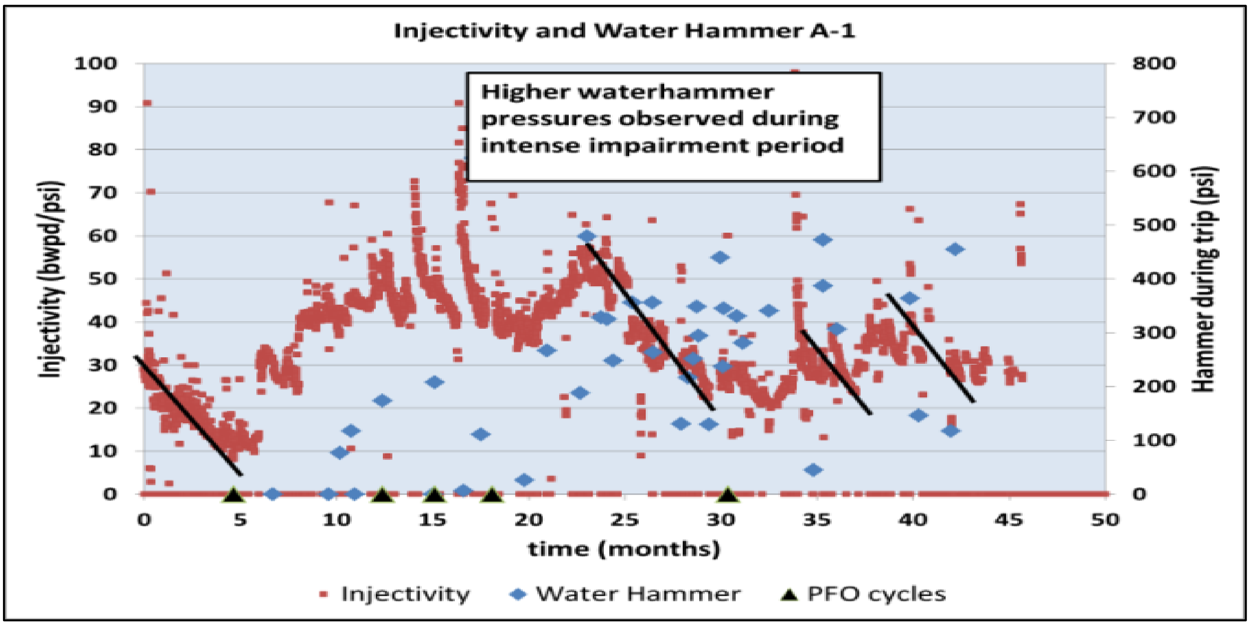

Figure E- 10: plot of injectivity index and water hammer pressures: showing high water hammer pressures during intense impairment period

Appendix F: Well Diagnostic Analysis

This was implemented to ascertain if the wells which data sets are used for the analysis are undergoing

Diagnostic Tools

Pressure-Rate Plot

This is the plot of bottom hole injection pressure against injection rate. It is mainly used in differentiating between wellbore plugging and fracture plugging. During matrix injection, the bottom hole pressure (BHP) is a direct function of injection rate and it increases as rate increases. This pressure remains fairly constant as rate varies once the formation is fractured. This constant pressure is called the fracture propagation pressure. The varying rate during this constant pressure period (fracture injection) shows that fracture growth laterally and transversely is occurring and this is observed by an increase in rate. (Ojukwu & van den Hoek, 2004)

A horizontal line along the FPP in principle can be used to define a fracture of a given formation. An observed alteration in the pressure regime of the formation could cause these parallel lines shift towards each other denoting gradual plugging of the formation while a wide gap between successive parallel lines could be interpreted as a sign of sudden plugging. Generally formation plugging can be observed as an increase in pressure occurring simultaneously with a decrease in rate (Ojukwu & van den Hoek, 2004). Figure F-1 illustrates this method of impairment diagnosis.

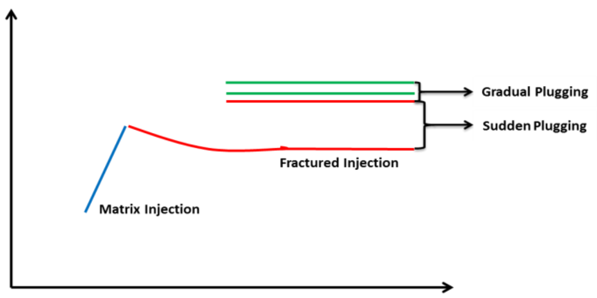

Figure F- 1: Pressure-rate plot diagnosis (culled from: Ojukwu & Hoek, 2004)

Hall Integral

The Hall plot analysis is a steady-state method, originally developed to analyze the water injection well performance in water flooding applications in oilfields (Hall, 1963). It permits a means of monitoring the water injectivity and its efficiency continuously and also provides a means to observe the change in some reservoir properties that occur during injection (Hall, 1963). The Halls method was based on Darcy's law for steady-state and the Newtonian flow of a well centered in a circular reservoir (Ojukwu & van den Hoek, 2004). It is a plot of $\sum(p_w - p_r)dt$ in psi.day against $\sum q_w dt$ in bbl which yields a slope given by:

$$HallSlope_{steadystate} = \frac{141.2\mu_w B_w\left\{\ln\left(\frac{r_e}{r_w}\right)\right\}}{k_w h_{eff}} \qquad \text{F- 1}$$

Ojukwu & van den Hoek, (2004) modified Hall technique by using it to quantify damage skin. This skin concept made it possible to quantify matrix damage/plugging observed at every upward slope or downward slope which shows fracture initiation. Successive downward slopes could be interpreted as fracture propagation or near-wellbore stimulation. If an initial fracture is observed, beyond this point successive upward slopes are interpreted as fracture plugging or wellbore plugging (Ojukwu & van den Hoek, 2004). The modified Hall slope is given as:

$$\boldsymbol{Modified\ Hall\ Slope} = \frac{141.2\mu_w B_w\left\{\ln\left(\frac{r_e}{r_w}\right)-\frac{3}{4}+S\right\}}{k_w h_{eff}} \qquad \text{F- 2}$$

Hall Derivative

Izgec & Shah Kabir, (2007) in their work introduced an analytic derivative method, a new formulation of the Hall analysis, to ascertain variables such as radial distance of the injection bank and pressure at the water/oil interface. Their method also solves the notion of single reservoir pressure assumed by Halls analysis, this is owing to the fact that the original Hall formulation was predicted using the tubing head pressure of the injector well and also ignoring the oil/water interface pressure at the flood front. The signature of the Hall integral is insensitive in revealing clues about subtle changes which may occur during formation fracturing or plugging but it was observed by Izgec & Shah Kabir, (2007) that the derivative of the modified hall integral provides definitive signatures about fracturing or plugging and this can be clearly used to provide unambiguous diagnosis of a well’s performance status when it is used in tandem with the Hall integral. The Hall derivative equation is:

$$D_{HI} = \alpha_1 W_i \left\{\ln\left(\frac{r_e}{r_w}\right) + S^*\right\}\text{-} \qquad \text{F- 3}$$

When both curves are used in tandem the diagnosis that can be carried out are:

1. The curves trace each other under a matrix- dominated flow devoid of fracturing or plugging.
2. The derivative plot goes below the Hall integral during a fracturing regime.
3. The derivative curve goes above the integral curve signifying plugging.

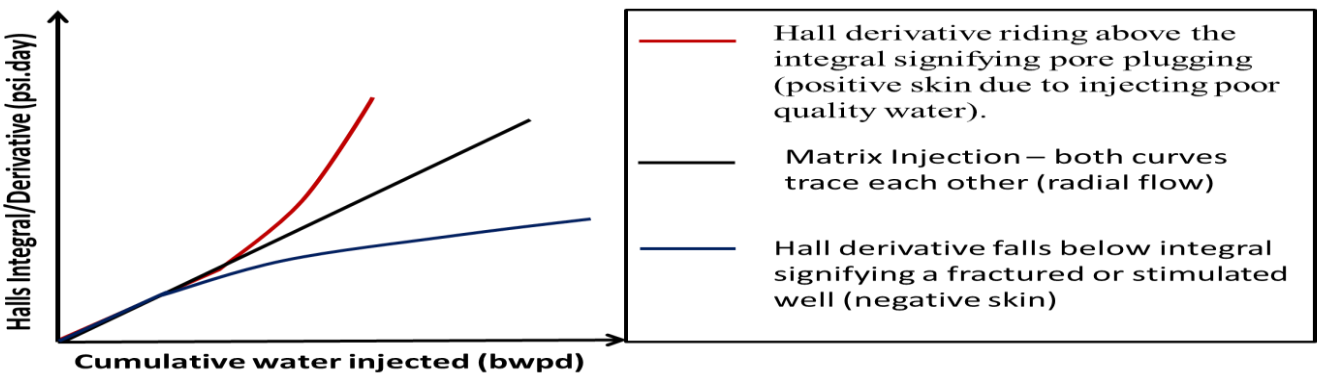

Figure F- 2: Halls Integral and Derivative Injector well Diagnostic analysis

This tool (figure F-2) can be used to monitor the evolution of skin with time unlike its pressure-transient counterpart, where time-derivative of skin is zero, skin is left intact when the cumulative injection derivative of the pseudo steady-state equation is sought (Izgec & Shah Kabir, 2007). The pseudo-skin which represents all resistance to injection can be obtained using the formula:

$$\boldsymbol{S^{*}=\frac{1}{0.868}\left[\frac{b}{m}-\log\left(\frac{k}{\phi\mu c_t r_w^2}\right)+3.23\right]} \qquad \textbf{F- 4}$$

$$\boldsymbol{b=\frac{P_i-P_{wf}}{q_n}} \qquad \textbf{F- 5}$$

$$\boldsymbol{m=\frac{162.6B\mu}{kH}} \qquad \textbf{F- 6}$$

Impedance Plots

This represents the inverse of injectivity plot and it can mostly be used to capture periods of fracture propagation while emphasizing transition periods between matrix and fracture injection regime. A rise in this plot denotes periods of transition from fracture regime of injection to matrix which is caused by severe fracture face skin while a fall signifies a transition from matrix to fracture regime. An extended low period illustrates a period of fracture propagation and growth. This plot will be used as a diagnostic tool to clearly show these different transition periods.

Diagnostic Analysis for Well A-1

Diagnostic analysis for the different wells was carried out using the pressure-rate plot, halls integral and derivative, pressure fall off (PFO) analysis, skin evolution with time and the fluid bank pressure of the injected water over time.

Figure F-3(a) emphasizes three injectivity regimes in the well's injection history: the matrix regime (radial flow), fracture growth and propagation regime and fracture face plugging. All the wells in the field display this kind of behaviour to injectivity. The matrix regime of injection for this injector lasted for 6 months and was marked by a continuous rise in bottom-hole pressure from about 4530psi (31Mpa) to about 6600psi (45.5Mpa), above the formation fracture pressure of 5000Psi (34.5Mpa).

This pressure increase was accompanied by a corresponding increase in injection rate within the first four (4) months of injection from 11,000bwpd ($1752m^3/day$) to about 45,000bwpd ($7165m^3/day$). This period of radial flow in which the bottom-hole pressure is a direct function of the injection rate (figure E-3(b)) was plagued significantly by pore space plugging as observed from the fourth (4) month of injection where it is confirmed by a gradual decline in the injection rate from about 35,000bwpd ($5573m^3/day$) to 12,000bwpd ($1910m^3/day$). The decline in rate was mainly due to plugging of the formation pore spaces which lead to a build-up in pressure that induced the formation of the first fracture which caused a

remarkable increase in injection rate from 12,000bwpd ($1910m^3/day$) to 52,000bwpd ($8280m^3/day$) above the frac-rate of 50,000bwpd ($7962m^3/day$).
In Figure F-3(c) a marked increase in injectivity between the 10th and 20th months from approximately 20bwpd/psi to 50bwpd/psi is observed. This was simultaneously marked by a noticeable decrease in skin from approximately 210 to a value averaging at 20. The decrease in skin was observed to be as a result of the transition from matrix injection (radial flow) regime to fracture injection regime.

The formation of a new fracture can be observed in the 20th month of injection in which there is a rise in injectivity from 35bwpd/psi to 60bwpd/psi. This is an evidence of fracture growth due to build-up in bottom-hole pressure as a result of continuous fracture face plugging by solids from the injected water. The skin used in this plot is the pseudo-skin that represents all kinds of resistance to injection. Furthermore, figure F-3(d) is a plot obtained from the modified Halls integral and derivative which when both curves are used in tandem an un-biased diagnosis of an injector wells performance can be carried out. It is clearly observed from these plots that the Halls derivative curve initially traces the integral at the start of injection signifying matrix injection regime but this regime is plagued by high pore space plugging as the derivative curve rides above the integral few months from the start of injection.

At the start of the fracture regime in the 6th month the derivative moves below the integral for a while (showing the formation of a new fracture). Later on, the derivative plot continually rides above the integral showing significant fracture face plugging.
The impedance plot (figure F-4) follows the same trend as the plot of skin evolution with time (figure F-3 (c)) and clearly depicts the cycle of transitions between matrix and fracture injection regimes. The trend of the impedance plot between the 25th and 30th month suggest a return to matrix injection regime owing to severe fracture face skin.

PFO Analysis (A-1)

Pressure Fall Off analysis data sets for well A-1 was interpreted. Although the data was a bit noisy, it gave more insight into the main cause of injectivity decline in the ailing wells. Signs of possible fracture closure and water hammer effect were identified in the early time of these plot and this went on to confirm that severe formation plugging and stunted fracture growth occurred during the injection history of all the wells
PFO analysis for this well is obtained from test carried out in the following months: 5th, 12th, 15th, 18th, and 30th month. They were all implemented during different injection regimes: 5th – matrix regime, 12th, 15th, and 18th during fracture regime, while the 30th was done during the period of significant fracture face

plugging. With this known, it is expected that these different analyses will give a clearer picture of the events occurring in the reservoir.

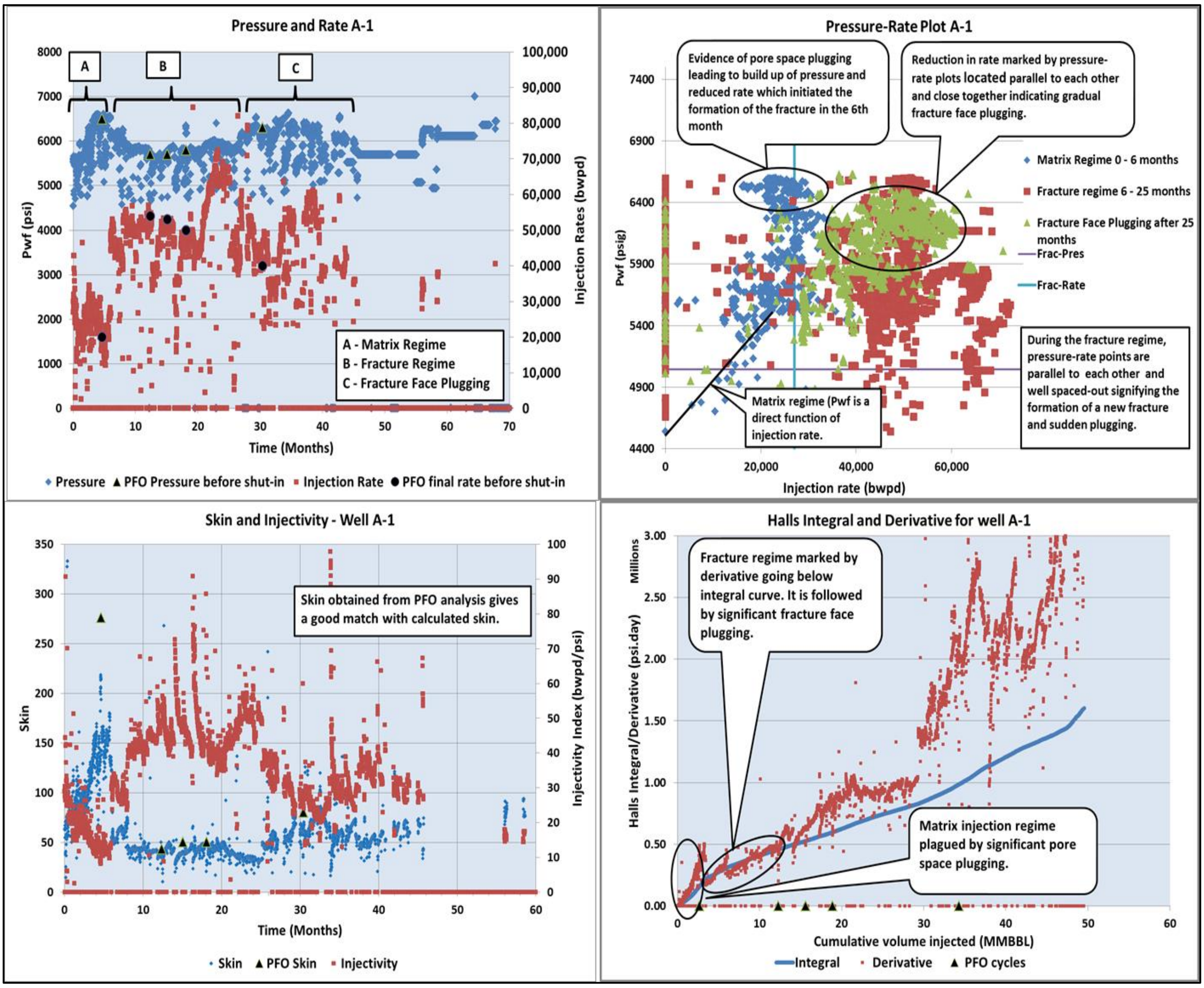

Figure F- 3: (a) Bottom-hole Pressure (P_{wf}) and rate with time (Top-left). (b) Pressure-Rate Diagnostic plot (Top-right). (c) Injectvity index and skin evolution with time (Bottom-left). (d) Modified Halls Integral and Derivative (Bottom-left)

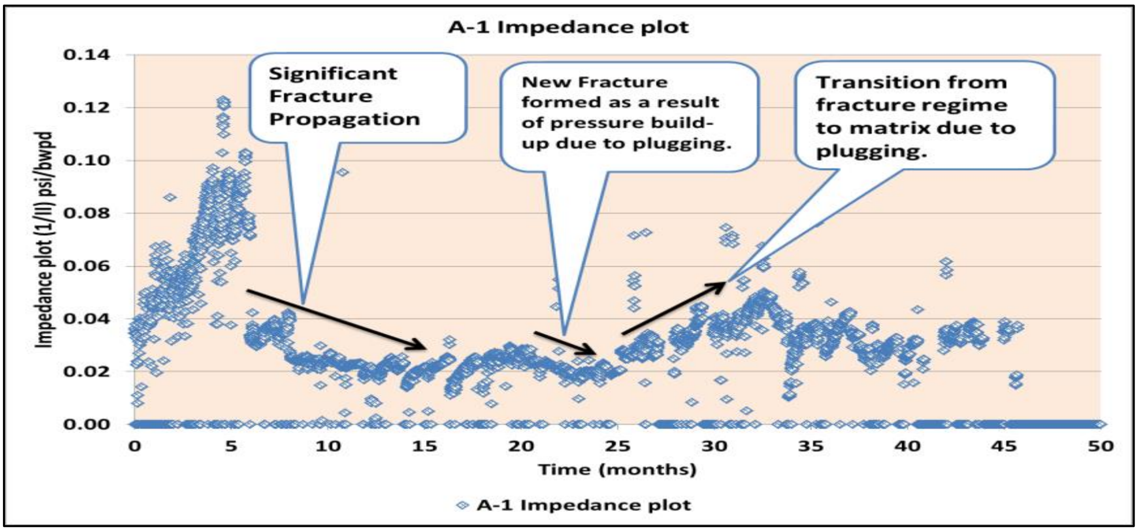

Figure F- 4: A-1 Impedance plot showing fracture-matrix transition

The bottom-hole pressure and its derivative were matched on a log-log plot to interpret the dominating characteristics of the wells during early time of shut-in. Also, most of the fall-offs exhibit linear behaviour when plotted with the root of time showing the presence of a fracture at early time. Results from the analysis are as illustrated in figure F-5 to F-9.

Figure F-5 is a PFO done in the 5th month and it can be observed that a very high skin of 276 was interpreted which masked the other events occurring during early time and confirms that severe formation plugging was occurring during this injection period of radial flow. Skin values of 43.1, 50.3 and 50.2 were interpreted in the 12th, 15th and 18th month denoting reduction and rise in skin owing to creation of new fracture and fracture face plugging respectively, also the approximately equal values of skin observed in the 12th and 15th month denote periods of significant fracture growth marked by relatively constant bottom-hole pressure. The skin recorded in the 30th month is 80.3 which marks a high rise in skin as compared to values recorded in subsequent months and suggest that fracture closure is occurring at a very high rate. These evolutions in skin tells a lot about the events occurring, however records also show that all derivatives converge towards the same radial flow stabilization (between 1-10hrs) permeability- thickness product (kh) values of $2.6 \times 10^5 mD.ft$ suggesting a very high average permeability of 5D. Furthermore multiple peaks are observed in the pressure derivative plot during the early time periods in the log-log plots (figure F-6 and F-7) and indicate possible fracture closure owing to fracture face skin. These peaks are not observed in the 5th month (figure F-5), PFO taken during matrix injection regime, and a reduced peak is seen in the 30th month, a period plagued by high fracture face skin and suggesting possible transition to matrix regime of injection.

Figure F-9 (a) to (d)–are plots of bottom-hole pressure against the square root of time clearly shows periods of linear flow in all cases (figure F-9 (a) – (d)) during the early time of shut-in. In figure 9(b) and (c), a kink is observed during this early time of linear behaviour and this could be as a result of fracture closure. Another school of thought is that it could be as a result of high water hammer pressures. Water hammer is a phenomenon that occurs during shut-in or well trip due to a sudden change in fluid velocity inducing pressure transients at the bottom-hole which is recorded and monitored using pressure gauges. They could be used to study the condition of the formation as high water hammer pressures denote a highly impaired formation. No kink was observed in the 30th month as shown in figure F-9(d) confirming possible fracture closure and high skin.

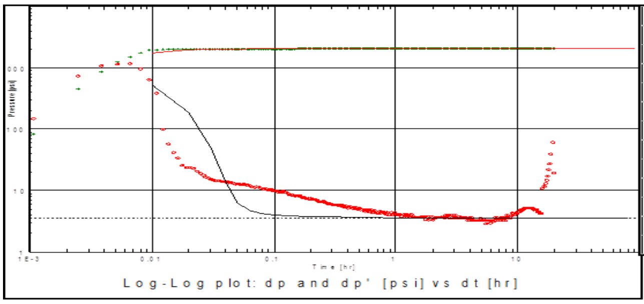

Selected Model		
Model Option	Standard Model	
Well	Vertical	
Reservoir	Homogeneous	
Boundary	Infinite	
Main Model Parameters		
TMatch	55400	[hr]-1
PMatch	0.139	[psia]-1
C	0.00176	bbl/psi
Total Skin	276	--
k.h, total	2.97E+05	md.ft
k, average	5400	md
Pi	4477.43	psia

Figure F- 5: PFO pressure and derivative plot for A-1 in the 5th month

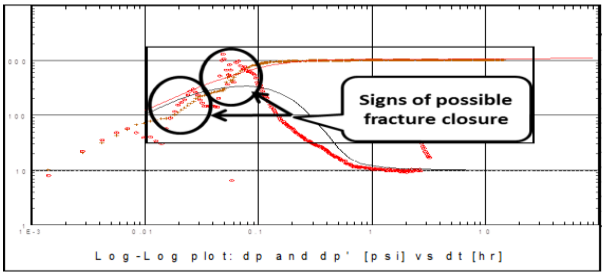

Selected Model		
Model Option	Standard Model	
Well	Vertical	
Reservoir	Homogeneous	
Boundary	Infinite	
Main Model Parameters		
TMatch	640	[hr]-1
PMatch	0.0509	[psia]-1
C	0.156	bbl/psi
Total Skin	43.1	--
k.h, total	3.04E+05	md.ft
k, average	5520	md
Pi	4557.24	psia

Figure F- 6: PFO pressure and derivative plot for A-1 in the 12th month

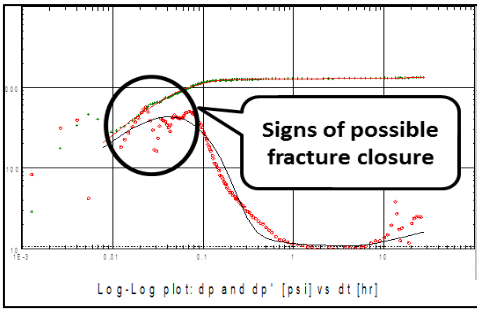

Selected Model		
Model Option	Standard Model	
Well	Vertical	
Reservoir	Homogeneous	
Boundary	One fault	
Main Model Parameters		
TMatch	1300	[hr]-1
PMatch	0.047	[psia]-1
C	0.074	bbl/psi
Total Skin	50.3	--
k.h, total	2.61E+05	md.ft
k, average	4750	md
Pi	2018.73	psia

Figure F- 7: PFO pressure and derivative plot for A-1 in the 15th month

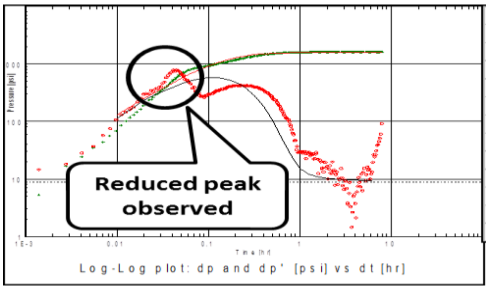

Selected Model		
Model Option	Standard Model	
Well	Vertical	
Reservoir	Homogeneous	
Boundary	Infinite	
Main Model Parameters		
TMatch	780	[hr]-1
PMatch	0.0561	[psia]-1
C	0.125	bbl/psi
Total Skin	80.4	--
k.h, total	2.97E+05	md.ft
k, average	5400	md
Pi	4784.03	psia

Figure F- 8: PFO pressure and derivative plot for A-1 in the 30th month – severe fracture face skin (possible transition to matrix regime of injection.

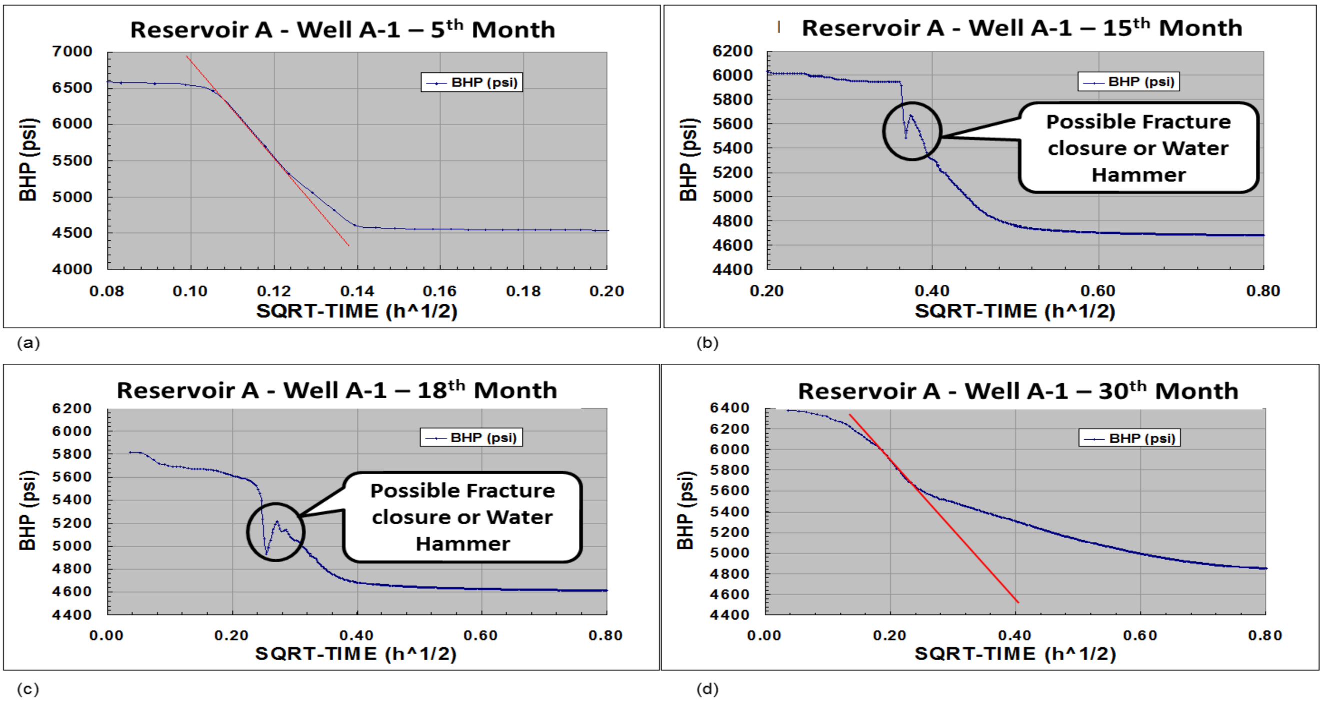

Figure F- 9: bottom-hole pressure of well A-1 against root of time. (a) 5th Month – Matrix injection regime. (b) 15th month – Fracture injection regime. (c) 18th month – fracture injection regime (d) 30th Month – period marked by significant fracture face plugging and possible transition to matrix regime (no kink is observed).

Diagnostic Analysis for Well A-2

To determine the injection regime of well A-2, its pressure-rate history data set was divided into three (3) carefully selected periods: Matrix Injection regime, Fracture Injection regime, and Fracture face plugging.

Figure E-11(a) is the pressure and injection rate history plot for 80months duration from the start of injection.

The different regimes of injectivity can be observed in figure F-10(a) and (b) in which during the first month of injection an increase in bottom-hole pressure from an initial value of 4371Psi to a value of 5000Psi which is the fracture pressure of the formation occurs. This period of matrix injection is characterized by a linear behaviour between the pressure-rate points (figure F-10(b)) as the injection rate increases with increase in pressure. The period of fracture regime which last from 0 - 18 months is plagued by significant plugging of the fracture; the pressure-rate points are parallel to each other but closely spaced signifying gradual fracture face plugging.

Figure F-10(c) shows the evolution of skin and injectivity index through time. An increasing trend in skin is observed from a value of 10 in the 25th month of injection to 35 in the 32nd month. This rise in skin is confirmed by a corresponding decline in injectivity from about 8obwpd/psi to 20bwpd/psi. A back flush operation was carried out on the well to restore injectivity in the 32nd month from 20bwpd/psi to 73bwpd/psi but this was short-lived as injectivity starts declining again in less than a month after the event, this again confirms severe plugging of the fracture. Five stimulation events were executed on the

32^{nd}, 38^{th}, 43^{rd}, 46^{th}, 53^{rd}, and 57^{th} months. The event on the 38^{th} month was a re-frac operation which restored injectivity from 22 to 52bwpd/psi. This restored injectivity was much lower than the result achieved using back flush. Subsequent attempts to use back flush returned a lower restored injectivity index than the previous attempts suggesting increased damage to the formation. Also observed from this plot is the parallel injectivity decline trend-lines which indicates the same mechanism of impairment (internal or external filter cake) is at play in all decline periods.

Finally, in figure E-10(d) the derivative curve traces the integral curve for about a month (matrix injection regime), it goes below it for less than a month after which it slowly rises above it denoting gradual fracture face plugging.

The impedance plot (figure E-11) clearly shows the transition to fracture flow after the first month of injection and the subsequent fracture-matrix transition throughout this wells injection history.

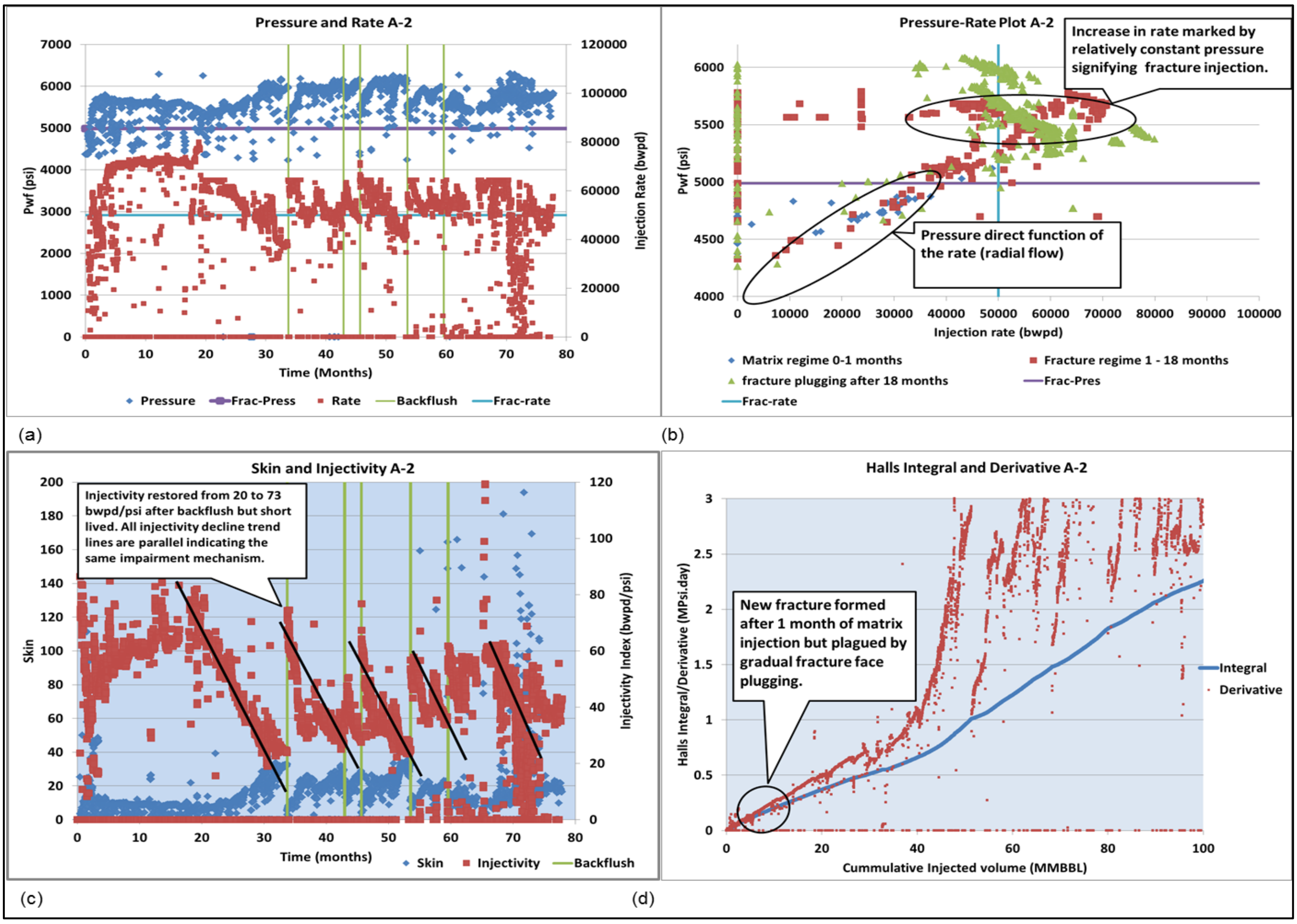

Figure F- 10: (a) A-2 Injection Pressure and Rate plot with time. (b) A-2 Pressure-Rate Diagnostic plot. (c) A-2 evolution of skin and injectivity index. (d) A-2 Halls Integral and Derivative Plot.

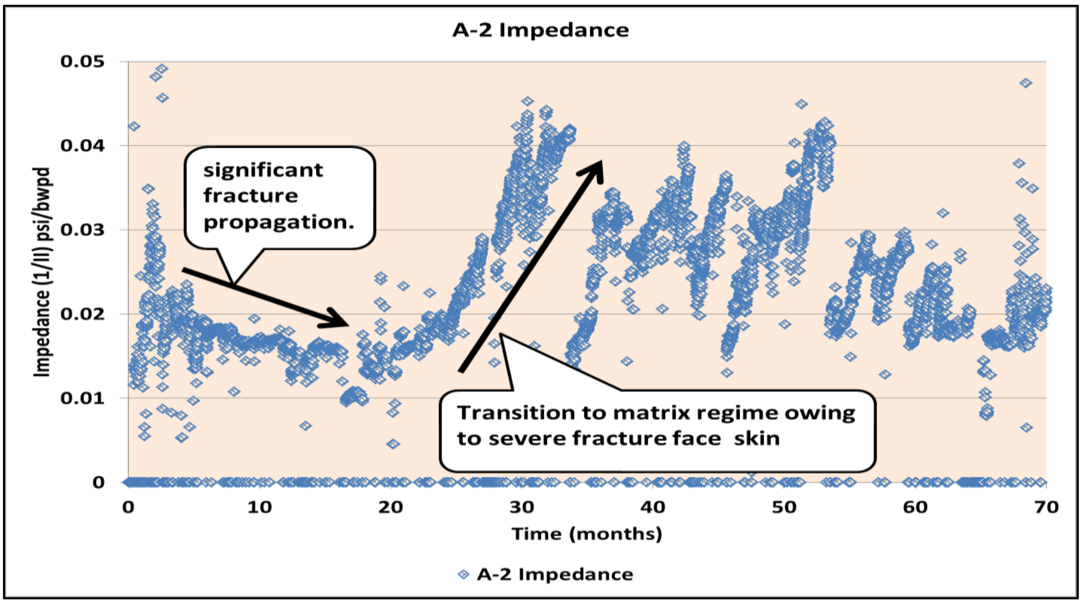

Figure F- 11: A-2 Impedance plot showing fracture-matrix transition

Appendix G: Lumped Parameter Analysis of the Dynamics of Deposited Particles in a Pore Volume

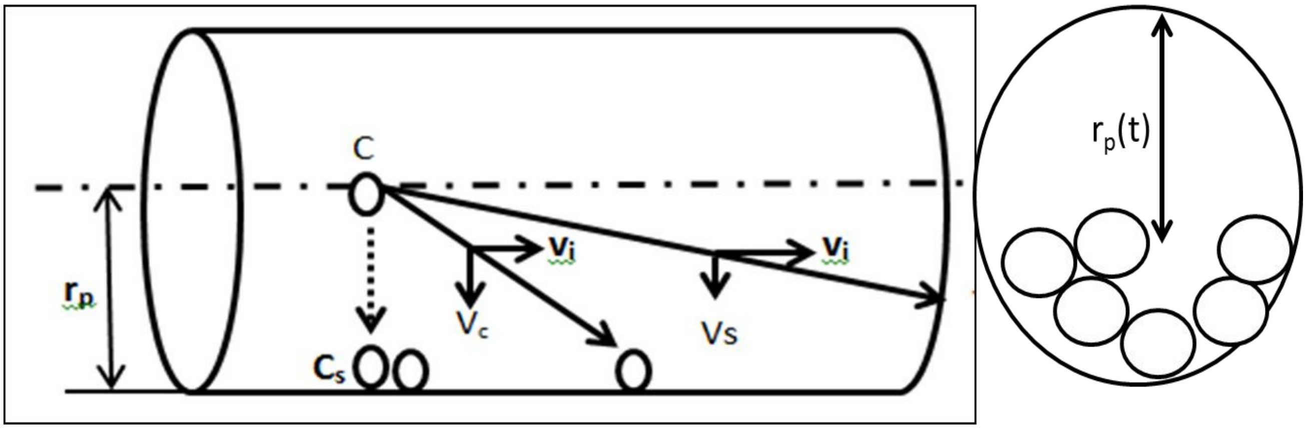

Figure G- 1: (a) the trajectory of particles before deposition; (b) the accumulation of particles in an isolated pore.

This analysis is an attempt to investigate the relative impact of injected particles concentration on amount of particles deposited/transported in the formation during injection, considering particles of different sizes using an isolated section of the porous medium.

A pore space of a given radius (r_p) and distance from injector is considered with a particle of a specific diameter (D_{pi}) flowing through it as shown in figure G-1a. Each transported particle has a different residence time of flow before deposition which is a function of its size, density and interstitial velocity. The residence time of a particle remains constant and will change if there is a change in the system's capacity as reflected in the pore radius of the formation. Using lumped parameter analysis, the dynamics of the deposited particles with time as used in the work of Lawal *et al*, (2010) can be obtained thus:

$$\boldsymbol{\rho_l v_c C = \rho_l v_c C_p + \rho_l r \frac{dC_p}{dt}} \qquad \textbf{G- 1}$$

C is the volume fraction of injected solids; C_p is the fraction of injected solids deposited.

The mass flow rate of particles injected

In this analysis accumulation at discrete points in the porous media is analyzed. Dividing through by $\rho_l v_c$ we have:

$$\boldsymbol{C = C_p + \frac{r}{v_c}\frac{dC_p}{dt}} \qquad \textbf{G- 2}$$

For this analysis, v_c is taken to represent the critical settling velocity of the particle which is the minimum vertical velocity required for particle transport. This implies that:

$$\frac{r}{v_c} = t_c = \frac{\pi[r(S_w)^2 - r_w^2]H\phi}{Q_t}\left[\frac{S_w}{F_w}\right]_{S_{wx}} \qquad \text{G- 3}$$

This is customized for a particle of a given size, it represents the time it takes for the particle to leave the flow stream in this analysis. It is assumed that if the injection rate is constant, all particles of a given size will get deposited at a particular distance (point) in the porous media and start accumulating as shown in figure G-1b. Other mechanisms of particle capture are not considered.

$$C = C_s + t_c\frac{dC_s}{dt} \qquad \text{G- 4}$$

C is the volume fraction of injected solids, C_s is the fraction of injected solids deposited.

From the condition of particle deposition: $V_s \geq V_c$; $\quad t_s = \frac{r_p}{v_s}$; $\quad t_c = \frac{r_p}{V_c}$

This implies for particle accumulation to begin $t_s \leq t_c$

$$t_s = \frac{18\mu_w}{(\rho_s - \rho_l)gD_p^2}\sqrt{\frac{k_o}{\phi_o}} \qquad \text{G- 5}$$

The solution to the equation F-4 is therefore:

$$C_s = C\left(1 - e^{-\frac{t}{t_c}}\right) \qquad \text{G- 6}$$

In the solution above t_c represents the time at which the concentration of deposits increases to 63.2% of the initial injected solids concentration and for the purpose of this study $3t_c$ is taken as steady state (Lawal et al, 2010). This equation will now be used to ascertain the impact of particles of a given diameter on pore radius reduction. The profile of injected particles with time for particles within 0.05µm to 5µm is illustrated using an initial injected solids concentration of 28ppm. The residence time of each particle is obtained using fractional flow theory and fitting a regression line to a plot of $t_c\ vs\ D_p$ as shown in figure G-2.

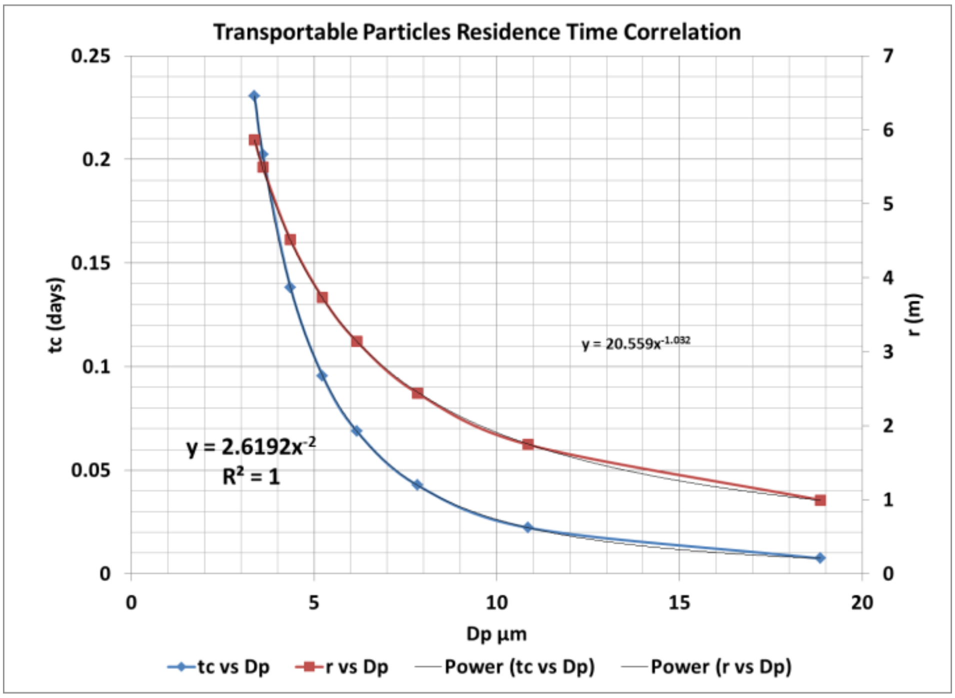

Figure G- 2: a correlation for particle residence time as a function of particle diameter from fractional flow analysis.

Figure G-3 (a) to (d) illustrates the effect of particle residence time on its transported/deposited concentration. From figure G-3 (a) and (b), for the case of 0.05 and 0.1 micron, it can be observed that concentration has negligible effect on the transportation of fine particles at submicron level as the transportation of the 0.05 and the 0.1 µm particles only reduce by 4.6% and 17.8% respectively at the end of 60days. From previous analysis in Appendix E on particle residence time, it was observed that these particles <1µm have a residence time >300days, hence they have negligible contribution to the accumulation of particles at the near-wellbore region of the injector. However, the injected particle concentration has a huge impact on the amount of deposits that will accumulate in the formation for large particles as these particles have a residence time < 1 day (0.12days for a 5µm particle). They get deposited at the immediate vicinity of the injector at relatively low rates of injection. The 5µm particle (figure G-3 (d)) leaves a very high concentration of deposits and very negligible fraction transported in <1day; hence, if particles larger than these are present in the injected sea water, a very large amount of deposits will accumulate at the near-wellbore region of the injector forming a low porosity filter cake. The amount of these large particles that gets deposited at the near-wellbore region of the injector increases with increase in particles concentration. It can also be inferred from this analysis that the larger the particles in suspension, the greater the impact of concentration on the amounts of solids deposited, that is, particle concentration has lower impact on permeability impairment due to sub-micron particles. This phenomenon has also been confirmed in the work of Pang and Sharma, (1997).

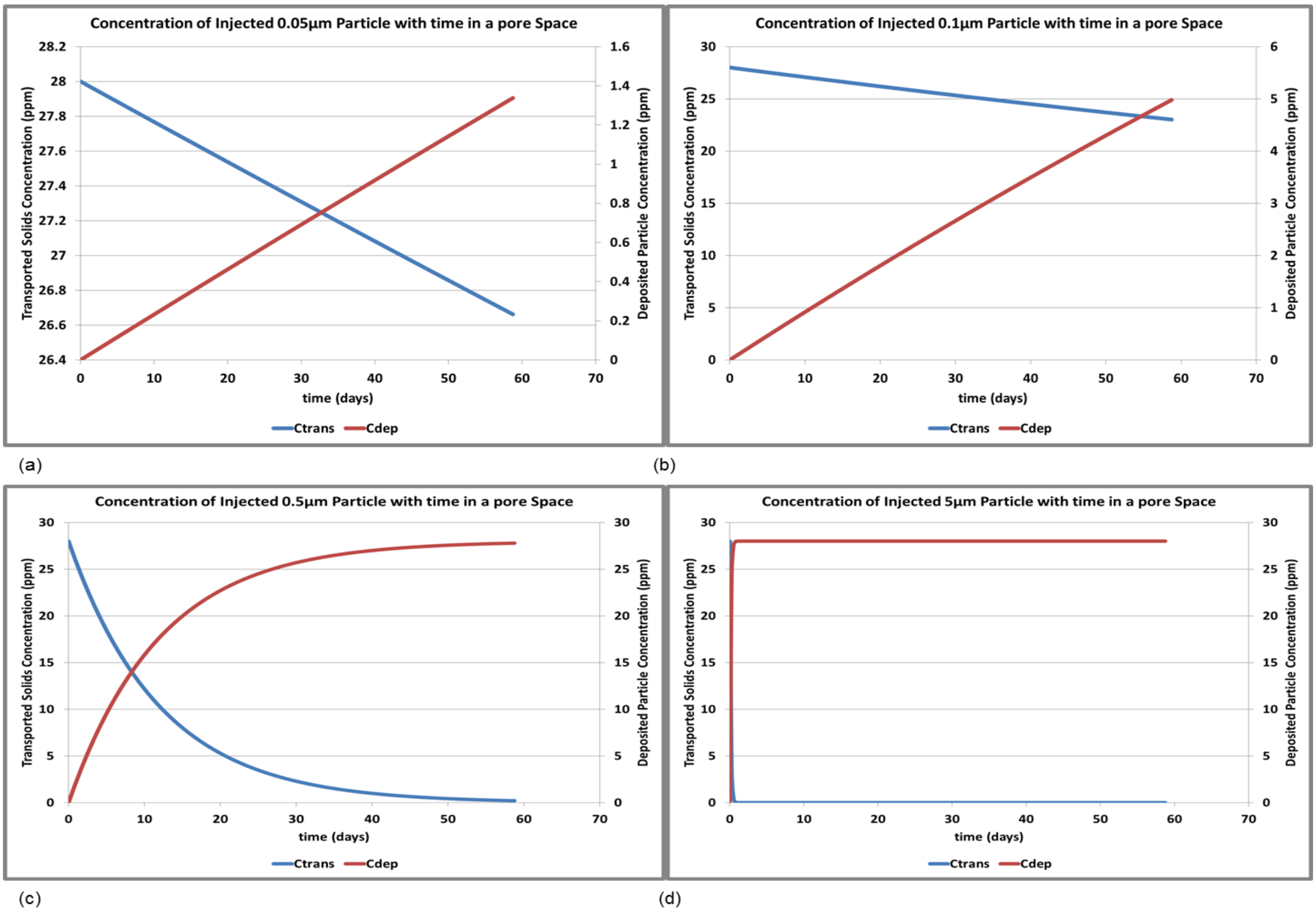

Figure G- 3: The relative impact of injected particles concentration on amount of particles deposited/transported considering particles of different sizes. (a) 0.05µm (b) 0.1µm (c) 0.5µm (d) 5µm